

***Delineation of subsurface fractures and conductors  
beneath Srisailam Formation using Very Low Frequency  
Electromagnetic Method in Amrabad north,  
Mahboobnagar district, Andhra Pradesh***

*Dissertation submitted in accordance with the requirements  
of the University of Hyderabad for the degree of*

**Master of Technology**

**in**

**Mineral Exploration**

**By**

**A.R.Mukundhan**

**(09ESDE03)**



**Centre for Earth and Space Sciences  
University of Hyderabad,  
Hyderabad - 500 046**

**2011**

# **CERTIFICATE**

It is to certify that, **Shri. A.R.Mukundhan**, sponsored candidate of Atomic Minerals Directorate for Exploration and Research, Department of Atomic Energy has carried out the Project Work titled “***Delineation of subsurface fractures and conductors beneath Srisailam Formation using Very Low Frequency Electromagnetic Method in Amrabad north, Mahboobnagar district, Andhra Pradesh***” at Centre for Earth and Space sciences, University of Hyderabad in partial fulfillment of the requirements for degree of M. Tech in Mineral Exploration under our joint supervision. It is further certified that the contribution is original in nature and had not been submitted either in part or whole elsewhere.

SHRI P. ALIPEERA  
Scientific Officer-F  
Atomic Minerals Directorate for  
Exploration and research  
Hyderabad-500629

DR. V. CHAKRAVARTHI  
Reader  
Centre for Earth & Space Sciences  
Hyderabad Central University  
Hyderabad-500046

PROF. A. C. NARAYANA  
Director  
Centre for Earth & Space Sciences  
Hyderabad Central University  
Hyderabad-500046

# CONTENTS

<i>Acknowledgment</i>	<i>i</i>
<i>Abstract</i>	<i>ii</i>
<b>Chapter –I Geology</b>	
1.1 Introduction	1
1.2 Study area	5
1.3 Approach to study area	5
1.4 Flora and fauna	6
1.5 Regional geology	6
1.6 Mineral Resources of Cuddapah basin	9
1.7 Geology of Srisailam sub-basin	12
1.8 Geology of the study area	14
1.9 Objective and scope of the work	17
<b>Chapter –II Methodology</b>	
2.1 Geophysics in mineral exploration	19
2.2 Previous geophysical studies in Srisailam sub-basin	21
2.3 Very Low Frequency Electromagnetic Technique	23
2.4 Data acquisition	34
<b>Chapter –III Filtering and Transformation of VLF – EM data</b>	
3.1. Introduction	37
3.2 Stacked profiles	38
3.3 Fraser Filter	38
3.4 Karous-Hjelt filter	40
3.5 current density Pseudosection	40
3.6 Level contour plans (Depth slices)	41
3.7 Interpretation based on filtering	41
3.8 Transformation of VLF-EM data and interpretation	44
<b>Chapter –IV VLF resistivity surveys and interpretation</b>	46
<b>Chapter –V VLF-EM and Magnetic data integration and Interpretation</b>	47
<b>Chapter –VI Modelling and Inversion of VLF-EM data and Interpretation</b>	
6.1 Introduction	49
6.2 Forward Modelling	50
6.3 2D Inversion of VLF- EM data	52
<b>Chapter –VII Integration with Geology and discussion</b>	58
<b>Chapter – VIII Conclusions</b>	64
<b>References</b>	66

## List of Figures

- 1.1 Location map of the study area
- 1.2 Geological map of Cuddapah Basin
- 1.3 Geological map of Srisailam and Palnad sub-basins
- 1.4 Lithostructural map of Srisailam sub-basin
- 1.5a Geological map of Mannanur – Amrabad sector, Mehboobnagar dt.,A.P
- 1.5b Geological section A-B line
- 1.6 Rose diagrams of the structural features observed in study area
- 2.1 Map showing various VLF transmitters around the globe
- 2.2 Figure showing interaction of primary EM field with conductor
- 2.3 Figure showing various components of primary and secondary EM fields
- 2.4 Ellipse showing tilt and ellipticity
- 2.5 Plot of depth penetration of VLF waves (m) verses resistivity (ohm-m)
- 2.6 Survey layout showing profile lines and station points
- 3.1 Stacked profiles of raw tilt (%) and ellipticity (%) data
- 3.2 Stacked profiles of low pass filtered tilt and ellipticity data
- 3.3 Fraser filter output of the study area
- 3.4 Karous-Hjelt (KH) filter output of the study area
- 3.5 Fraser filter pseudo sections of the profiles showing conductor axis
- 3.6 Karous-Hjelt (KH) filter pseudo sections of the profiles showing conductor axis
- 3.7 Depth slices prepared using Fraser filter data
- 3.8 Depth slices prepared using Karous-Hjelt (KH) filter data
- 3.9 Plot showing ratio of tilt/ellipticity Vs distance-quality of conductor
- 3.10 Hilbert Transform output Image of In-phase data
- 3.11 Amplitude of Analytical signal Image of In-phase data
- 3.12 Profiles showing depth to the top of the conductor using empherical method
- 4.1a Fraser filter output of the study showing VLF resistivity profile lines
- 4.1b Measured apparent resistivity profiles
- 5.1 Profiles (N2200 and N 1800) showing VLF in-phase and Magnetic anomaly

- 5.2 Superimposed map of 3D inverted map with Fraser filter contours
- 6.1 Description of 2D model parameters
- 6.2 2D-Model for N-2200 line
- 6.3 VLF- Electromagnetic field
- 6.4 Generalized flow chart for the finite element method for 2D Inversion
- 6.5 2D Inversion model along profile line N1800
- 6.6 2D Inversion model along profile line N2000
- 6.7 2D Inversion model along profile line N2200
- 6.8 2D Inversion model along profile line N1000
- 6.9 2D Inversion model along profile line N4400

## **List of tables**

- 1.1 Stratigraphy of Cuddapah Super Group and Kurnool Group
- 1.2 Geological succession of study area
- 2.1 Geophysical methods and operative physical property
- 2.2 Global VLF transmitters and their frequency
- 2.3 Various types of VLF receivers

## **ACKNOWLEDGEMENT**

I express my pleasure and deep sense of gratitude to Shri. P.B.Maithani, Director, Atomic Minerals Directorate for Exploration and Research (AMD), Hyderabad for permitting me to pursue M.Tech. in Mineral Exploration course, at University of Hyderabad. I extend my sincere gratitude and thanks to Shri P. S. Parihar, Shri K. Umamaheswar, and Dr.M.K.Roy Additional Directors, AMD, Hyderabad for their encouragement and support. I am also thankful to Dr.P.V.Ramesh Babu, Regional Director, Dr. K.K.Achar, Deputy Regional Director, and Shri S.J Chavan, Incharge, Srisailam Investigations, South Central Region for their constant support and encouragement.

I am extremely grateful to Prof. A. C. Narayana, Director, Centre for Earth and Space Sciences (CESS), University of Hyderabad for providing all necessary facilities for the present study and also for his continuous encouragement during the entire tenure of two years at CESS.

I feel immense pleasure and deep sense of indebtedness to my mentors as well as supervisors Shri. P.Alipeera, Scientific Officer-F, EGPG Group, AMD, Hyderabad, and Dr. V. Chakravarthi, CESS, UOH Hyderabad for their support and encouragement and guidance from time to time during the field work and also during processing of the data.

I am indebted to my colleague and friend Dr. V. Rameshbabu, ASRS group, Hyderabad who was the inspiration behind this work and providing all the literature and software during processing. He was with me all throughout this work. Without his support I would not have completed this work.

The help extended by Shri R. L. Narasimha Rao, Incharge, Exploration Geophysics Group, AMD, Hyderabad, for providing the necessary instrument facilities is greatly acknowledged. I am thankful to Shri Rajeev Ranjan, Shri.M.Venakteshwaralu, M.Chandrashekar and Shri.Pal, all my M. Tech colleagues for their memorable company during the M.Tech course. I am thankful to Shri.H.S. Rajaraman, Scientific Officer, SCR for the support during the field work and also processing the data.

I am also thankful to all my colleagues in South Central Region, especially Dr. G. Nagendra Babu, Scientific Officer, SCR and Shri. M.S.M.Deshpande, Scientific Officer, for their support during this course. Special thanks are to Shri. Krishnakant Parashar, with whom I carried out the field work for the present study.

I sincerely thank my Father who has been my source of constant inspiration, wife Gomathi and sons Mohnish and Karthik for their co-operation and support for completion of this work.

## **Abstract**

*The Project work on “Delineation of subsurface fractures and conductors beneath Srisailam Formation using Very Low Frequency Electromagnetic Method in Amrabad north, Mahboobnagar district, Andhra Pradesh” was carried out with an objective to decipher the fracture zones/ conductors occurring in the basement below Srisailam sediments which may host uranium mineralization. The study area form a part of the Amrabad outlier close to the main Srisailam sub-basin of the Cuddapah basin.*

*The Srisailam sub-basin occurring in the northern parts of Cuddapah basin is well known for its uranium potentiality. Substantial uranium resources have already been established in three uranium deposits namely Lambapur, Peddagattu and Chitrial in three separate outliers of the Srisailam Formation. Uranium mineralisation in these deposits is essentially confined along the unconformity between the basement granites and overlying sediments of Srisailam Formation. Also, the outline of the ore bodies indicates the uranium mineralisation generally follow the trend of the basement fracture. The Amrabad outlier of the Srisailam Formation is also having similar lithostructural setup as that of the three outliers, where uranium mineralisation is established. From uranium exploration point of view the Amrabad outlier is largely unexplored since this outlier forms a part of the Rajiv Gandhi Tiger Sanctuary (RGTS). Ground geophysical surveys were carried out for the first time in the area north of Amrabad.*

*An area of 10 sq km was covered by VLF-EM surveys using the IRIS make T-VLF receiver unit of Centre of Earth and Space Sciences (CESS), University of Hyderabad. The frequency of 17100Hz transmitted by UMS, Moscow was used for the entire survey since this transmitter falls approximately in the NNW – SSE direction of the study area, coinciding with the expected anomalies along the N-S direction. The profiles were kept at 200m interval and the station spacing was kept at 25m. VLF data such as tilt and ellipticity was collected along twenty six profiles with the total no of data points being 1924.*

*The stacked profiles of the raw data and filtering methods such as Fraser and Korous- Hjelt indicates two dominant trends of the conductors along NNE- SSW and NW-SE directions. The NNE-SSE trend is the older one as this trend is offset by the later NW-SE trend. The conductors have lengths ranging from 400m to 1200m with*

*widths ranging from 50 to 150m. Pseudo sections and depth slices of the Fraser and Korous-Hjelt filtered outputs of the VLF in phase data indicates the continuity of the conductors at depths also and the strength of the conductors increase with depth. VLF-resistivity surveys along two selected profiles have confirmed the presence of the conductors, besides throwing light on the width and the quality of the conductors.*

*The results obtained by filtering and transformation processes, prompted for modeling of the VLF- EM data. Both 2D forward modeling and 2D inversion were attempted for first order interpretation. Results of the forward modeling using the known geological parameters of the area closely matches with the observed VLF data. 2D inversion of the VLF data along five profile lines has brought the presence of conductors (low resistivity zones) along two well defined directions corroborating with the inferences from filtering process. Resistivity values obtained by the 2D inversion of VLF-EM data fall within the range of basement fractures. It is inferred that the low resistivity values are due to the presence of sulphides, alteration minerals and water in varying proportions in structurally weak zones such as fractures of 100 -150m width. Thus the VLF-EM survey in north of Amrabad area has narrowed down the target areas for future subsurface exploration.*

*The entire thesis is organized in to eight chapters as discussed below. Chapter I deals with the regional geology, geology of the study area and the mineral wealth of Cuddapah basin, Chapter II deals with the methodology adopted and utility of very-low frequency technique in exploration of natural resources both in India and abroad and the results of orientation surveys along with survey layout for present study. Chapter III elaborates in detail the filtering and transformation studies and their interpretations. This chapter includes preparation of pseudosections and depth slices of VLF-EM data. Chapter IV outlines the results obtained from VLF resistivity surveys. Chapter V discusses integration studies of magnetic and VLF-EM data. The procedure of 2D forward modelling and 2D inversion processes, its results and interpretation are discussed in Chapter VI. Chapter VII deals with the integration of observed geophysical indicator parameters with geology of the area. Chapter VIII details the conclusions of the present geophysical study.*

# CHAPTER - I

## GEOLOGY

### 1.1. Introduction

According to conventional wisdom, the world is unlikely to run out of energy in the near future. However, current patterns of energy production and use have destructive impacts on the environment and in recent years, environmental issues such as possible climate change resulting from greenhouse gas emissions have thrown the spotlight onto the links between energy and the global environment. At the same time, there is a need, especially in developing countries, for higher levels of energy supply for sustaining their economic development. At present, 'energy poverty' hinders the economic and social development of very large number of people.

Coal, oil, gas and nuclear energy are the major sources of primary energy, followed by renewable combustible wastes (biomass, animal products, municipal wastes, and industrial wastes), hydro, and other sources. The ever increasing demand for energy in its all forms like hydrocarbons, gas hydrates, coal etc has an implicit compulsion to explore more and more the hidden subsurface resources with the state of art of technology. In this direction geotechniques play an important and indispensable role. However, it is to be noted that these energy sources are not devoid of environmental degradation. Today, the world faces the consequences of global warming caused possibly by the ease of fossil fuel and hence there is a resurgence of interest in nuclear power. This resurgence is driven partly by the need of more electricity for increasing population and higher per capita consumption. But we also need sources of energy that do not emit carbon-di-oxide (CO<sub>2</sub>) and other green house gases (CFC) which cause global warming.

Further hydropower, thermal power and other renewable energy sources have reached its criticality and they may highly unlikely meet the future demand. It may not be a hyperbole to state that the entire world is in a danger of approaching energy depletion in the decades to come unless a source of long term salvation is developed. In view of the above reasons nuclear power can possibly be the only alternate solution to meet the future demands without much concern on global warming.

Mineral exploration is the process of finding ore (commercially viable concentrations of minerals) to mine. Mineral exploration is a much more intensive, organized and professional form of mineral prospecting and, though it frequently uses the services of prospecting, the process of mineral exploration on the whole is much more involved. Uranium exploration which is at the front end of the nuclear fuel cycle utilizes many techniques to decipher its subsurface concentrations. The main objective of any exploration program is to progressively narrow down the target to further detailed exploration. Recent advancements in uranium exploration has advocated an integrated study of geological, geophysical and geochemical data.

Fourteen principal types and as many as forty seven sub-types of uranium deposits have been identified worldwide (Dalkhamp, 1980). These deposits occur in various geological environments ranging in age from Upper Achaean to recent. Of these, three principal uranium mineralisation types, such as the Proterozoic Unconformity related type, the Proterozoic iron oxide breccia type and the Mesozoic-Cenozoic sandstone type accounts for more than 60% of total uranium resources of the world. The Proterozoic unconformity related uranium mineralisation type is spatially and temporally associated with Lower – Middle Proterozoic unconformity owing to the

favorable physico-chemical conditions existed then. The nature of the basement and the structures within constitute a crucial role in serving as suitable conduits for the movement of metalliferous fluids and localizing the deposits. These deposits constitute for the high grade, large tonnage uranium deposits. The classical examples of such deposits occur in the Athabasca basin, Saskatchewan, Canada and the Pinecreek geosyncline, Australia (Mathews et al., 1997). Geophysical methods in general and electromagnetic methods in particular have been successfully employed in these areas for establishing the controlling features associated with uranium mineralization as deep as 500 meters below the ground surface.

The Very Low Frequency electromagnetic method (VLF-EM) is one of the methods of geophysical exploration used for exploring shallow concealed mineral deposits, also used for identifying associated structures and alteration zones in the reconnaissance, semi-detailed stage of exploration.

In India, the Lower – Middle Proterozoic unconformity is represented at the base of the Fourteen Proterozoic sedimentary basins. Out of these, the Cuddapah basin of the Dharwar Craton is a known uranium 'province', and holds its importance since uranium mineralisation has been established in its various stratigraphic levels.

In Srisailam sub-basin of the northern part of Cuddapah basin, uranium mineralisation occurs along the unconformity between the Lower Proterozoic basement and Middle-Upper Proterozoic cover sediments. Sustained exploration by AMD over the past two decades had established substantial uranium reserves in this part of the basin by identifying three deposits at Lambapur, Peddagattu and Chitrial areas. Mineralisation in these deposits is confined to the unconformity with most part (> 85%) in the

basement (Sinha, et al., 1995). The ore body outline of these deposits have one long dimension and two short dimensions indicating the control of fractures/ reactivated basement structures for the formation of these deposits. Uranium mineralisation in these deposits occurs at a depth of 70mts from the surface.

VLF-EM studies carried out in one of the deposits of the northern parts of Cuddapah basin, in Chitrial main block (Rajaraman, 2010) have indicated positive correlation between the EM conductors and the mineralized basement fractures. Besides VLF-EM method has been successfully utilized in the study of the uranium mineralized basement fractures in the southeastern margin of Chhattisgarh basin (Rameshbabu, 2007).

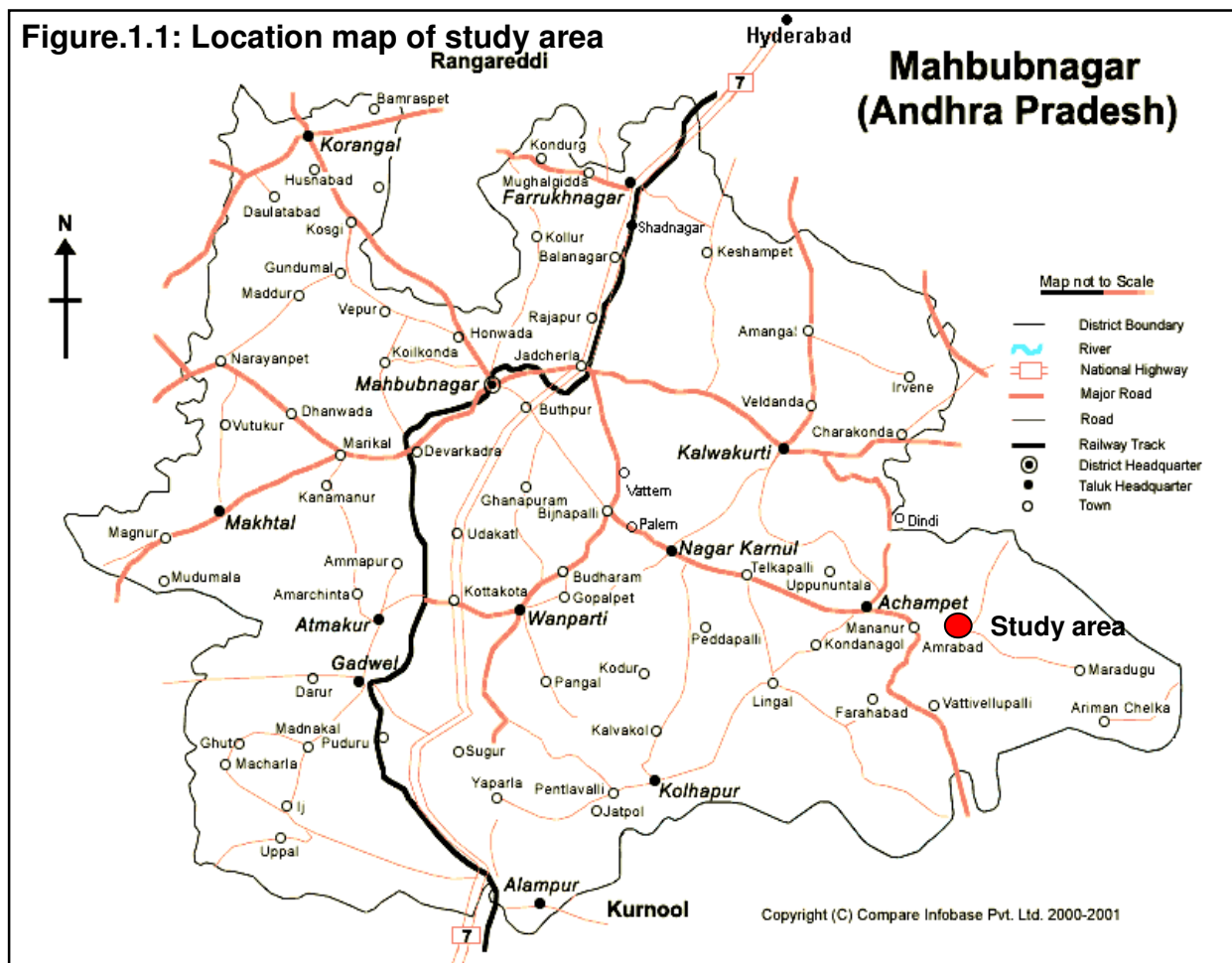
The present study area also lies in the northern margin of Srisailam sub-basin, southwest of the Chitrial outlier, and hold immense potentiality to host unconformity related uranium mineralisation owing to the similar lithostructural setup of the study area. The present study of “***Delineation of subsurface basement fractures and conductors beneath Srisailam Formation using Very Low Frequency Electromagnetic methods in Amrabad North, Mahboobnagar District, Andhra Pradesh***” is aimed to decipher and quantify the basement fractures and conductive zones using the above geophysical parameters used in similar geological setup, in an entirely unexplored sector of Amrabad outlier of Srisailam sub-basin. Ground geophysical surveys were carried out for the first time in the area. By this the ultimate aim of the present study is to narrow down the target for future subsurface exploration in this part of Srisailam sub-basin and also to standardize the VLF – EM indicator parameters controlling the uranium mineralisation.

## 1.2. Study Area

The study area covers about 10 sq km, forms a part of Amrabad outlier (latitude  $16^{\circ}25'00''$  to  $16^{\circ}27'49''$ N and longitude  $78^{\circ}49'13.7''$  to  $78^{\circ}49'00''$ E, Survey of India Toposheet No. 56L/15) which lies in northern margin of Srisaillam sub-basin, to the southwest of the Chitrial outlier, having similar lithostructural setup as that of the outliers in the northern part of Srisaillam sub-basin. The area is an unexplored part of the Srisaillam sub-basin since the entire area is part of the Rajiv Gandhi Tiger Sanctuary.

## 1.3. Approach to study area

The study area falls in Survey of India Toposheet No.56L/11 and 15 and is in Mahboobnagar district of Andhra Pradesh. Amrabad - Mannanur is approachable



through national highway NH-7 from Hyderabad via Jadcherla–Achempet route (179 km) or by Kadthal main road of Hyderabad – Srisailam state highway via Kalwakurthy (138 km) with a bus journey of about 2.30 to 3.00hrs by either route (**Fig.1.1**). Nearest railway station is Jadcherla, which is located about 95 km NW of Mannanur. The topography of the area is mainly flat of 250-300 m RL, with gentle slope towards the east.

#### **1.4. Flora and fauna**

The entire study area falls in Srisailam Tiger reserve. This is the country's largest tiger reserve. The Srisailam sanctuary is spread over an area of 3568 sq. km. It comprises of the several plateaus of the Nallamalai Hills, the most famous being the Amrabad Plateau in the northern section. Dry deciduous mixed forest with scrub and bamboo thickets provide shelter to a wide range of animals. A variety of forest types can also be found in the gorges and valleys. The terrain is rugged and winding gorges slice through the Nallamalai hills. Spotted Deers, Mouse Deers, Black Bucks, Sambhars, Chousingha Nilgai, Wild Boars, Indian Giant Squirrels, Tree Shrews, Rayels, Mugger Crocodiles, Wild Dogs, Jackals, Wolves, Foxes, Sloth Bear, Panthers and Tigers are the animal attractions of this sanctuary. Quite a number of bird species are present in Nagarjunasagar-Srisailam Tiger Reserve.

#### **1.5. Regional Geology**

The crescent-shaped Cuddapah basin exposed in the eastern margin of the Dharwar Craton covers an area of about 44,000 sq km and contains aggregated sediment-volcanic litho sequence of 12,000 m and is the second largest Proterozoic basin of India, after the Vindhya. The western margin of the basin is marked by the

profound unconformity between the basement comprising Peninsular Gneissic Complex and granites of Lower Proterozoic age (2400-2600 Ma), and intruded by basic dykes (1500-1800 Ma) (Kale et al., 1991), whereas the eastern margin of the Cuddapah basin has a thrust contact with the Eastern Ghat Mobile Belt (EGMB). The sediments of the Cuddapah Basin belong to the Cuddapah Supergroup and Kurnool Group of rocks. The stratigraphy of the Cuddapah Basin was initially compiled by King (1872). The classification scheme proposed after the systematic structural mapping and sedimentological studies by Nagaraja Rao et al., (1987), widely followed in the geological fraternity is given in **table 1.1**.

**Table 1.1: Stratigraphy of Cuddapah Super Group and Kurnool Group**

<b>Age</b>	<b>Group</b>	<b>Formation</b>	<b>Lithology</b>
Late Proterozoic	<b><i>Kurnool</i></b>		Carbonate facies Fine Clastics
~~~~~ <b>Unconformity</b> ~~~~~			
Middle Proterozoic	<b><i>Srisaïlam</i></b>		Quartzite and shale
		~~~~~Angular Unconformity~~~~~	
		Cumbum	Phyllite/slate, Quartzite, Dolomite
	<b><i>Nallamalai</i></b>	Bairenkonda quartzite	Quartzite and shale
		~~~~~Angular Unconformity~~~~~	
Early Proterozoic to Middle Proterozoic	<b><i>Chitravati</i></b>	Gandikota Tadpatri	Quartzite and shale Shale, tuff, dolomite with intrusive
		Pulivendla quartzite	Conglomerate and quartzite
		~~~~~Disconformity~~~~~	
		Vempalle	Stromatolitic dolomite, chert, breccia with basic flows/intrusives
	<b><i>Papaghni</i></b>	Gulcheru quartzite	Conglomerate quartzite and shale
~~~~~ <b>Angular Unconformity</b> ~~~~~			
<b>Archaean and Dharwar Super Group</b>			Granite gneiss, granite and amphibolites

Although exact age data is not available for the entire sequence, lithostratigraphic correlations with limited age dates, have established that the age of the sediments of Cuddapah Supergroup and Kurnool Group ranges from Lower Proterozoic to Upper Proterozoic, over a span of nearly 1000 Ma (Ramakrishnan & Vaidhyanathan, 2008). The sediments of Cuddapah Supergroup are laid in four well distinguishable sub-basins (**Fig.1.2**). The Papaghni and Chitravati Groups of sediments are laid in The Papaghni sub-basin, the Nallamalai Group in Nallamalai sub-basin and the sediments of Srisailam Group in Srisailam sub-basin. The sediments of Kurnool Group are laid in Kurnool and Palnad sub-basins of the Cuddapah basin. The basement for the Cuddapah basin is marked by giant mafic dyke swarms especially in the northwestern and southwestern margins. The dykes outside the Cuddapah Basin do not cut across the sediments; many of the faults in the basement seem to continue into the sediments. E-W dykes are predominant in the southern part. In the southeast, dominant NW-SE and NE-SW oriented dykes appear along with some E-W trending dykes (Radhakrishnan et al., 2007). In the western part, the dominant trend is WNW-ESE to NW-SE. In the northern part, the dominant trend is WNW-ESE to N-S with minor emplacements oriented in NE-SW direction (Murthy et al., 1987). The basin is 440 km in length along its eastern margin and 145 km across its widest part (Vaidhyanathan., 2008; Valdia, 2010). Kalia et al., (1979) discussed the deep crustal, low-angle thrust along the eastern concave margin of Cuddapah Basin, along which the metamorphics and gneisses of the Eastern Ghats Granulite have been thrust over the sediments (Ramakrishnan & Vaidhyanathan, 2008).

## 1.6. Mineral resources of Cuddapah Basin

Cuddapah Basin is a store house of many mineral deposits, starting from the oldest Papahgani Group to youngest Kurnool Group of sediments; the basin is known for its many metallic and non metallic mineral potential (Nagaraja Rao et al., 1987 and Ramam et al., 1997). Brief details of the mineral potential of Cuddapah basin is given below.

**Asbestos:** Major occurrences of asbestos is confined to the Pulivendla belt in southern margin of Cuddapah Basin and are confined to narrow zones of serpentinization that are developed along the lower and upper contact of dolerite sill with the Vempalle dolomite.

**Baryte:** Cuddapah basin contains 90% of the known barite reserves of the country and 25% of world reserves. Two types of baryte have been reported such as vein and bedded type. Vein types are hydrothermal origin is found in Vempalle belt. They contain 95 % BaSO<sub>4</sub>. Bedded baryte is occurring in Mangampeta in the form of two lensoid bodies. Volcanogeneic origin is attributed to the Mangampeta barite.

**Base metal:** Base metal occurrence in the Cuddapah Basin is located in three formations Vempalle , Tadpatri and Cumbum. Occurrences are concentrated in a few well defined belts. Agnigudala belt, Zangamrajpalle-Varikunta belt, Rayavaram-Chinnavanipalle belt, Gani-Kalva belt, Pulivendla belt. These belts are known for the occurrence of lead-zinc and copper mineralizations in the form of veins, veinlets, pockets and thin sheets.

**Building stone:** Flaggy horizons of Narji limestone are extensively used as flooring stones and popularly known as 'Cuddapah Slabs'. Chips of dolomite and serpentinized

dolomite of Vempelle dolomite are widely used in mosaic floor tiles. Good quality slates are being mined from Cumbum Formation of Prakasam district.

**Diamond:** Diamond has been reported from two geological environments in the Cuddapah Basin. They are conglomerates of Banganapalle age and detrital Krishna gravels of Quaternary age. Basal conglomerate of Banganapalle is potential source of diamonds. Gravels of Krishna river includes the majority of the ancient diamond workings. The world's famous Koh-i-noor, Regent or Pitt were discovered from these gravels. These gravels are also famous for other gem minerals such as garnet, zircon, topaz and kyanite.

**Limestone:** Large cement grade limestone resources occur in Narji Limestone of Kurnool and Palnad sub-basins. Chemically, CaO content in these limestone varies between 50 to 54%. A small reserve of chemical grade limestone is found within Vempelle Formation in Dronachalam area in Kurnool district. The chemical grade limestone is suitable for manufacture of soda ash/calcium carbide occurs as detached lensoid bodies within Vempelle dolomite. Their formation is attributed to dedolomitization of dolomite limestone. Chemically, they analyse 49 to 54% CaO with low magnesia and silica.

**Uranium:** Cuddapah Basin is also known to host various type of uranium mineralization from the oldest to youngest sequences. Two major types of uranium mineralisations occur in Cuddapah basin. They are the stratabound type and the unconformity related type. The Vempelle Formation of Papaghni Group consisting of dolomitic, stromatolitic impure limestone hosts the syn-sedimentary strata bound uranium deposits at Tummalapalle – Rachakuntalapalle sector in the southwestern

sector of the basin. Uranium occurs in two bands over 7 km length with 2.20 m average thickness. The ore body shows homogenous, uniform distribution with uranium minerals such as pitchblende and coffinite with molybdenite as byproduct. Ore tonnage is 29 million tones with average grade of 0.050%.U<sub>3</sub>O<sub>8</sub>. Uranium occurrences have also been reported from the Chitravati Group in the form of strata bound hosted by quartzite (Nagabhushana, 1997).

In the northwestern margins of Cuddapah basin prior to 1990, ground radiometric surveys by AMD, was mainly focused in the basement granites for possible vein type uranium mineralization and later the focus was shifted for unconformity related uranium mineralization between the basement and overlying Srisailam Formation. This resulted in locating a number of uranium anomalies both in the basement granites and quartzites of Srisailam Formation. The first breakthrough was achieved by locating uranium anomalies along the unconformity between the basement granite (Mehboobnagar granite) and the overlying Srisailam sediments in the Lambapur outlier which is one of the few dissected outliers of Srisailam Formation in the northern margin of Srisailam sub-basin (Umamaheshwar et al., 2008). Further detailed exploration in Lambapur and adjacent outliers has established three uranium deposits namely Lambapur, Peddagattu and Chitrial.

In these deposits uranium ore body occurs along the unconformity contact between the early Proterozoic, fertile basement granite and Srisailam-arenaceous cover sediments. The rich pods are confined to the fracture zones and weathered basic rocks occurring in the basement granite (Mukundhan et al., 2009). Uraninite and pitchblende are the main uranium minerals along with minor proportion of galena (Umamaheswar et

al., 2008). The geological setting of Srisailam sediments over the Cumbum shale/phyllite is similar to the classical unconformity setting of Athabasca Basin and is the future target (Sinha et al., 1995) and forms future target areas for exploration.

Owing to the similar lithostructural characteristics of the Lambapur-Chitrial area, exploration was carried out in the adjacent Palnad sub-basin. This resulted in locating a number of uranium anomalies and establishing the Koppunuru uranium deposit close to the unconformity between the basement granite and sediments of Kurnool Group wherein currently, the potential anomalous zones are being actively explored for proving subsurface mineralization (Umamaheshwar et al., 2008).

The Kurnool-Palnad sub-basin in the northern part of Cuddapha Basin is also hosting the uranium mineralization, wherein the mineralization is hosted by granite as well as Banganapalle quartzite. In the Palnad sub-basin, at Koppunuru-Dwarakapuri, the uranium ore body occurs both in the Banganapalle quartzite of the Kurnool Group and along the unconformity between the basement granite and the Banganapalle quartzite. Uranium minerals in the Koppunuru deposit are pitchblende, coffinite, phosphuranylite (Ca-U-Phosphate) and metazeunerite (Cu-U-arsenite) associated with sulphides of copper, lead and iron. Uranium association with carbonaceous matter and intergranular sericite clay matrix is common in quartzite above the unconformity (Umamaheswar et al., 2008).

### **1.7. Geology of Srisailam Sub-basin**

The Srisailam Formation, the youngest unit of the Cuddapah Supergroup, developed in the Srisailam sub-basin forms a very prominent plateau with an extent of around 3000 sq km in the northern part of the Cuddapah basin. It is mainly an

arenaceous unit with subordinate shale intercalations and generally shows sub-horizontal dips due southeast, and attains a maximum thickness of 300m. Along the northern margins, the sediments of Srisailam Formation directly overlie the basement rocks consisting of Achaean gneisses and schist belts (Peddavoora Schist belt) and granites, basic dykes, pegmatites and quartz veins of paleo Proterozoic ( $2268\pm 32$  Ma to  $2482\pm 70$  Ma) age (Pande, B.K. et al., 1988). Whereas, along the southeastern margin the Srisailam Formation is underlain by Nallamalai Group with an angular unconformity. Along its northern fringes this sub-basin has a highly dissected topography resulting in the formation of a number of flat topped outliers of Srisailam Formation within the basement rising up to 100 to 150 m above the ground level. The Lambapur, Peddagattu and Chitrial uranium deposits are located in three such separate outliers detached from the main Srisailam sub-basin (**Fig.1.3**).

Lithostructural studies for the evaluation of fracture system in parts of Srisailam-Palnad sub-basins based on high resolution satellite data, indicated three generation of dykes with various trends such as N-S or NNE-SSW and E-W or ENE-WSW trending dykes along with minor NE-SW or NW-SE (**Fig.1.4**). Evaluation of fracture system indicated NNE-SSW and ENE-WSW trending major faults (Abhinav Kumar, 2007).

The Srisailam Formation is mainly an arenaceous unit with glauconite-bearing ferruginous quartzite alternating with minor shale units and attains maximum thickness of over 300 m. It has sub-horizontal dip and lies with an angular unconformity over Nallamalai Group. Based on mineralogy such as glauconite, in Srisailam sediments, the environment of deposition inferred as tidal flat to shallow marine.

The Srisailam sub-basin is bounded by NE-SW trending lineaments gives rise to the elliptical shape with NE-SW axis. The NE-SW lineament defining the northeastern part of the Nallamalai sub-basin limits the southeastern boundary of the Srisailam sub-basin. Primary sedimentary structures such as stratification, ripple marks, cross-stratification (both linear and trough), laminations and syn-sedimentary deformation structures are present within the thin layer of grey shale just above the unconformity.

### **1.8. Geology of the Study Area:**

The surveyed area forms a part of the main Srisailam sub-basin of Cuddapah basin. The area lies to the southwest of Chitrial outlier. The area comprises basement consisting of various types of granites with mafic and quartz intrusions unconformably overlain by the unmetamorphosed sediments of Srisailam Formation. In the basement, of all the types, the coarse grained biotite granites dominate others and cover vast areas. The coarse grained biotite granites are followed by pink granites and highly chloritised granites (occurring especially surrounding Amrabad area). Megascopic examinations of the granites indicate quartz, K-feldspar, plagioclase, biotite as the major minerals with minor hornblende. The basement consists of enclaves of metasedimentary rocks (Chavan,S.J., 2011).

The metasedimentary enclaves in the basement comprises various types of amphibolites, metaquartzites (showing sedimentary structures), and gneisses showing ptygmatic folding. Such features indicate the possible sedimentary origin of the granites. Granites are mostly grey in color but attain pink color in the surroundings of the ferruginised, fractured basic dykes. Basic dykes of at least two generations were

observed in the surveyed area varying in thickness from 2 to 10m, mostly trending along N-S and NW-SE directions. Rose diagrams indicate a dominant N-S trend followed by NW – SE directions of quartz veins and basic dykes.

The overlying sediments of Srisailam Formation are unmetamorphosed and mainly comprised of quartzites with intercalations of shale. The sedimentary sequence starts with a band of shale–siltstone-sandstone alternations overlain by a thick sequence of massive quartz arenites. Thickness of the sediments is around 60 m. The general stratigraphic succession of the area is **table 1.2**.

**Table 1.2: geological succession of the study area**

Age	Formation	Lithology
Middle Proterozoic	Srisailam Formation	White, massive quartzite
		Quartzite-shale intercalation
		Pebbly/ gritty quartzite
~~~~~Unconformity~~~~~		
Lower Proterozoic	Basement Granite	Quartz / Pegmatitic veins Basement Granite & intrusive basic dykes

The sediments generally show very shallow dips of  $<10^{\circ}$  towards southeast. However, reversal in dip direction with steep dip are observed close to the two major faults of the area, namely the Nallavagu and Nekkantivagu faults (**Fig.1.5a**) A geological section along line A-B is shown in **figure 1.5b**.

## Structure

The surveyed area exposes the unconformity between the basement granites and overlying sediments of Srisailam Formation along high rise escarpment faces developed due to basin margin faulting with a general E-W trend. The unconformity between the basement and the overlying sediments is sharp. Because of heavy cover of talus at most of the places the unconformity between the basement and cover sediments is not exposed at most of the places. Besides the basement comprises a number of basic dykes which mostly trend along N-S and NW-SE directions. It is observed that all the major structural features in the surveyed area trends along N-S and NW-SE directions. The fracture trend rose diagram of the basement indicate a dominant N- S trend followed by NNE-SSW trend.

Besides the basement granites are traversed by chlorite veins of different lengths and widths. This conspicuous feature is particularly widespread in the granites surrounding Amrabad village. In general the chlorite veins show an anatomizing pattern. However the rose diagrams of the chlorite vein direction also show a dominant N-S direction followed by minor E–W direction (**Fig.1.6**). Some of these chlorite veins also show very high order radioactivity.

All these features of the area (basic dykes, Chlorite veins, quartz veins and fracture trends) indicate the predominance of the N-S structural grain in the surveyed area followed by its component shear fracturing along NE-SW and NW-SE directions. Two regional scale basin marginal faults (namely the Nallavagu and Nekkantivagu -as mentioned in the literature, demarcated by aerial photo interpretation) occur cross

cutting the sediments. Both these faults were observed in ground and trend along NNW-SSE direction.

### **1.9. Objective and Scope of the Work**

The study area lies in southwest of the well known uranium deposits at Lambapur, Peddagattu and Chitrial, and also forms a part of the main Srisailam sub-basin (**Fig.1.3**). Since in these deposits the uranium mineralization is controlled by basement fractures and associated alterations such as ferruginization and chloritization near the unconformity zone, understanding the basement fracture system is essential for further detailed exploration in the area. Very Low Frequency - EM method (VLF-EM) can delineate conductive zones in the subsurface, their orientation and depth persistence. Demarcation of such conductive zones will be useful to target the areas for future exploration, besides the same analogy may also be extended in the deeper parts of basin. The scope of the work includes

- Carry out VLF-EM geophysical surveys in parts of the main Srisailam sub basin, owing to the continuity of the similar lithostructural setup of Chitrial - Lambapur - Peddagattu uranium deposits,
- Understand the electromagnetic signatures of the basement fractures since, ground geophysical surveys have not been carried out in main Srisailam sub basin till date,
- Delineation of EM conductors which may host uranium mineralisation,
- Processing and filtering of the VLF-EM data and qualitative and quantitative interpretation of the data,

- 2D-Inversion of the acquired VLF-EM data to know the nature and geometry of the causative bodies,
- Integration of the geophysical data with the geology of the area,
- By combining above all, the main objective is to narrow down target area for subsurface exploration.

## **CHAPTER - II**

### **METHODOLOGY**

#### **2.1. Geophysics in Mineral Exploration**

The science of geophysics applies the principles of physics to the study of the Earth. Geophysical investigations of the interior of the Earth involve taking measurements at or near the Earth's surface that are influenced by the internal distribution of physical properties. Analysis of these measurements can reveal how the physical properties of the earth's interior vary vertically and laterally. By working at different scales, geophysical methods may be applied to a wide range of investigations from studies of the entire earth (Kearey, 2002) to the exploration of a localized region of the upper crust for engineering or other purposes. Geophysical explorations provide a relatively rapid and cost-effective means of deriving information on subsurface geology. In the exploration for subsurface resources the methods are capable of detecting and delineating local features of potential interest and can optimize exploration programmes by maximizing the rate of ground coverage and minimizing the drilling requirement.

#### **Geophysical survey methods**

Geophysical surveying methods can be broadly classified into those that make use of natural fields of the earth and those that require the input into the ground of artificially generated energy. The natural field methods utilize the gravitational, magnetic, electrical and electromagnetic fields of the earth, searching for local perturbations in these naturally occurring fields that may be caused by concealed geological features of economic or other interest. Artificial source methods involve the generation of local electrical or electromagnetic fields that may be used analogously to natural fields, or, in

the most important single group of geophysical surveying methods, the generation of seismic waves whose propagation velocities and transmission paths through the subsurface are mapped to provide information on the distribution of geological boundaries at depth. Generally, natural field methods can provide information on Earth properties to significantly greater depths and are logistically simpler to carry out than artificial source methods.

A wide range of geophysical surveying methods exists, for each of which there is an 'operative' physical property to which the method is sensitive. The methods are listed in **Table 2.1**. The type of physical property to which a method responds clearly determines its range of applications. Other considerations also determine the type of methods employed in a geophysical exploration programme.

**Table.2.1: Geophysical methods and operative physical property**

<b>Method</b>	<b>Measured parameter</b>	<b>Operative physical property</b>
Seismic	Travel times of reflected/refracted seismic waves	Density and elastic moduli, which seismic waves determine the propagation velocity of seismic waves
Gravity	Spatial variations in the strength of the gravitational field of the Earth	Density
Magnetic	Spatial variations in the strength of the geomagnetic field	Magnetic susceptibility and remanence
Electrical		
Resistivity	Earth resistance	Electrical conductivity
Induced polarisation	Polarization voltages or frequency-dependent ground resistance	Electrical capacitance
Self potential	Electrical potentials	Electrical conductivity
Electromagnetic	Response to electromagnetic radiation	Electrical conductivity and inductance
Radar	Travel times of reflected radar pulses	Dielectric constant

## **2.2. Previous geophysical studies in Srisailam sub-basin**

**Airborne gamma ray spectrometric data:** Interpretation of Airborne gamma spectrometric data of Devarkonda block indicated an average of 5.6 ppm uranium, 36 ppm thorium and 2.98% potassium. Anomalous uranium zones are found to fall in Kasarajupalli which lies SE of Chitrial area (Abhinav kumar, 2007).

**Aeromagnetic studies:** Magnetic data interpretation indicated that the western limb of the Peddavuru schist belt in the Northern part of the basin is bounded by a NW-SE trending fault lineament. A series of WNW-ESE trending basement faults in the Srisailam plateau with progressing down throw towards SSW culminating in a wedge shaped down-faulted block bounded by the Atmakur and Gani-Kalava faults have been identified. ENE-WSW trending Gani-Kalava fault and its extension might have oscillated facilitating the deposition of variable quantum of sedimentation in the Srisailam-Palnad sub-basins. Modelling of aeromagnetic data (Babu Rao, et al., 1987) has indicated a source depth of 400 m located on the Narji limestone whose maximum thickness ranges from 300-350 m, underlain by 70 m of Banganapalli quartzite.

**Gravity studies:** Gravity studies over the adjoining granite-greenstone terrain in between Closepet granite in the west and the Cuddapah Basin in the East indicated alternating gravity highs and lows corresponding to the synformal greenstones and upwelled granitoids respectively. These belts trend in a NW-SE to N-S direction, indicating the eastward convexity. The Srisailam quartzite is indicated as a gravity low forming the Srisailam plateau, bounded by the Kurnool and Macherla anomalies. (Kesavamani et al., 1996). Prominent gravity highs in the northern part are the

Mahaboobnagar-Achampet high and Macherla high. These two zones are collinear and inferred to form the extensions of the known Gadwal, Peddavuru and Medavaram greenstone belt.

**Ground magnetic and Transient Electro-Magnetic (TEM) studies:** Ground magnetic and TEM surveys have been conducted by AMD in Peddgattu outlier, which has the geological setting similar to that of the study area. Magnetic survey revealed the presence of E-W block faulting, concealed basic dyke and NW-SE trending faults. The depth estimation using inverse slope method indicated a 80 m depth for a concealed basic dyke and that has been confirmed by drilling. Further interpretations reported are E-W trending dyke and NW-SE trending major fault system. Controls of uranium mineralization for the Peddagattu uranium deposits are identified as NW-SE trending fault in sub-block III and E-W trending dyke in sub-block II. The TEM studies along five profiles indicated a low order conductor along the NW-SE trending fault and its conductivity was attributed to fractured/pulverized quartzite saturated with ground water (Ramakrishna et al., 1997).

**Gravity and VLF – EM studies in Chitrial Main block:** An area of 5 sq km was covered by ground magnetic and VLF – EM surveys in Chitrial main block, where uranium mineralization is hosted by the basement granites along the unconformity between the basement and the overlying sediments of Srisailam Formation. These surveys have established the control of conducting fracture zones which are showing magnetic lows as the loci of uranium mineralization in the area (Rajaraman, 2010 and Chavan, 2010).

### **2.3. Very Low Frequency Electromagnetic Technique**

The very low frequency electromagnetic (VLF-EM) method is well established for rapid geological mapping and detection of buried conductive targets. The method makes use of the signal radiation from military navigation radio transmitters as a source. There are about 42 global ground military communication transmitters (ABEM) operating in VLF frequency range of 15-30 kHz (**Table 2.2**). These stations, located around the world, generate signals which are effectively used for variety of applications including navigation and communication, groundwater detection or contamination, soil engineering, cultural detection, ionospheric, meteorological, archeological and VLF band transmission studies, mineral exploration, mapping of fault zones etc. (Sundararajan et al., 2007). VLF-EM surveys which make use of single frequency signals (15 to 30 kHz) from remote VLF transmitters are rapid and useful for reconnaissance geological mapping, where the sedimentary cover is thin. The VLF method has proved to be an effective exploration tool for massive sulphides, graphites, carbonaceous shales, sheared contacts and fracture zones. Therefore, during the last few decades, it has been employed worldwide to identify conducting features in mineral exploration, geological, engineering and environmental problems. (Ramesh Babu et al., 2007, 2008 and Sundararajan et al., 2007). Although the VLF-EM method has been widely used for the last over three decades to map shallow subsurface structural features of varying interests, the interpretation of the observed VLF-EM anomalies is mainly carried out using anomaly curves and nomograms (Kaikkonen, 1979; Saydam, 1981). Fraser and Hjelt filtering and subsequent contouring of the observed responses are the most common practice to derive qualitative information about the subsurface (Fraser, 1969; Karous and Hjelt; 1983). Multidimensional numerical modeling and

inversion are needed to determine quantitatively geometrical and physical subsurface parameters from VLF anomalies.

## **Theory**

The theory of the VLF-EM technique is well described in literature (Paterson and Ronka, 1971). In a far field, above uniform earth, the ground wave of the vertically polarized VLF radio wave has three field components namely radial horizontal electric field ( $E_x$ ), vertical electric field ( $E_z$ ) and a tangential magnetic field ( $H_y$ ). When these three fields encounter electrically conducting ore bodies in the subsurface, eddy currents are induced causing the secondary fields to radiate outward from these conductors. Thus, the measurement of the total field (primary + secondary) at the surface of the earth can help in detecting conductive structures located in the study area. Though this range is very low for radio transmission, it is higher than that used in standard low frequency electromagnetic geophysical methods (1-3 kHz). The sources for the VLF measurement are fixed transmitters used for communication that represent vertical electric dipoles, situated at several locations (**Table 2.2**) around the world (**Fig. 2.1**). The radio signals are transmitted either as ground waves or waves guided by the solid earth and the conducting ionosphere. At sites far from the source, the primary electromagnetic field resembles a vertical plane wave with the electrical field nearly vertical, and the magnetic field horizontal. According to the electromagnetic theory, conductive bodies beneath the surface become the source of a secondary field (with vertical and horizontal components), which is shifted in phase relatively to the primary one. The major advantage of VLF method is that a personal transmitter is not needed to produce the primary EM wave, which saves time and reduces exploration costs.

**Transmitter:** VLF transmitters are complex structures with 200 to 300m high towers. One or more of these towers can carry the antenna current. The VLF transmitter stations radiate electromagnetic waves in the 3 to 30 kHz. The waves are generated by currents traveling up and down the vertical tower. The current on the antenna begins to flow upward, reaches maximum, then dies away to zero. Then it begins to flow down the antenna, reaches maximum and, as before, dies away to zero. This process is continued at the frequency of the station, that is, the current oscillates. Magnetic fields form concentric circles about this vertical line of current. The circles are centered on the antenna and parallel to the ground. An electric field is oriented vertically at right angle to the magnetic field. As the current oscillates so do these associated magnetic and electric fields. The fields build, move outward, and are pinched off as the current returns to zero. All over the world there are many VLF transmitters (**Fig. 2.1**) and are listed in **table 2.2**.

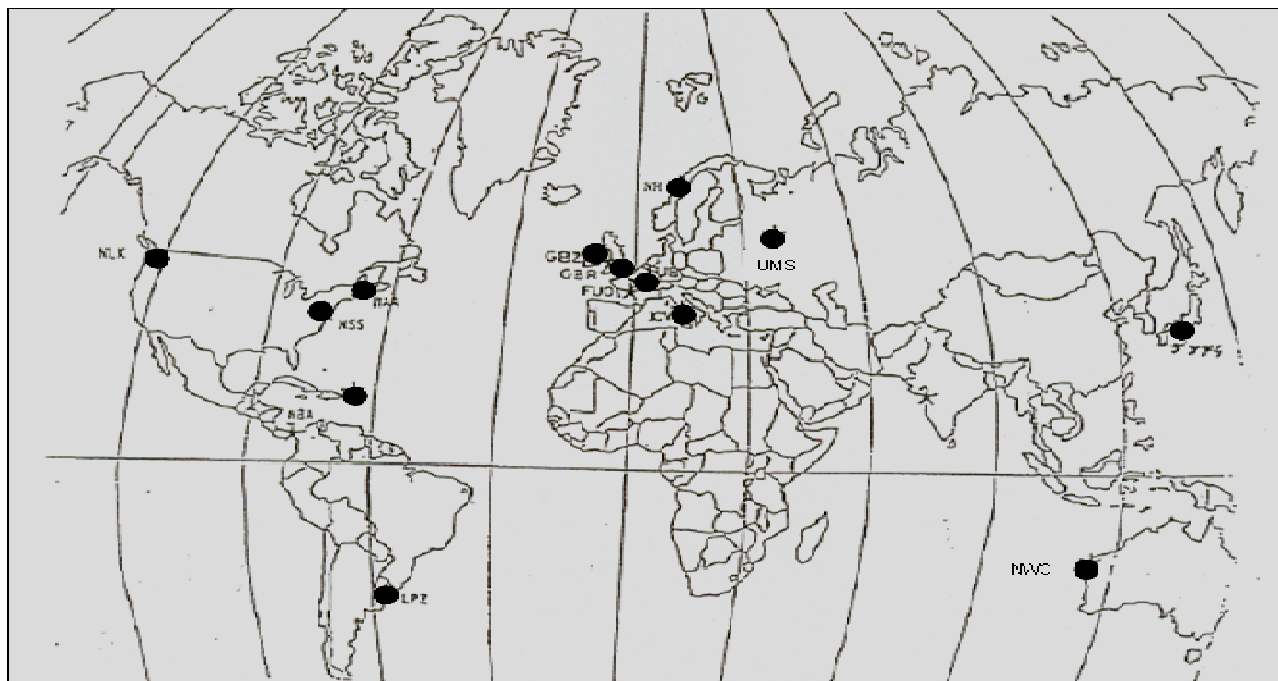


**Fig.2.1: Map showing of main VLF transmitters**

**Table 2.2: Global VLF transmitters and their frequency**

<b>SIGN</b>	<b>FREQUENCY kHz</b>	<b>LOCATION</b>	<b>COUNTRY</b>	<b>POWER (KW)</b>
FUO	18.3	Cateauroux	France	1000
VTI	15.1	Bombay	India	
VTX	15.2, 17.0,16.3 & 19.2	Tirunelveli	India	
GBR	16.0	Rugby	Grande Bretagne	750
FUB	16.8	Saite Assise	France	250
<b>UMS</b>	<b>17.1</b>	<b>Moscow</b>	<b>USSR</b>	<b>1000</b>
JJF4	22.2	Ebino	Japan	
HN	17.6	Hegaland	Norvege	
NAA	24.0	Cutler	USA	1000
NSS	21.4	Annapolis	USA	100
GBZ	19.6	Dunfries	Grande Bretagne	
ICV	20.2	Rome Tavolara	Italy	500
NWC	22.3	NW Cape	Australia	1000
NWM	23.4	Lualualei	Hawaii	300
LPZ	23.6	Buenos Aires	Argentina	
NBA	24.0	Balboz	Panama	



The closed loops of current which circulate in a confined, conductive body are vortex currents. Consider a conductor placed in a resistive host. The VLF field causes charges to form on the surface of the body, which produce a secondary electric field (**Fig. 2.2**). The magnetic field cutting across the conductor has an electric field which circulates above it and that drives closed loops of current within the body. This current circulates within the conductor. These currents produce a secondary magnetic field which adds to the primary magnetic field. Disturbances caused by this secondary field in the primary field are the anomalies sought. The secondary magnetic field associated with the vortex currents is very diagnostic regarding the geometry and electrical properties of the conductive body. The electric fields associated with vortex current flow only arise from variable secondary magnetic fields; no charge accumulation occurs. Vortex currents produce secondary magnetic fields, but no secondary electric fields.

Galvanic currents flow on a regional scale about the VLF transmitter and that produces secondary electric fields by both charge build up and time variable magnetic fields. It produces many spurious responses due to sensitivity to small conductivity contrast and anomalous responses may also be produced more resistive features. Galvanic currents produce both secondary magnetic and electric fields. The electric fields are mainly produced solely by charge accumulation not by variable secondary magnetic field.

**Receiver:**

The receiver used for the VLF data collection was provided by the University Centre for Earth and Space Sciences, University of Hyderabad. The instrument is known as T-VLF and is manufactured by IRIS Instruments, France. It is a portable microprocessor based instrument weighing less than 6kg and it can be back-mounted by the user. The

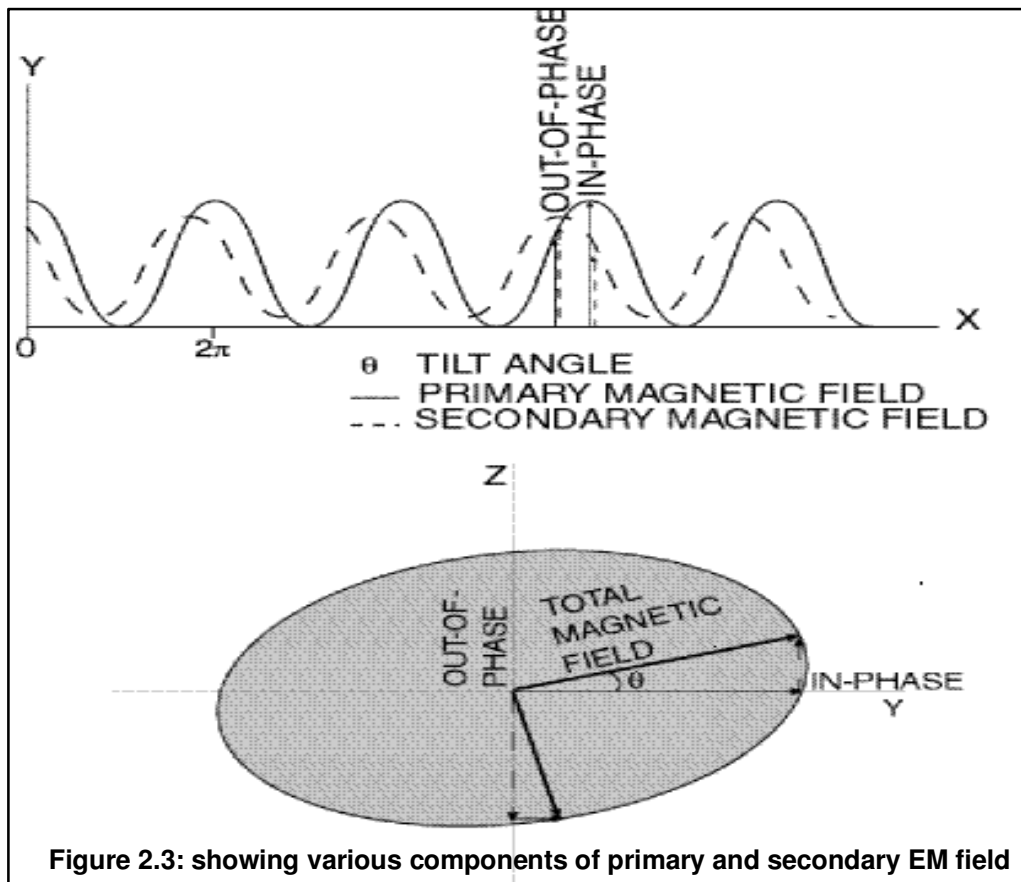
specialty of this instrument is that no orientation of the operator with respect to the direction of the transmitter is required. It has three low noise magnetic sensors that measure the components of VLF field. Tilt or horizontality of the sensor unit is neither required since two inclinometers correct for tilted positions. Low noise magnetic sensors and digital filtering permit to carry out good quality measurements. Besides, a quality factor is given at each measurement to control the quality of data. The receiver can be operated in two mode such as tilt angle mode and resistivity mode. **Table 2.3** gives the various type of commercially available receivers.

**Table 2.3: Various types of VLF receivers**

Receiver model	Manufacturer
VLF-3/4	Scintrex
EM-16R	Wadi
T-VLF	IRIS Instruments, France
EDA-OMNI	Scintrex
DHVLF-EM	Scintrex

### **VLF parameters measured**

Whatever the source (vortex and or galvanic) of the secondary magnetic field, the secondary magnetic field will be oriented in unique direction and is represented by a vector that can point in any direction. The primary magnetic field is totally horizontal and oriented right angle to the line connecting the observation point to the transmitter. These two vectors add up and resulting vector traces out an ellipse with time, which oscillates at VLF frequency (**Fig. 2.3**). The orientation of the ellipse is arbitrary and is greatly extended along the direction of primary field. The resulting ellipse is known as



polarization ellipse. The total field is measured in VLF survey because there is no

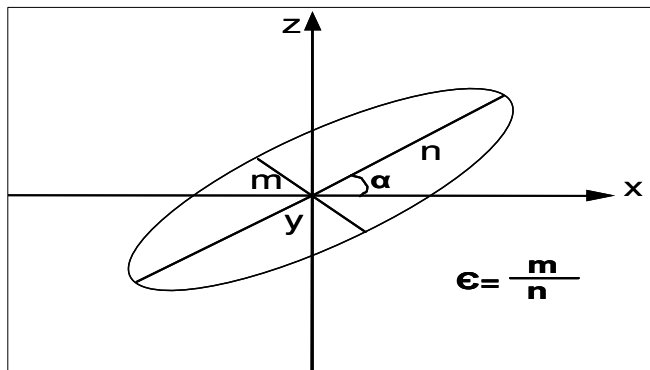


**Figure 2.4: Ellipse showing tilt & ellipticity**

convenient means to separate the primary and secondary fields. Two parameters measured by VLF receivers are; the tilt ( $\alpha$ ) of the major axis of the polarization ellipse, and ratio of the minor to major axis referred to as the Ellipticity ( $\epsilon$ ) (**Fig. 2.4**). Wright

(1988) has demonstrated that the tilt is approximately equal to the inphase part of vertical component ( $H_{ZR}$ ) and the Ellipticity approximately equals to the quadrature or out of phase part of the vertical component ( $H_{ZI}$ ).

The VLF waves travel over the earth's surface and directly downward regardless of the angle of incidence, with both the fields parallel to the surface. The magnetic field is perpendicular to the line connecting the observation point to the transmitter and the electric field is parallel to the line. Both the fields diminish as they travel into the earth. The electric field leads ahead of the magnetic field by  $\pi/4$  radians or 45 degrees. Both the fields are continually phase shifted by the same amount as they travel into the earth. Here comes the concept of skin depth ( $\delta$ ). This is the depth at which the amplitude of the wave drops to 0.368 or approximately 1/3 of its initial value. Likewise, both the magnetic and electric fields are phase shifted by  $1/\delta$  radians relative to their initial timing at the earth's surface. A ratio can be formed between the magnetic and electric fields. Using this ratio, the apparent resistivity can be calculated using the following equation popularly known as Cagniard's equation.

$$\rho_a = \frac{1}{\omega \mu_0} \left| \frac{E_y}{H_x} \right|^2$$

$$\varphi_a = \pi/4 \quad \text{or } 45^\circ$$

Where  $\rho_a$ =apparent resistivity;  $\omega=2\pi f$ ;  $f$ =frequency;  $\mu_0=4\pi \times 10^{-7}$ ;  $\varphi_a$ = apparent phase angle. The Cagniard's equation yields the true resistivity if the ground is homogenous and isotropic and the phase angle ( $\varphi$ ) = 45°. However, if the ground is heterogenous, the resistivity is termed as apparent resistivity and for the layered earth  $\varphi > / < 45^\circ$  depending on the resistivity of the upper layer.

### Depth of Investigation:

Both the magnetic and electric fields diminish in amplitude as they penetrate the earth, this effect quantified as skin depth parameter ( $\delta$ ). The skin depth is the depth at which the wave falls to approximately one third of its initial amplitude. For all practical

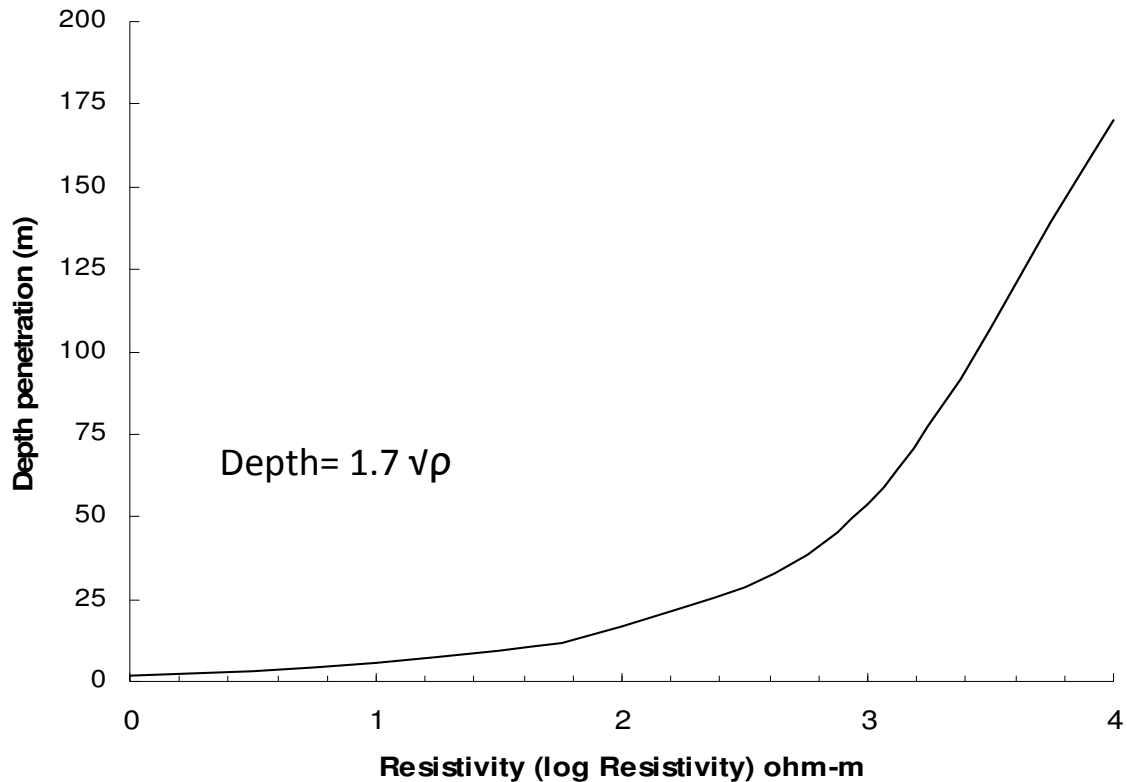


Figure 2.5: Plot of depth penetration of VLF waves (m) verses resistivity (ohm-m)

purposes, the wave can be considered as having finished at this point. However the wave must penetrate to the target and return to the surface to be detected. Thus, if a target is half a skin depth beneath the surface, the received signal is that of wave having traveled full skin depth. Maximum depth penetration is half a skin depth of the medium surrounding and or overlying the target. **Fig. 2.5** gives the details of determining the depth penetration for a given conductivity/resistivity of the host rock as suggested by Wright (1988).

## **Application of VLF technique**

Originally, the VLF technique has been developed for communication purpose. Transmissions in the VLF band were first experienced in 1910-1912. The method enjoyed wide application for long range communications. After the World War II, the applications have dominated particularly for submarine communications. However, the signals generated by the VLF stations can be exploited for a variety of applications. Soil engineering studies, cultural detection, ionospheric studies, meteorological studies, archeological studies and VLF band transmission studies. Paal (1965) has discussed the prospecting of ore bodies based on VLF radio signals. VLF method has been extensively used for identifying the buried faults, conductivity changes in the sedimentary cover (Oskooi and Pedersen, 2005) and identifying the potentials ground water bearing fracture zones (Sundararajan et al., 2007).

VLF is an effective reconnaissance geophysical tool for mapping geoelectric features. It may be used wherever an electrical conductivity contrast is present between geological units. This may include mapping of faults, groundwater investigations, overburden mapping, mineral exploration etc.

Ground and airborne VLF electromagnetic surveys have been used successfully to delineate electrical conductors and also to map the geological contacts (Wright, 1988). Mineral exploration is one of the main fields of application. VLF surveys in general can be conducted in various platforms such as airborne, ground and borehole. Air borne resistivity technique gives the spatial variation of conductivity and related structural features on regional scale (Mathews, et al., 1997). The VLF technique in association

and resistivity techniques have been extensively applied crystallines of south India (Sundararajan et al., 2007). Application of VLF technique has also been tested in the borehole logging, recently (Mwenifumbo et al., 1997). In Athabasca basin, uranium is found to be associated with the graphite conductors. Subsurface VLF conductors have been reported by Markandeylu et al., (2001) in Shillong Basin, wherein the unconformity type uranium mineralization is expected. The ground VLF surveys have been successfully utilized for uranium exploration in Raigarh district, M.P. (Ramesh Babu et al., 2008).

## **2.4. Data Acquisition**

### **Orientation Survey**

Before starting the geophysical surveys orientation surveys and reconnaissance radiometric surveys in the area resulted in locating a number of radioactive anomalies both in the basement and also along the unconformity between the basement granites and the overlying sediments of Srisailam Formation. The aim to carry out geophysical surveys in this outlier is to trace the subsurface extension of the fractures and basic dykes hosting these anomalies, beneath the sedimentary cover of Srisailam Formation. An area of around 300 sq km was covered by rapid reconnaissance geologic and radiometric surveys. The radiometric surveys resulted in locating the following important radioactive anomalies in parts of Amrabad outlier. The details of these anomalies are given below (Mukundhan and Krishnakant, 2011).

**Bamanpalle:** Uranium mineralisation was recorded in fractured ferruginised basic dyke, within granites, approximately 500m from the unconformity contact between the basement granites and the cover sediments. The basic dyke trends along N-S

direction. Intense fracturing and ferrugenisation renders the radioactive rock brownish colour. The fracture zone extends for 10m x 1m with variable radioactivity of 2-10 xbgc with very high radioactive spots of 30xbgc. Intense ferrugenisation in the basic dyke and its surroundings, has rendered the granites in the surrounding a pinkish color. Samples have assayed upto 0.44%  $U_3O_8$ .

**Kuppagattu:** uranium mineralisation was recorded along the unconformity between the basement granites and cover sediments at Kuppagattu hillock. The granites are highly weathered and ferrugenised which are overlain by shale/quartzite intercalation of Srisailam Formation. Radioactivity is spotty in nature and distributed over a patch of about 50m length. Samples have assayed up to 0.046 %  $U_3O_8$  .

During the orientation surveys, structural data were collected both in the basement and in the sediments. It was observed that the all the linear features such as lineaments, basic dykes and fractures in the basement have a major N-S trend followed by NE-SW and NW-SE trends (**Fig. 1.6**). An area of 10 sq km was marked for geophysical surveys by orientation surveys.

### **Survey Layout**

An area of 10 sq km has been covered by VLF EM survey by using the IRIS make T-VLF receiver. Since the expected basement geological features such as fractures, basic dykes and quartz veins the transmitter lying exactly in the N-S or NW-SE direction was searched, for maximum conductor coupling. For this work, the transmitter UMS Moscow, Russia, transmitter with frequency 17.1 KHz was used. The transmitter has power of 1000 KW. The profile to profile distance was kept at 200m in N-S direction and

the station interval was kept at 25m in E-W direction. A total of 26 E-W, profile lines (N-00 to N-5000) were completed. The length of each profile lines varies from 1000 to 2000m with '0' station being the eastern extremity and '-2000' being the western extremity. For all references in this thesis the distance indicated is the distance from the eastern extremity for that particular profile. Using the frequency of 17.10 KHz, the VLF-EM parameters such as Tilt (%) and Ellipticity (%) were recorded at every station in all the 26 profiles. Total numbers of data points are 1924. The profiles were running over the cover rock-Srisailam sediments with an objective to infer the signal related to N-S geological features. The base map of the area with profile lines and stations is given in **(Fig 2.6)**.

## CHAPTER – III

### FILTERING AND TRANSFORMATION OF VLF-EM DATA

#### 3.1. Introduction

The IRIS make T- VLF receiver read directly the in-phase and quadrature components in digital form of vertical secondary magnetic field as percentage of the primary horizontal magnetic field, expressed as tilt% and ellipticity %. As mentioned it has been shown that the tilt is approximately equal to the In phase component and the ellipticity is approximately equal to the out of phase component of the vertical component (Wright,1988). Although in VLF, both the in-phase and quadrature components contain valuable diagnostic information, only few schemes exist for extracting this information and relating the observed anomalies to their causative sources.

VLF in-phase data often yield complex patterns which require considerable study for proper interpretation of the profiles. The most popular form of presenting VLF-EM 2D data over a given area is in the form of stacked profiles. The software Oasis-Montaj (GEOSOFT) was used for the purpose. Two filtering techniques popularly known as Fraser filter and Karous-Hjelt filter are commonly used for processing the VLF- EM data, by which the demarcation of the conductor is possible. A Matlab based graphical user interface software VLFPROS (Sundararajan et al., 2006) available at <http://www.iamg.org/CGEditor/index.htm> for processing and semi quantitative interpretation of VLF-EM data, was extensively used for the present study for filtering of the data and preparation of pseudo depth sections. In addition, Hilbert transform and amplitude of analytical signal analysis was also carried out for finding the depth

to the top of the conductor using empirical methods. The details of processing techniques adopted and the interpretation are discussed below.

### **3.2. Stacked profiles**

These are profiles along each survey line plotted on a 2D plane in the same relative position as the lines (Sundarajan et al., 2006). The VLF in-phase and out-of-phase data was plotted along each survey line on a map in the same relative position as the lines; shown in (**Fig 3.1**). Both tilt (%) and ellipticity (%) are plotted as stacked profiles. In such plot, use raw data is clumsy and the cross-overs are not that clear. Also the variations in the out of phase data plotted as stacked profiles are much smaller than the corresponding in-phase component. The anomalies in the out-of-phase data are so small, in the order of noise in the data, the identification of the cross overs is difficult. Hence for all the filtering processes and interpretation, the in-phase data was used. However the out of phase data was utilized in the qualitative interpretation for the quality of the conductors in the area and also in 2D inversion of VLF-EM data. In the stacked profiles, in order to overcome the high frequency noise the data was smoothed by using low pass filter and plotted as stacked profiles (**Fig 3.2**). The cross-overs from positive to negative of the tilt (%) from left to right in all the profiles lines were connected by solid lines to infer the trend of the conductor axis. Two prominent trends of conductors along NNW-SSE and NNE-SSE were demarcated, which correlates well with expected N-S trend in the area. Also 4-5 disconnected conductor axes could be marked on the stacked profile.

### **3.3. Fraser Filter**

In the absence of numerical modeling the Fraser and Karous-Hjelt filtering techniques have been proved to be effective because they provide simple scheme

for interpretation of the VLF data. The Fraser filter is a linear filtering technique analogous to passing the in-phase data through a band pass filter. Fraser filtering converts somewhat noisy, non-contourable in-phase components to less noisy, contourable data which ensures greatly the utility of VLF-EM survey. This filter involves running a four-point weighted average using the weights of +1, +1, -1, -1. The simple digital filter operator passes over the in-phase or tilt component (Fraser, 1969, 1981). The process involves mathematically convolving the shape of an expected anomaly along the various profiles. When this anomaly outline match with one in the measured data, a large positive number results. Noise in the data, reverse the cross-over, and long rolling responses are all suppressed. This yields either negative or low positive values. The filter phase shifts all frequencies by  $90^\circ$  and it turns cross over into peaks or troughs. This filter exhibits a band-pass response that is it greatly diminishes either noise or long rolling responses.

Traditionally, the filter's length is simply set to span four data points; however, the filter could be lengthened to span more number of points. Since the deeper anomalies will have longer wave lengths, the deeper anomalies can also be resolved by increasing the length of the filter to span any number of points. If results from several different filter lengths are to retain relative magnitudes, then the additive total from the filtering should be divided by the number of data points spanned. Very sharp responses indicate shallow source and conversely; the broader anomalies indicate progressively deeper sources. The contouring connects responses from line to line and curves to delineate the trend of conductive zones.

### 3.4. Karous-Hjelt (KH) Filter

This filter technique is a more generalized and rigorous form of the Fraser filter but is directly derived from the concept of magnetic fields associated with current flow in the earth. From the filtered VLF inphase component, one obtains the equivalent current densities at a constant depth which would cause a magnetic field. That is the filter attempts to determine the current distribution responsible for producing the measured magnetic field. Determination of the filter coefficients is a fairly a simple mathematical process. The optimized filter (Karous and Hjelt, 1983) is expressed as follows:

$$\Delta z/2\pi I_a (\Delta x/2) = 0.0102H_{.3} - 0.059H_{.2} + 0.561H_{.1} - 0.561H_1 + 0.059H_2 - 0.102H_3$$

Where  $\Delta z$  is assumed thickness of current sheet,  $\Delta x$  is distance between the data points and also the depth to the current sheet location of the calculated current density is beneath the centre point of the six data points. The values of H are the normalized vertical magnetic field anomaly at each of six data points.

### 3.5. Current density pseudo-section

Pseudo-section is the type of filtered output. According to Ogilvy and lee (1991), the pseudo sections of current density provides good visualization of targets such as mineralized veins, fractures, vertical stratigraphy that produce vertical and subvertical conductors. The pseudo sections are produced by processing a data profile with filters of various lengths. As the length of the filter increases, response from increasing depths is successively emphasized. When these outputs are arranged on a section, such that greater depths correspond to longer filters, then the section should approximately resemble the current pattern in the ground. The anomalies are positive areas with a widening down section. The larger amplitudes reflect increased conductivity and or size. Deeper responses are rounded and

shallower ones come to a peak. A trend of the response to either side down section indicates a dip in that direction.

### **3.6. Level contour plans (Depth slices):**

For exactly knowing the disposition of the conductors, interpreted through Fraser filter, Karous-Hjelt filter and the pseudo sections contour plans at various depths are prepared. The processed data for the preparation of such level contour plans are obtained from the pseudosections prepared from Fraser and KH filters.

In the present study, after initial plotting of the in-phase and out of-phase data, as stacked profiles and low pass filtering of the data, filtering techniques such as Fraser and KH filters were applied. Further, pseudo sections using both Fraser and KH filters were prepared. Besides, contour level plans (depth slices) were prepared using both Fraser and KH filters. These are detailed below.

### **3.7. Interpretation based on filtering**

As mentioned above the location of the conductor axis were marked by the cross over responses of the VLF low pass filtered in-phase data, plotted as stacked profiles. In this two prominent trends of conductors along NNW-SSE and NNE-SSE were demarcated, which correlates well with expected N-S trend in the area. After this Fraser filter and KH filter were applied to the data.

The Fraser filter output of the study area (**Fig 3.3**), which converts the cross over's into peaks and identifies the location of the conductors, indicates two prominent trends of the conductors, the major one along the NNE-SSW direction and the other along NW-SE direction. The conductors trending along NNE-SSW direction shows broader outlines, are offset broadly by the conductors of NW-SE direction (along N-2500). This indicates that the NNE-SSE direction in the area is older than the NW-SE direction. This fact is further evidenced by the fact that the NW-SE trend shows

good continuity in the entire study area, whereas the NNE-SSE trend is detached. Based on the outline of the positive contours of the Fraser filtered data, it is observed that the width of the conductors vary from 100 to 150m. The length of the NNE-SSW trending conductors vary from 400m to 1200m and the NW-SE trending conductors vary from approximately 400 to 600m.

The Karous-Hjelt (KH) filtered output of the study area (**Fig 3.4**), resembles more or less the Fraser filter output. The KH filter mainly indicates the distribution of current density in the sub surface, which produces the observed magnetic anomaly. The matching of the Fraser and KH filtered outputs, confirms the presence of the conductors. The directions and outlines of the conductors marked by the Fraser filter are also confirmed by the KH filtering of the data. Besides the trends outlined by these filtering methods also matches with the structural trends observed in the area depicted as rose diagrams (**Fig 1.6**). It is pertinent to mention that, the study area is covered by the sediments of Srisailam Formation and the offset of the NNE-SSE trend by the NW-SE trend is not observed on the surface. Such clear offset which is indicative of strike slip faults, has been demarcated by the present VLF-EM studies. Demarcation of these concealed strike slip faults in the area will be helpful in future, in planning of the boreholes in the area.

As a next step, in order to understand the depth persistence of the conductor, current density pseudo depth sections were prepared for all the 26 profiles using both Fraser filter and KH filters. Careful study of the pseudo section can throw light on the quality of the conductor as high current density values should reflect good conductors. The pseudo depth sections prepared using KH filters of the study area (**Fig 3.5**) confirms the interpretation made by the Fraser and KH filters that two trends of the conductors along NNE-SSW directions exist. And the strength of the

conductors increase with depth giving an inverted conical outline from the surface to bottom. According to Ogilvy and Lee (1991), such conical outlines of the conductors with the maximum current density in the centre indicate a linear vertical body such as a dyke or fracture zone, with limited width extent. The direction of the greater slope of the contours along one direction indicates the dip of the body. However in the present study the conducting bodies seem to be vertical, since slope of the contours are equal in both the directions, except a few. Also the conductors trending along both the NNE-SSE direction and NW-SE directions are of equal strengths indicated by their current densities.

The pseudosections prepared using Fraser filter corroborates well with the interpretation by the KH filter pseudosections (**Fig 3.6**). However in the Fraser filter pseudosections the inverted cones generated by the conductors are broader and are well defined. This feature is well marked in the case of NNE-SSW trending conductors indicating the quality of the conductors.

The depth slices for the study area for the conductors at 25, 50, 75 and 100m were prepared using both Fraser and KH filters. The depth slices prepared for the study area using Fraser filter indicates the continuity of the surface features even at depths of 100m and with depth the outlines of the conductors becomes broader (**Fig 3.7**). In the KH filter depth slices maximum current density occurs at depths between 50 and 75m (Fig 3.8), which is also the depth of the expected unconformity between the basement granites and the overlying sediments of Srisailam Formation.

A qualitative method to determine the conductivity of the host rock having fracture zone, was given by Wright (1988). The ratio of in-phase to quadrature can be used for this purpose. If the ratio is more than one, host rock possesses the better conductivity. The ratio in all the twenty six profiles of the study area is varying from -

65 to 54 indicating the presence of moderately conductive fracture zones located within highly resistive host rock (**Fig 3.9**).

### **3.8. Transformation of the VLF data and interpretation:**

Hilbert transform for the interpretation of VLF-EM data in analogy with the magnetic anomalies was applied successfully in the detection of uranium mineralized basement fractures of Raigarh area (Rameshbabu et al., 2007). The application of the Hilbert transform to the in-phase component shifts the phase of all spatial frequencies by 90°, that is, it turns crossovers into peaks or troughs. These peaks can be interpreted in terms of conductors. Thus, the Hilbert transform can be deciphered somewhat similarly to the Fraser filter, or, the Hilbert transform and the Fraser filter do a similar job to some extent. Here, the application of the Hilbert transform to the in-phase component of VLF-EM data is computed profile-wise and then imaged. The Hilbert transform output (**Fig 3.10**), of the study area exactly corroborates with the results of the Fraser and KH filters discussed above. Also the Hilbert transform output of the area clearly brings out two definite trends along NNE-SSW and NW-SE directions.

Similarly the amplitude of the analytic signal is being used extensively to locate subsurface targets besides estimating the depth to the top based on certain characteristic points in the interpretation of VLF-EM (Sundararajan et.al., 2011). A similar approach for the location of basement fractures and subsequent interpretation was carried out for the detection of mineralized basement fractures of Raigarh area (Rameshbabu et.al., 2007) using the in-phase component of VLF – EM data. The amplitude of the analytical signal precisely locates the position of the conductor. The analytical image output of the present study (**Fig 3.11**), more or less

matches with the trends of the fractures obtained by the Fraser and KH filters and Hilbert transform.

Sundararajan et al, (2011), proposed an empirical method for precisely locating the depth to the top of the conductor by combining the profiles of VLF in-phase, Hilbert transform and the amplitude of analytical signal. This method was adopted to interpret the VLF-EM signals along two selected profiles N 2200 and N 4600 were chosen for the purpose. All the three profile lines such as Low pass filtered in phase, Hilbert transform and amplitude of analytical signal were plotted in a single plot with suitable scales (**Fig 3.12**). In both the profiles the depth to the top of the conductor is less than 25m. This interpretation is utilized in further data processing such as 2D modeling.

By the above methods of filtering such as Fraser, Korous-Hjelt filters pseudosections and depth slices and the transformations such as Hilbert and analytical signal analysis the location of the conductors could be marked. Two well defined trends of the conductors along NNE-SSW and NW-SE directions were demarcated. In addition by the above analysis the offset of the older NNE-SSW trending conductors by the later NW-SE trending conductors could also be marked. These observed features closely match with the geology of the area and the expected trends of the causative bodies. In addition, using empirical methods, the depth to the top of the conductor could be estimated.

During the course of the field work, resistivity surveys were carried out for confirming the presence of conductors and also to know the quality of the conductor. It is discussed in the following chapter.

## CHAPTER - IV

### VLF RESISTIVITY SURVEYS AND INTERPRETATION

After initial processing of the VLF in phase data of all the profiles and marking the location of the conductors based on the cross over responses, resistivity surveys were carried out along two selected profiles to check and confirm the presence of conductors.

Two profiles of 400 m each along N-1800 and N2000, from 1000m west to 1400m west, were carried by resistivity surveys. For measuring resistivity, the T-VLF instrument was turned to resistivity mode with an electric line of 10m used as a standard length to measure the electric field along the line. Apparent resistivity values were measured at each station. The measured apparent resistivity values were plotted as profiles (**Fig. 4.1a and 4.1b**).

The apparent resistivity values ranges from 1 to 2500 Ohm-m. Plotting the apparent resistivity profiles, it was observed that low resistivity zones are intercepted, exactly above the conductors marked by the VLF in-phase data. This feature is evident in both the profiles. In N1800 profile the width of the low resistivity zone is less compared to the profile line N2000. In Fraser filter output of the VLF in-phase data also, similar feature is observed.

Form the VLF resistivity surveys the presence of conductors are confirmed and the initial interpretation made by plotting stacked profiles, Fraser filter and Karous-Hjelt filters for the location and width of the conductors area also confirmed. Besides the survey has given an idea about the quality of the conductor.

## CHAPTER - V

### VLF-EM AND MAGNETIC DATA INTEGRATION AND INTERPRETATION

In order to increase the quality of interpretation and to reduce the degree of ambiguity, magnetic surveys were also carried out in the study area. Accordingly magnetic data was studied in combination with the VLF-EM in-phase data of the study area. During the course VLF- EM data collection, magnetic data was also collected along the same twenty six profiles, following the same grid (Krishnakant.P., 2011). Integrated studies were carried out along the profiles in which the conductors were intercepted. Besides, the Fraser filtered output which exactly marks the location of the conductors, was superimposed on the 3D inverted magnetic output of the area. The results are discussed below.

The diurnal corrected magnetic intensity of the study area varies from -129 gammas to 60 gammas. Plotting of the magnetic data in the profiles along which conductors were intercepted exactly at the same locations indicate a crude positive correlation in the cross over locations and magnetic highs. However this cannot be generalized since the amplitude of the magnetic high is not much (**Fig. 5.1**).

In order to understand the spatial distribution of magnetic signatures with VLF conductors, the contour maps of 3D inverted magnetic data and Fraser filtered in-phase data were superimposed. The superimposed map indicates very important observations in the study area. The 3D-inverted magnetic contour map essentially shows the basement configuration of the study area. The topography of the basement varies from -45m to -99m from the surface and the northern and southern parts showing basement lows and a broad central part showing a basement high (**Fig. 5.2**). Besides the contour

map shows many E-W faults/fractures, which are mostly sympathetic to the basin margin faults responsible for the formation of the basin. The 3D basement configuration also brought out significant N-S trending faults criss-cross the major trends over the basement (**Fig. 5.2**)

Uranium mineralisation in other parts of Srisailam sub-basin, such as Lambapur, Peddagattu and Chitrial are mostly controlled by the N-S, NNE-SSE, NW-SE cross faults which are mostly across the basin margin with a general E-W trend. Hence, the NNE-SSW trends of the conductors demarcated by the VLF-EM data can be the future targets for further exploration. The depth of the unconformity between the basement and overlying sediments estimated from magnetic data inversion is used in 2D modeling of the VLF-EM data.

## CHAPTER – VI

### MODELING AND INVERSION OF VLF EM DATA – INTERPRETATION

#### 6.1. Introduction

VLF –EM data of the area was further subjected to modeling and quantitative interpretation with ultimate aim to decipher the disposition, depth and geometry of the conductive bodies thereby narrowing down the target area for subsurface exploration in the area. In this direction both 2D forward modeling and also 2D inversion of the VLF-EM data was attempted. The 2D forward modeling was done by a freeware named EM2DMODEL and the inversion was done using software (freeware for academic purpose) known as Inv2DVLF. For both the models to be accurate a complete knowledge of the resistivity of various formations was required. For this the resistivity surveys carried out along two profiles were mostly utilized, besides using some data from the published literature.

From the data processing such as filtering and transformations two trends of the conductors along NNE-SSW and NW-SE directions could be delineated. It was also inferred that the NNE-SSE direction is older than NW-SE direction. Attempt was made to model to know the conductor characteristics along both these directions. Forward modeling was done for the major NNE-SSW trending conductor along 2200 profile line. Whereas in the 2D-inversion process, the conductors trending along both the directions were considered. In total five profile lines (N1000, N1800, N2000, N2200 and N4400), showing good response in the pseudo sections, were considered for 2D-inversion process. Of the five profiles for 2D-inversion N1800, N2000 and N2200 are for the NNE-SSW trending conductors and the

profiles N1000 and N4400 were selected for NW-SE trend and there by this process an idea about the entire surveyed area can be obtained.

## 6.2. Forward Modeling:

The VLF primary horizontal magnetic field is parallel to the survey lines and normal to the strike of the 2D conductive structure like fractures, hence produce maximum coupling between the conductor and field. The primary magnetic field, which has no vertical component in the absence of an anomalous conductor, induces a vertical secondary field component when it interacts with a 2D conductive body, resulting in elliptical polarization of the total magnetic field. The tilt of the major axis of the ellipse and the axes ratio are the two field parameters recorded in VLF EM survey. These two parameters depend on the ratios of vertical to horizontal magnetic field components and their phase difference.

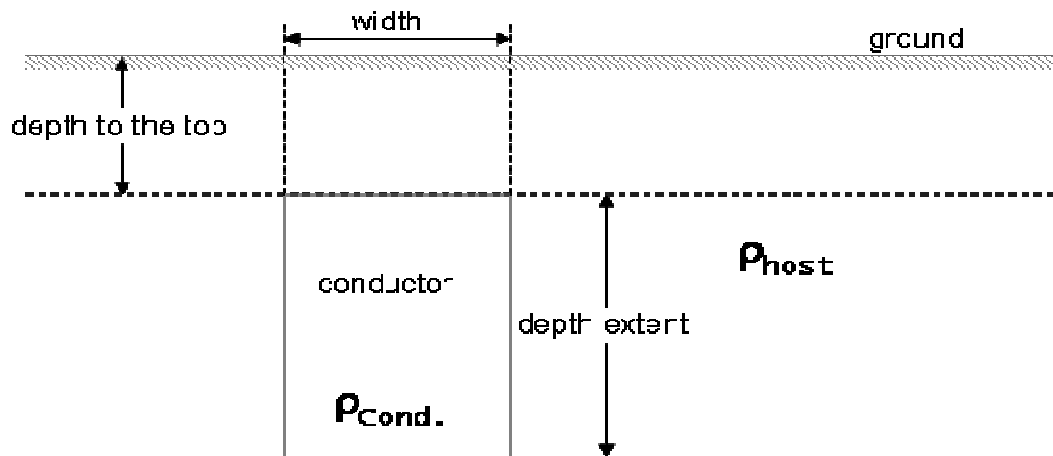


Figure 6.1: Description of model parameters

Four-parameter have been used in the modeling of VLF EM data. These four parameters are peak-to-peak vertical in-phase and axes ratio responses designated by  $\alpha_{\text{max}}$  and  $\epsilon_{\text{max}}$ , and the horizontal distances between the primary peak in inphase axes-ratio responses. These four parameters depend on the conductance and

geometry of the conductor and resistivity of the host rock (Wright, 1983). In the study area, the Srisailam sediments rest unconformably above the basement crystallines and are cross-cut by the fracture zone. Based on the observations, a model consisting of both sheet and layered case is used in this study to quantify the results (**Fig. 6.1**). 2D forward modeling was attempted for N2200 profile line which show good cross over responses. Based on the magnetic data inversion, the depth to the unconformity was kept at 55m. The fracture zones were kept vertical for simplifying the problem.

### **Results of the Profile N-2200**

The model response of conducting fracture zones, were studied ,using a profile length of 1100m with 100 elements in the E-W direction and 20 elements in depth for getting information up to a depth of 100m. The in-phase data of the profile shows two clear cross over from negative to positive by moving west to east. The resistivity of the granite was taken as 3000ohm-m, the sediments as 1800 ohm-m and the fracture zones as 10ohm-m and 50ohm-m. The model closely approximates a geological situation of study area, where the fracture has a long strike length. The tilt angle anomaly corresponding to low resistivity indicating the fracture zone is clearly depicted. The top of the fracture zone is centered at the inflection point of the anomaly (**Fig. 6.2**). The observed and computed tilt angle along with the resistivity profile shows perfect matching in the cross over areas from east to west thereby validating the model. For comparison the Fraser filter pseudo section is also given along with the model. By the modeling two fracture zones having widths of 100-150m were interpreted having cross over at 125m and 1025m from east. One thin fracture

zone having width of around 50m has been interpreted at 625m from east. The RMS obtained for this model is 1.2.

### 6.3. 2D - Inversion of the VLF-EM data.

Although 2D forward modeling of the VLF-EM data was closely approximated for the real geological situation in the area, the minute fluctuations and inflexions in the VLF-EM data could not be taken care of. This warranted numerical modeling of the data. VLF-EM modelling is implemented using an algorithm and software (freeware for academic purpose) developed by Monterio et al., (2006) for in-phase and out-of-phase components based on a 2D regularized inversion approach by Sasaki (1989, 2001). Assuming a 2D conductivity distribution (**Fig. 6.3**) striking along the direction of X and the profile along the direction of Y, the in-phase and quadrature components of the vertical magnetic field ( $H_z$ ) are measured using the local horizontal magnetic field ( $H_y$ ) as the phase reference. At each measurement site it is possible to define a scalar tipper B given by  $H_z = B H_y$ .

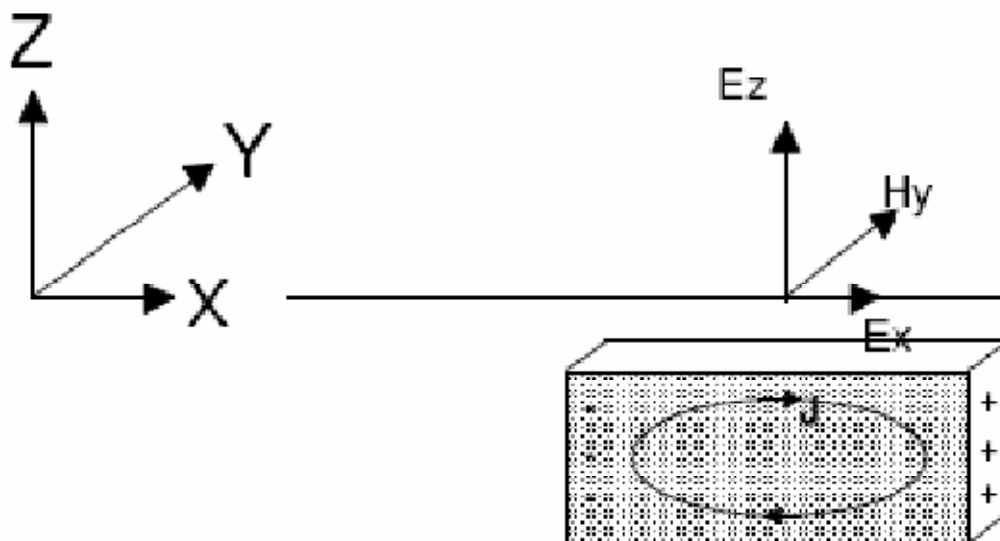


Figure 6.3. VLF- electromagnetic field

The tipper B is a complex quantity originated by the time lag between horizontal and vertical components of the magnetic fields due to the electromagnetic induction phenomena. The tipper does not exist over a homogeneous earth (or over a layered earth). Over a 2D earth, the tipper varies along the measuring profile showing the strongest variations in the vicinity of resistivity contrasts. The real and imaginary (or in-phase and out-of-phase) components of the tipper in the case of the VLF-EM method are usually expressed as percentage.

The software "Inv2DVLF" for 2D regularised inversion of VLF-EM data developed based on a forward solution using the finite element method (Monterio et al., 2006) is available for inversion. The pre requisite of this inversion software needs an appropriate number of coordinates in x, y directions and number of layers. The software Inv2DVLF was used for the inversion of VLF data of the present study. The details of input and output parameters to this inversion scheme is discussed below.

### **Input and Output Parameters for Inv2DVLF**

The forward modelling of Inv2DVLF is based upon the finite-element method (FEM) and the inversion on the regularization method. Therefore, a graded spacing in both vertical and horizontal directions should be used for the FEM computation and a block-division of the area of interest should be specified. The Inv2DVLF (Monterio et al., 2006) runs over an input file generated by PrepVLF. The inputs to PrepVLF are the coordinates of the finite-element mesh of the earth-model block, observed in-phase and out-of-phase components of the tipper along with location and its topography. The output of PrepVLF which contains all the information necessary for the inversion to be performed by Inv2DVLF viz., number of iterations (usually between 20 and 30), the Lagrange parameter (usually 0.03, but it depends on the

problem). Finally, Inv2DVLF generates information of the inversion process, final model and the input data and model responses along with the sensitivity of the model. **Fig. 6.4** illustrates the inversion procedure (Monterio et al., 2006).

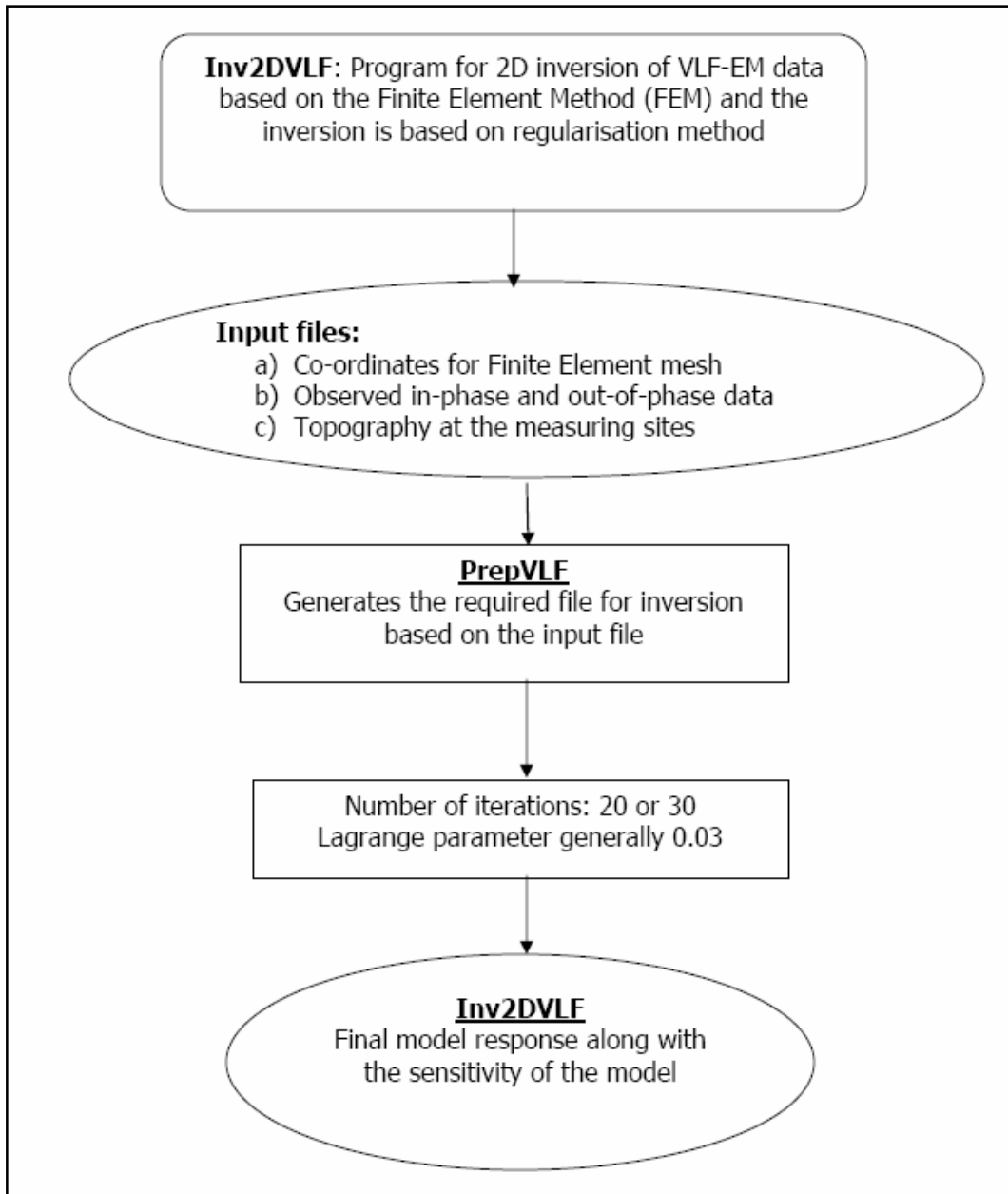


**Figure 6.4. Generalized flow chart for the finite element method for 2D Inversion**

For the present study, VLF-EM modelling of the in-phase and out-of-phase components was carried out at a transmitter frequency of 17.10 kHz with an initial

half space resistivity of 2000 ohm-m based on the recorded resistivity values along two profiles. As the terrain is plain, topography was taken as zero during the computation. The skin depths for the models are approximately 100 m, although the program by itself calculates the parameters for greater than 200m depths.

### **Inversion and Interpretation for profiles N1800, N2000 and N2200**

The inverted models N1800, N2000 and N2200 are presented in **Fig. 6. 5, 6.6 and 6.7** respectively. These profiles correspond to the NNE-SSW trending conductors.

It is pertinent to mention that the inversion process was carried out initially using raw data and then by the low pass filtered data for getting refined output. These comprises the inverted output of the raw data, low pass filtered data along with Fraser filtered pseudo section. The profiles of the observed and computed data are also presented in the figures.

The original in-phase data of profile N1800 comprises a cross over at around 1125m west, confirming the presence of a conductor. The Fraser filter pseudo section also confirmed the inference by showing a peak over the cross over. The inverted model of the profile (**Fig. 6.5**) shows a clear low resistivity zone between 1100 to 1200 W. The inverted model carried out for the profile using the low pass filtered data further refines the low resistivity zone. The low resistivity zone extends to depth of around 100 m. The measured apparent resistivity profile between 1000m to 1400m west exactly shows the low resistivity zone in the same zone, there by confirming the presence of the conductor and also validating the 2D inverted model. The dip of the low resistivity zone is not clear in this profile.

Similar to profile N 1800, the profile N 2000 comprises a cross over at around 1050m W and lies in the northern continuity of the same conductor inferred in the N1800

profile. The Fraser filter and KH filter pseudo sections confirmed the presence of the conductor by showing peaks over the cross over and inverted cone structure thereby confirming its depth continuity. Also the Fraser and KH filters show slight dip of the body towards west. The inverted models both from raw data and also low pass filtered data (**Fig.6.6**) shows the presence of a low resistivity zone exactly over the cross over and the inverted cone structures in the pseudo sections. In the inverted model the dip of the conductor is around 70 to 80° towards west. The measured apparent resistivity profile of the same line also confirms presence of the low resistivity zone and thereby the conductor. Also by this 2D inverted model, the continuity of the low resistivity in the NNE direction is inferred. The mean width of the low resistivity zone is around 100 m and extends up to a depth of around 120m. The inverted model of low pass filtered data further refines the low resistivity zone.

Further 200 m north of N 2000 profile, N 2200 profile also shows a cross over around same zone in the NNE continuity of the low resistivity zone inferred above, thereby confirming its continuity. Fraser and KH filters also confirm presence of a conductor. The 2D inverted model of the of the raw data not only confirms the continuity of the conductor, but also the dip of the conductor along westerly direction (**Fig. 6.7**). These conductor characteristics were already inferred for the same profile by the forward modeling. The width of the conductor has a maximum of 100m with a depth extent of around 100m. It is to mention the RMS error for the all the profiles lies between 2 and 3.

#### **Inversion and Interpretation for profiles N 1000 and N 4400**

After inverting profiles showing conductor axis along NNE-SSW direction, attempt was made to characterise the conductor having NW-SE trend by 2D inversion process. For this two profiles showing good cross over response one at northern

portion of the study area (N 4400) and one at the southern portion of the study area (N 1000) was selected.

Raw data profile of N 1000 shows a cross over at 1050 m west. Presence of conductor was confirmed by the peak above the cross over in the Fraser and KH filtered outputs. 2D inverted output of the profile confirms a wide low resistivity zone of around 200 m from 1000 m west to 1200 m west (**Fig.6.8**). The depth extent of the low resistivity zone is shallow compared to the NNE-SSW trending conductors. The inverted model of the low pass filtered data further resolves the low resistivity two conducting bodies which are connected. Also the low resistivity zone does not show any asymmetry there by inferring that the conductors are vertical or sub vertical.

The profile N 4400 is in the northern portion of the study area shows a cross over at around 1150 m west. This was confirmed by the 2D inverted model of the profile in this profile as in the N 1000 profile the depth extent of the low resistivity zone is shallow of less than 100 m (**Fig.6.9**). However the width of the low resistivity zone is more compared to the NNE-SSW trending conductors. The RMS error for the two profiles lies between 3 and 4.

By the above analysis such as 2d forward modelling and 2D inversion of the raw and low pass filtered in-phase and quadrature components, presence of low resistivity zones having resistivity as low as  $<10$  Ohm-m within a highly resistive terrain such as granite could be inferred. The conductor characteristics such as depth extent, width of the body were inferred by the 2D inversion of the data.

## **CHAPTER - VII**

### **INTEGRATION WITH GEOLOGY AND DISCUSSION**

The northern margin of the Srisailam sub-basin of the Cuddapah basin of Dharwar Craton, presents a highly dissected topography with a number of outliers exposing the sediments of Srisailam Formation of Middle-Upper Proterozoic age, overlying the basement crystallines of Lower Proterozoic age. The basement comprises a number of varieties of granites, basic dykes and quartz veins. This Lithostructural setup makes these outliers ideal to host unconformity related uranium mineralisation. In this pursuit, substantial uranium resources have been established by AMD in three deposits in Lambapur, Peddagattu and Chitrial in three separate outliers with same names.

The study area covering 10 sq km, forms a part of Amrabad outlier, southwest of the Chitrial outlier where substantial uranium resources have been established by sustained exploration efforts by AMD during the past decade. The study area has similar lithostructural setup as that of the other outliers of Srisailam Formation, which gives an idea about its uranium potentiality. Exploration could not be taken up in Amrabad outlier because of the constraints of the Rajiv Gandhi Tiger sanctuary. Also the study area is close to the main Srisailam sub-basin and the interpretations based on geophysical surveys in this outlier can be extended to the main Srisailam sub-basin.

Uranium mineralisation in already explored outliers like Chitrial, Peddagattu and Lambapur is localized along the unconformity between the basement granites and overlying sediments of Srisailam Formation mostly hosted by the granites and is controlled by structures, having one long dimension. Also, uranium mineralisation is associated with sulphides, and hydrothermal alteration has played a major role in

localizing these deposits. Expecting that these features will give good electromagnetic response and keeping the analogy of similar lithostructural setup, VLF-EM surveys were carried out in parts of Amrabad outlier. Also, shallow nature of the uranium mineralisation (less than 70m) depth and the terrain condition prompted for VLF-EM surveys in this area. The entire procedure from data collection, filtering and transformation, 2D modeling and Inversion carried out is outlined below.

- 1) An area of 10 sq km was covered by VLF-EM surveys using IRIS make T-VLF instrument, with frequency of 17100Hz, transmitted by UMS, Moscow. Both tilt (%) and ellipticity (%), which represent the in-phase and quadrature components respectively were measured in 1924 stations, spread over in 26 profile lines with profile spacing distance of 200 m along N-S direction and station interval of 25 m in E-W direction. The target for such surveys is to delineate the N-S trending structures, which is the dominant trend in the area. The transmitter was selected for obtaining maximum EM response.
- 2) The stacked profiles of raw data and low pass filtered output shows clear cross over response, indicating thereby the presence of conductors.
- 3) Filtering procedures such as Fraser and Karous – Hjelt methods have defined the extent of the conductors. Besides the Fraser and KH filter outputs have brought to light two definite trends of the conductors along NNE-SSW and NW-SE directions. It could also be inferred that the NNE-SSE trend is older than the other, by the offset relationship between the two.
- 4) As a next step in filtering, current density pseudodepth sections were prepared for all the 26 profiles using Fraser and KH filter data. Pseudodepth sections

qualitatively confirm the presence of the conductors, with typical inverted conical features. Also the pseudosections reveal continuity of the conducting zones in the adjacent profiles. Stacking of the pseudosections as profiles, also confirms the two trends of the conductors elucidated by the Fraser and KH filter outputs.

- 5) The depth slices (level contour plans) of the area indicate the continuity of the conductors even to the depth of 100 m. Besides, one important observation in the depth slices of the KH filter output is the current density occurs between depths between 50 and 75m, which is the expected depth of the unconformity in the area.
- 6) The Hilbert transform and the amplitude of the analytical signal output of the VLF in-phase data clearly brings out the two trends of the conductors and also their offset inferred from the Fraser and KH filter outputs. Further, the empirical method of obtaining the depth to top of the conductor by plotting the in-phase, Hilbert and amplitude of analytical signal profiles of the same line gives a depth of around 25 m.
- 7) Study of correlation of VLF-EM data with the magnetic data of the same area gives a crude positive magnetic anomaly in the zones of EM cross over. The inverted magnetic anomaly map clearly brings out the basement topography of the area from which the depth to the unconformity can be estimated.
- 8) VLF- resistivity surveys carried out along two profiles N1800 and N2000 of 400m length from 1000 to 1400m west has brought out correlatable low resistivity zone in both the profiles. The resistivity surveys have helped not only in demarcation of the low resistivity zone and also to have an idea about the probable resistivity

in the area for different formations. This information was extensively used in the 2D modeling of the VLF-EM data.

- 9) All the inferences and the qualitative interpretations made by the filtering and transformation exercises warrants modeling of the VLF-EM data. This procedure was aimed in obtaining the quantitative information of the conductors, for future sub surface exploration in the area.
- 10) 2D forward modeling was attempted for N 2200 profile which shows good cross over response. The model response for two conductors of 100-150 m width and one thin conductor of 50m width, with the unconformity level of -55 m from surface, fits well with the observed in phase profile area. The resistivity of the basement was kept at 3000 Ohm-m and sediment with 1800 Ohm-m. The resistivity of the conductors was kept between 10 -50 ohm-m. This matches well with the real geological situation in the area. Such low resistivity zones within highly resistive formations can be due to intense fracturing of the host rock followed by hydrothermal alteration leading to the formation of sulphides, alteration minerals and iron oxides, besides water in the conductive fracture zones. These zones may be the future targets for subsurface exploration.
- 11) As a next step, for differentiating the conductors along NNE-SSW and NW-SE directions, 2D inversion of the VLF-EM data was attempted by using a freeware named 'Inv2DVLF'. For this the profiles N1800, N2000 and N2200 showing conductors along NNE-SSW direction and profiles N1000 and N4400 were selected showing conductors along NW-SE direction.

- 12) 2D inversion of the profiles showing conductors along NNE-SSW direction clearly elucidates low resistivity zones of 100 – 150m width with depth extent of more than 100m. Also the inversion has brought out the westerly dip of the conductors with angle of around  $70^{\circ}$ . These low resistivity zones are well correlatable with the adjacent profiles thereby confirming their strike continuity. Also, the 2D inversion for the profile N2200 corroborates with the 2D forward modeling done the same profile.
- 13) 2D inversion of profiles N1000 and N4400 profiles for the conductors along NW-SE strike direction also show low resistivity zones of 100 -150m, but having shallower depth extent that of the NNE-SSW trending conductors. Also these low resistivity zones are nearly vertical in contrast to the other set of conductors.
- 14) Hence it can be inferred that the study area is affected by at least two structural deformation phases along older NNE –SSW direction and later NW-SE direction. By the 2D inversion process the subtle differences in their geometry could be outlined.
- 15) The structural studies in the area also support the interpretation. The low resistivity zones may represent structural weak zones affected by intense alteration and deposition of sulphides and iron oxides along with water. With the knowledge that uranium mineralisation occurs along the structural weak zones involving hydrothermal systems, these low resistivity zones form future target areas for subsurface exploration.
- 16) Subsurface exploration in the known uranium deposits, occurring in the surrounding outliers has brought to light the control of the structures and zones of

their intersection for rich grade mineralisation. In this regard the low resistivity zones brought by 2D inversion along two directions, and their intersection zones form the primary targets for subsurface exploration by drilling in the area.

- 17) By these processes the ultimate aim of present study to narrow down the target for future subsurface exploration is fulfilled.

## **CHAPTER - VIII**

### **CONCLUSIONS**

Very Low Frequency – Electromagnetic (VLF-EM) surveys were carried out for the first time in an entirely unexplored sector of Amrabad outlier close to the main Srisailam sub-basin, owing to its uranium potentiality of the area for hosting fracture controlled unconformity related uranium mineralisation. The aim of the present surveys is to narrow down the target for future subsurface exploration and also to characterize the EM signatures for future geophysical exploration programmes in the area. Following salient features could be brought out by the VLF-EM surveys in the area.

1. The surveys have brought to light the presence of subsurface conductors in two different strikes along NNE-SSW and NW-SE directions. The based on their relationship as inferred by the filter outputs the NNE-SSW direction is older which are offset by the younger W-SE direction.
2. Based on the pseudodepth sections and depth slices prepared from both the Fraser and KH filter data, the strike and the depth continuity of these conductor zones could be qualitatively inferred.
3. The results of the data transformations such as Hilbert and amplitude of analytical signal, also corroborate with the conclusions drawn from the Fraser and KH filtering of the data.
4. VLF-resistivity surveys along two profiles showing cross over, has brought out low resistivity zones within the highly resistive formations, thereby confirming the presence of the conductors.

5. Results of 2D forward modeling of the using the known geological factors of the area, closely matches with the observed data thereby inferences such as the width of the conductors, depth to the unconformity and the resistivity values of the conductors can be utilized for the future exploration programmes in the area.
6. 2D inversion of the VLF-EM data along five profile lines has clearly brought to light the presence of low resistivity zones along two different directions and the subtle difference in their geometry and disposition.
7. The low resistivity of  $<100$  Ohm-m obtained for the conductors, by 2D inversion, can be assigned for the presence of sulphides, alteration minerals (produced by intense alteration of the host rock) and water in varying proportions in the structurally weak zones within the basement or slightly above the basement.
8. Hence it is concluded that the conductors (low resistivity zones) outlined by qualitative methods (Fraser, KH and pseudo sections) and quantitative methods (2D Forward modeling and 2D inversion) and the zones of their intersection can be the future targets for subsurface exploration.
9. Based on the experience gained during this work, it is recommended that the VLF survey can be extended to the other areas in Srisailam sub-basin, wherein the sediment thickness must be less than 70m and the depth of investigations is around 100m.
10. The results obtained by the VLF-EM surveys can be corroborated by applying any one of the ground EM surveys to further narrow down the target and Induced Polarization (IP) surveys to characterize the nature of the sulphides.

## REFERENCES

- Abhinav kumar and Sunil Kumar (2007): A report on evaluation of Srisailam and Palnad sub basins using Geographic information system for identifying target areas, using information gathered over the years by regional and AMD Hqrs. Unpublished Report, AMD, DAE, Hyderabad.
- Adepelumi, A.A., Kim, M.J.Yi.J., Ako, B.D. and Son, J.S. (2006): Integration of surface geophysical methods for fracture detection in crystalline bedrocks of southwestern Nigeria. *Hydrogeology Journal*,14, p.1284-1306.
- Babu Rao, V., Atchuta Rao, D., Rama Rao, C.H., Sharma, B.S.P., Bhaskara Rao, D.S., Veeraswamy, K. and Sharma, M.R.L. (1987): Some salient results of interpretation of aeromagnetic data over Cuddapah Basin and adjoining terrain, south India. *Memoir of Geological Society of India*, no.6, p.295-312.
- Chavan,S.J.,(2011) Unpublished Achievement report of Srisailam Investigations, AMD, Hyderabad.
- Chavan,S.J.,(2010) Unpublished Achievement report of Srisailam Investigations, AMD, Hyderabad.
- Dhalkhamp,F.J.,(1980) Uranium ore deposits, Spriger Verlag Berlin(West)
- Fraser, D.C (1969): Contouring of VLM-EM data, *Geophysics*, 34, p.958-967.
- Fraser, D.C (1981): A review of some useful algorithms in geophysics. *Canadian Institute of Mining Bulletin*, v.74 (828), p.76-83.
- Kaikkonen, P. (1979): Numerical VLF modeling, *Geophysical Prospecting*, 27, p.815-834.
- Kale, V.S., and Phansalkar, V.G. (1991): Purana Basins of Peninsular India: a review, *Basin research*, 3,p.1-36.
- Kalia, K.L., Roy Choudhury, K., Reddy, P.R., Krishna, V.G., Hari Narain, Subotin, S.I., Sollogub, V.B., Chekunov, A.V., Kharetko, G.E., Lazrenko, M.A., and Ilchenko, T.V., (1979): Crustal Structure along Kavali-Udipi Profile in the Indian Peninsular Shield from Deep Seismic Sounding: *Journal of Geological Society of India*, v.20, p.307-333.
- Karous, M. Hjelt, S.E., (1983): Linear filtering of VLF dip-angle measurements. *Geophysical prospecting*, 31, p782-794.

Kesavamani M., Rao, N.B.K. and Rama Rao., J.V. (1997): Characteristics of Granite-Greenstone Basement below the Cuddapahs: A Geophysical Insight. *Journal of Indian Geophysical Union*, v.1, no.1, p.27-39.

King (1872): The Kadapah and Kurnool Formations in the Madras Presidency. *Geological Survey of India, Memoir 8*, p.1-346.

Krishnakant,P., (2010): Unpublished M.Tech dissertation work (in progress, Personnel communication), University of Hyderabad.

Markandeyulu and Subhash Ram (2001): Detailed geophysical surveys in Mawlaingut area, East Khasi Hills district, Meghalaya, Unpublished Brief annual Report (Field Season 2000-01), AMD, DAE, Hyderabad

Mathews, R, Koch. R., Lappin.M., (1997): Advances in integrated exploration for unconformity uranium deposits in western Canada. In "Proceedings of Exploration 97: Fourth Decennial International Conference on Mineral Exploration" *edited by* A.G. Gubins, 1997, p.993-1024.

Mernagh, T.P., Wyborn, L.A.I. and Jagodzinski, E.A. (1998): Unconformity-related U±Au±platinum-group-element deposits. *AGSO Journal of Australian Geology and Geophysics*, 17(4), p.197-205.

Mithilesh Sharma, Rai, A.K., Nagabhushana, J.C., Sinha, R.M., and Vasudeva Rao, M. (1995): Cuddapah Basin and its environs as first order uranium target in the Proterozoics of India. *Exploration and Research for Atomic Minerals*, v.8. p.127-139.

Monteiro, S.F.A., A. Mateus, J. Figueiras, M. A. Gonçalves, 2006, Mapping groundwater contamination around a landfill facility using the VLF-EM method – a case study: *Journal of Applied Geophysics*, Vol. 60, pp. 115-125.

Mukundhan,A.R., and Krishnakant,P., (2011): Unpublished brief annual report, AMD, Hyderabad.

Mukundhan,A.R., Saravanan,R., Reddy,S.V.S., Chavan,S.J., Ramesh Babu,P.V., (2009) Geochemical characteristics of the mineralized granites of Peddagattu uranium deposit, Nalgonda district, Andhra Pradesh; National symposium in Advances in atomic mineral science in India during 50 year period:1959-2009; Abstract volume, AMD,July-2009.

Murthy, Y.G.K., Babu Rao., Gupta sarma, D., Rao, J.M., Rao, M.N. and Bhattacharji, S. (1987): Tectonic, petrochemical and geophysical studies of mafic dyke swarms around the Proterozoic Cuddapah basin, South India. In:H.C. Halls and W.H.Fahrig, W.H. (Eds.), *Mafic dyke swarms*. Geological Association of Canada, Newfoundland, Canada, Special paper No.34, p.303-316.

Mwenifumbo, C.J., Elliott, B.E. and Cinq-Mars, A. (1997): Field Evaluation of a Four-component Downhole VLF-EM Logging System. In "Proceedings of Exploration 97: Fourth Decennial International Conference on Mineral Exploration" *edited by* A.G. Gubins, 1997, p. 541–544.

Nagabhushana (1997): Tummulapalle Rachakuntapalle uranium deposits, Cuddapah district, Andhra Pradesh: Economic appraisal and exploration history. Training course handbook, v.3. Part III, AMD, Hyderabad

Nagaraja Rao, B.K., Rajurkar, S.T., Ramalingaswamy, G. and Ravindra Babu (1987): Stratigraphy, and evolution of Cuddapah Basin, Geolocial society of India, memoir no. 6, pp.33-86.

Nagaraja Rao, B.K., Rajurkar, S.T., Ramalingaswamy, G. and Ravindra Babu, B. (1987): Stratigraphy, structure and evolution of the Cuddapah Basin. In: Purana Basins of Peninsular India, Geological Society of India, Memoir 6, p.33-86.

Narayanaswami, S.(1966): Tectonics of Cuddapah Basin. Journal of Geological Society of India, v.7, p.33-50.

Ogilvy, R. D., and Lee, A. C., (1991): Interpretation of VLF-EM in-phase data using current density pseudosections: Geophysical Prospecting, Vol. 39, pp.567-580.

Oskooi and Pedersen (2005): Comparison of VLF and RMT methods. A combined tool for mapping conductivity changes in the sedimentary cover. Journal of Applied Geophysics, 57, p.227-441.

Paal, G. (1965): Ore prospecting based on VLF-radio signals. Geoexploration, v.3, p.139-147.

Pandey, B.K., Prasad, R.N., Sastry, D.V.L.N., Kumar, B.R.M, Suryanarayana Rao, S., Gupta, J.N., Rb-Sr whole rock ages for the granites from parts of Andhra Pradesh and Karnataka, In: Fourth national symposium on mass spectrometry, Indian Institute of Science, Bangalore, India. (1988) EPS-3/1.

Paterson, N. R., and V. Ronka, 1971, Five years of surveying with the Very Low frequency Electromagnetic method: Geoexploration, Vol. 9, pp. 7-26.

Philip Kearey, Michael Brooks, Ian Hill., (2002): An Introduction to Exploration Geophysics; Weiley-blackwell publish.

Radhakrishna, T., Krishnendu, N.R. and Balasubramonian, G. (2007): Mafic dyke magmatism around the Cuddapah Basin: Age constraints, Petrological characteristics and geochemical inference for a possible magma chamber on the southwestern margin of the basin, Journal of Geological society of India, v.70, p.194-206.

Rajaraman, H.S., (2010): Data acquisition, processing and Interpretation of Very Low Frequency Electromagnetic responses in Chitrial Main Block of Srisailam sub-basin, Nalgonda district, Andhra Pradesh, unpublished M.Tech dissertation thesis, University of Hyderabad.

Ramakrishna, P., Dash, J.K., Narasimha Rao, B. and Tiku, K.L. (1997): Report on preliminary geophysical surveys at Peddagattu outlier, Nalgonda district, Andhra Pradesh (Field season 1996-97). Unpublished Report of Exploration Geophysics Group, AMD, Hyderabad.

Ramakrishnan, M. and Vaidhyanathan, R. (2008): Geology of India, v.1, Published by Geological Society of India. p.492-509.

Ramam, P.K., and Murthy, V.N. (1997): Geology of Andhra Pradesh, Geological Society of India, Bangalore.

Rameshbabu, V., (2007): modeling and inversion of magnetic and VLF-EM data for uranium exploration, Raigarh district, Chhattisgarh, India, unpublished PhD thesis, Osmania University, Hyderabad.

Ramesh Babu, V., Subash Ram, Srinivas, R., Veera Bhaskar, P. and Bhattacharya, A.K. (2008): VLF surveys for U exploration in Dulapali area, Raigarh district, Madhya Pradesh. Journal of geophysics, India, vol. 25, No. 2&3. p.27-33.

Ramesh Babu, V., Subhash ram and N. Sundararajan, (2007), Modeling and inversion of magnetic and VLF-EM data with an application to basement fractures - A case study from Raigarh, India: Geophysics, SEG, USA, Vol. 72. Sept.-Octo., 2007.

Saydam, A. S., 1981, Very low frequency electromagnetic interpretation using tilt angle and ellipticity measurements: Geophysics, Vol. 46, pp. 1594-1606.

Sasaki Y., (1989), Two-dimensional joint inversion of magnetotelluric and dipole-dipole resistivity data: Geophysics, Vol. 54, pp. 254-262.

Sasaki, Y., (2001), Full 3-D inversion of electromagnetic data on PC: Journal of Applied Geophysics, Vol. 46, pp. 45-54.

Sinha, A. (1990): Interpretation of ground VLF EM data in terms of vertical conductor models. Geoprospection, v.26, p.213-231.

Sinha, R.M., Shrivastava, V.K., Sarma., G.V.G., and Parthasarathy, T.N. (1995): Geological favourability for unconformity related uranium deposits in northern parts of the Cuddapah Basin: Evidences from Lampapur uranium occurrence, Andhra Pradesh, India. Exploration and Research for Atomic Minerals, v.8, p.111-126.

Sundararajan, N., Nandakumar, Narsimha Chary, M., Ramam, K. and Srinivas, Y. (2007): VES and VLF - an application to groundwater exploration, Khammam, India. The Leading Edge.

Sundararajan, N., Ramesh Babu, V., Chaturvedi, .A. K., (2011) Detection of basement fractures favourable to uranium mineralization from VLF-EM signals. Journal of geophysics and engineering, Vol.8, p.330-340.

Sundararajan, N., Ramesh Babu, V., Prasad, N. S., and Srinivas, Y., 2006, VLFPROS – A MATLAB code for processing of VLF-EM data: Computers & Geosciences (Elsevier), Vol. 32, pp. 1806-1813.

Sunil S.Gandhi (1995): An overview of the exploration history and genesis of Proterozoic uranium deposits in the Canadian Shield. Exploration and Research for Atomic Minerals, v.8, p.1-47.

Umamaheswar, K., Achar, K.K., and Maithani, P.B. (2008): Proterozoic Unconformity Related Uranium Mineralization in the Srisailam and Palnad Sub-Basins of Cuddapah Basin, Andhra Pradesh, India

Valdia, k.s. (2010): The Making of India: Geodynamic Evolution. Macmillan publishers India Ltd. India.p.175-182.

Verma, M.B., Som, A., Latha, A., Umamaheswar, K. and Maithani, P.B. (2008): Geochemistry of host granitoids of uranium deposit at Chitrial area, Srisailam Sub-Basin, Nalgonda district, Andhra Pradesh. Memoir Geological Society of India, no.73, p.37-54.

Wright, J.L (1988): VLF interpretation manual, EDA Instruments (now Scintrex Ltd.).Concord. Ont.

# CHAPTER-I GEOLOGY

## **CHAPTER-II**

# **METHODOLOGY**

**CHAPTER-III**  
**FILTERING AND**  
**TRANSFORMATIONS**  
**OF VLF-EM DATA**

**CHAPTER-IV**  
**VLF RESISTIVITY SURVEYS**  
**AND**  
**INTERPRETATION**

**CHAPTER-V**  
**VLF-EM AND MAGNETIC DATA**  
**INTEGRATION- INTERPRETATION**

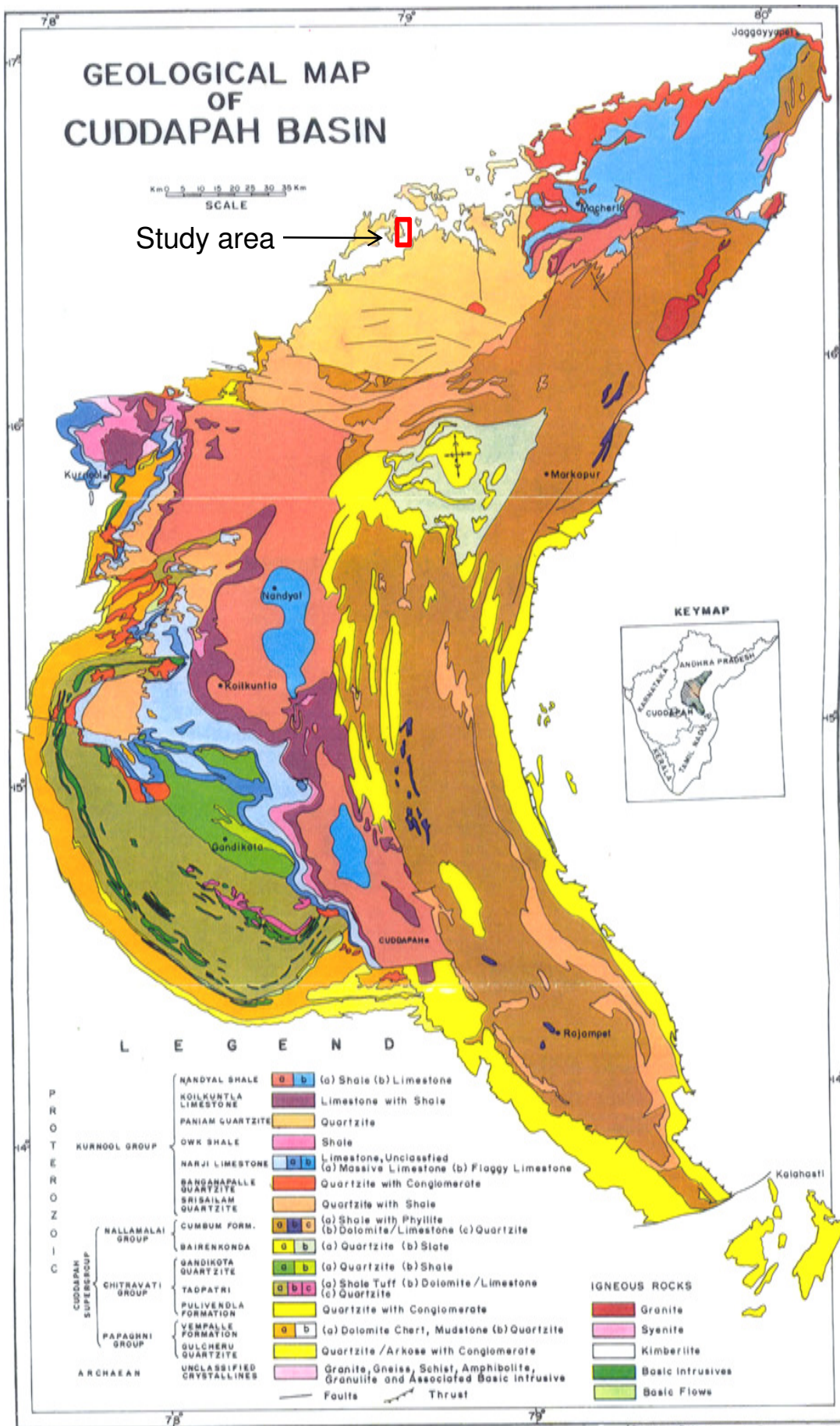
**CHAPTER-VI**  
**MODELING AND INVERSION**  
**OF VLF-EM DATA**

**CHAPTER-VII**  
**INTEGRATION WITH**  
**GEOLOGY**  
**AND DISCUSSION**

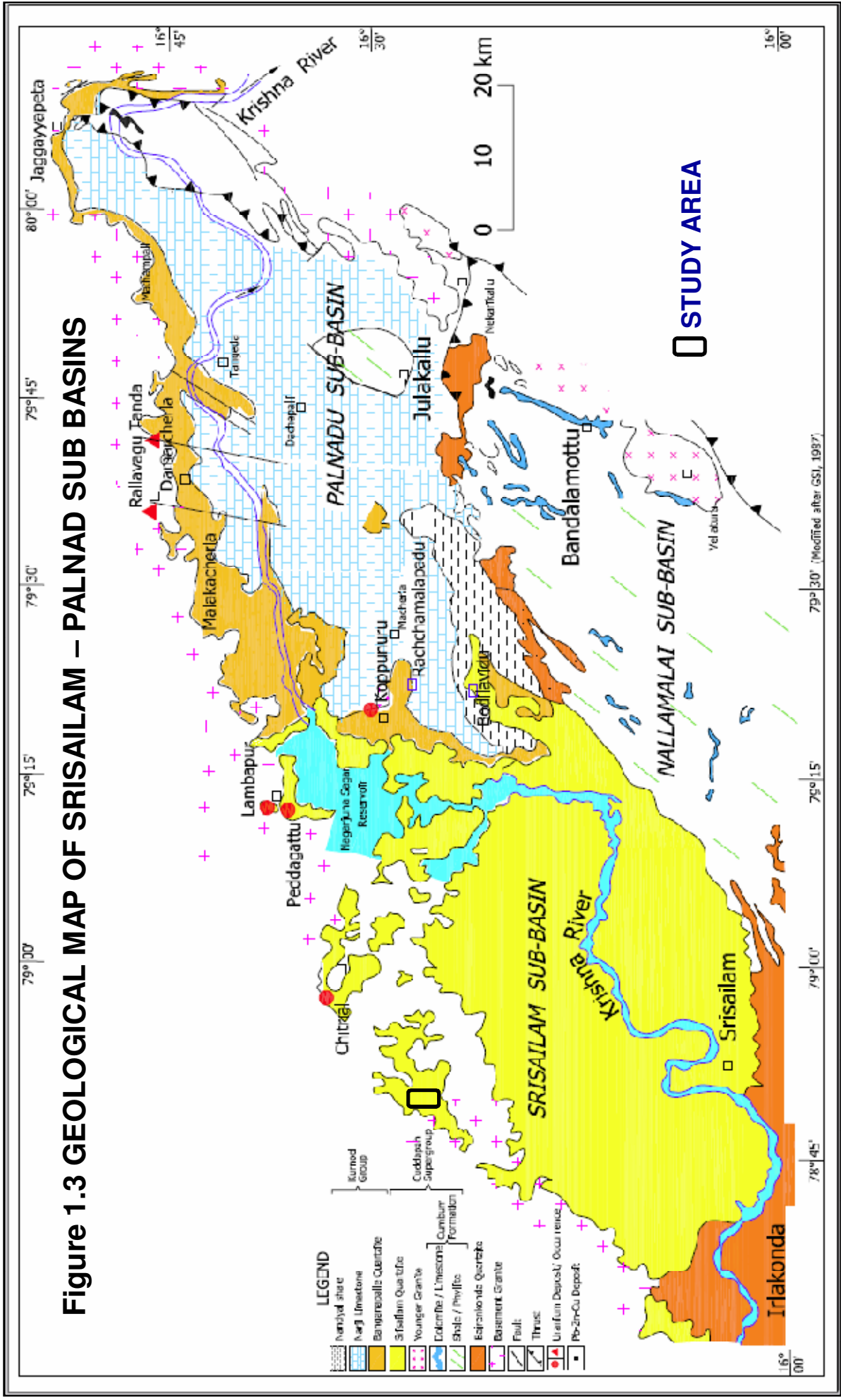
# CHAPTER-VIII

# CONCLUSIONS

# REFERENCES



**Figure 1.3 GEOLOGICAL MAP OF SRISAILAM – PALNAD SUB BASINS**



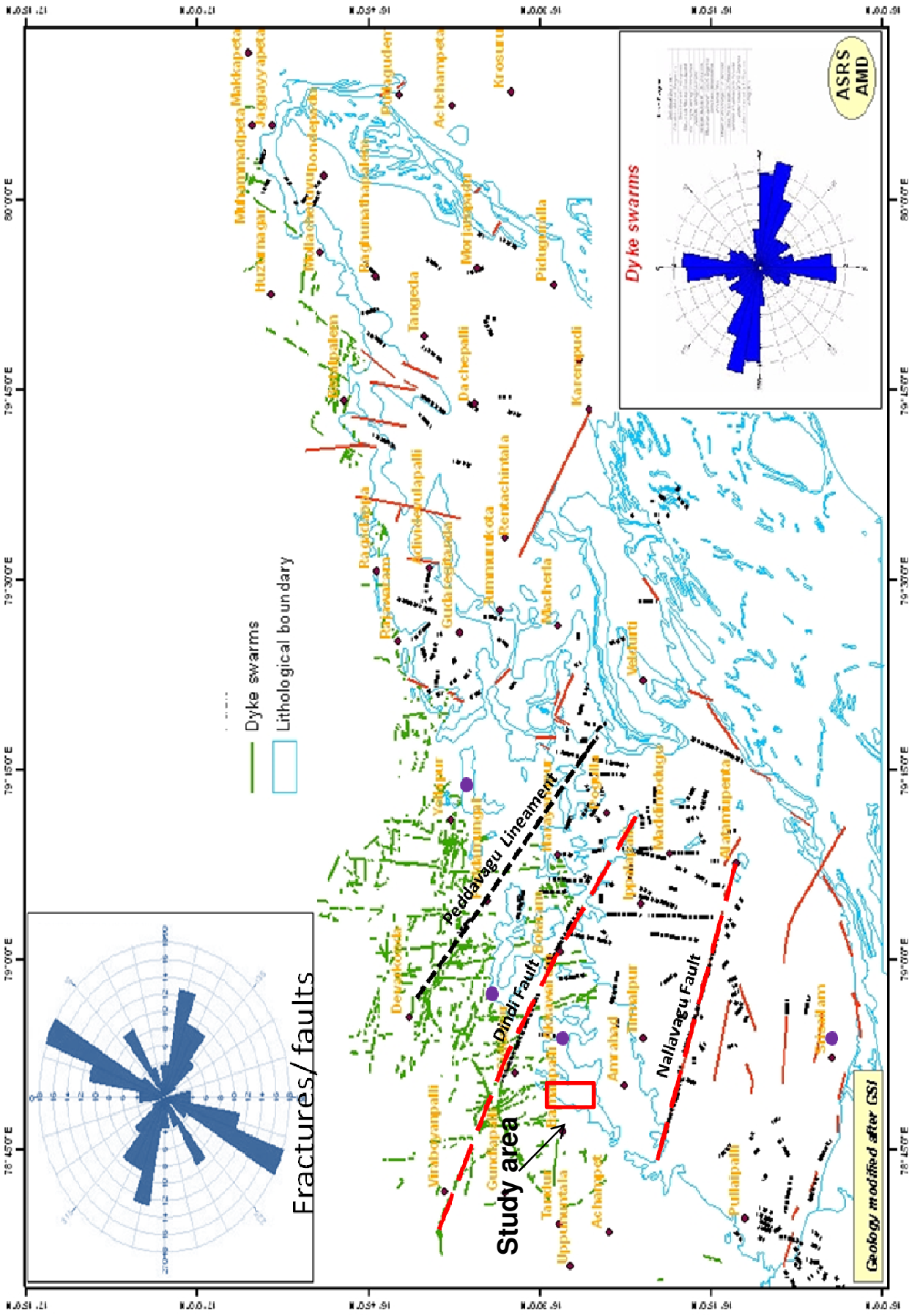
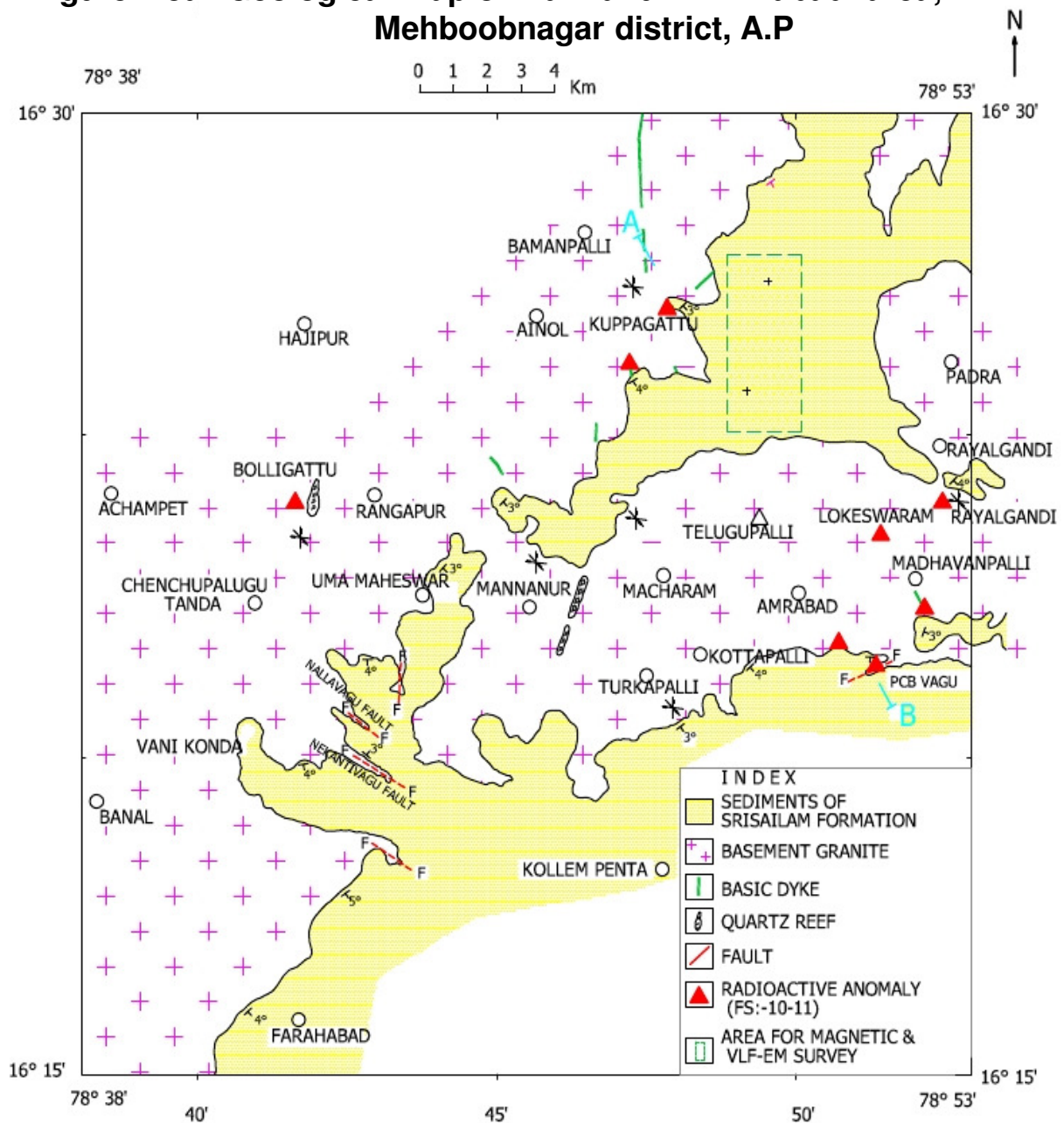
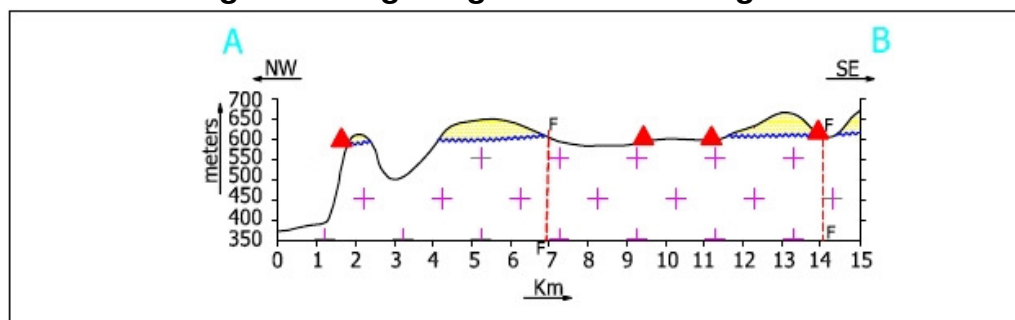


Fig.1.4: Lithostructural map of Srisaillam sub-basin (source ASRS, AMD)

**Figure 1.5a : Geological map of Mannanur – Amrabad area, Mehboobnagar district, A.P**



**Figure 1.5b: geological section along A - B**



(Map source : AMD,SCR)

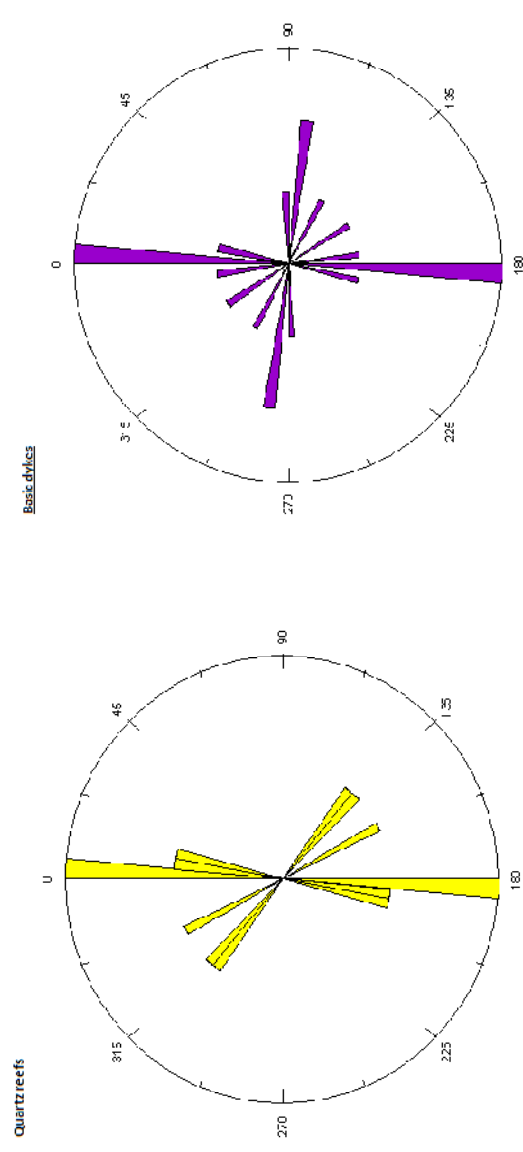
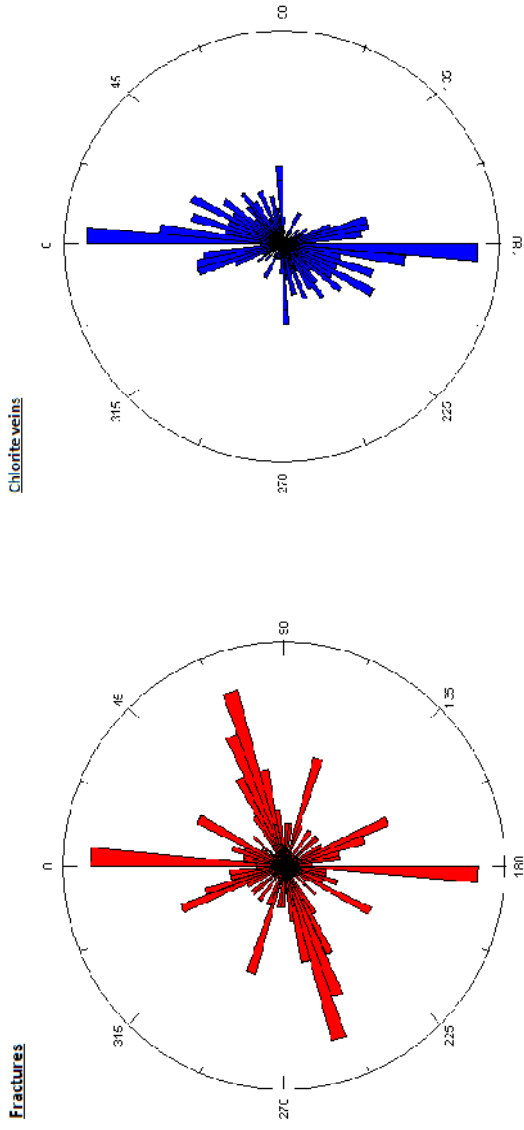
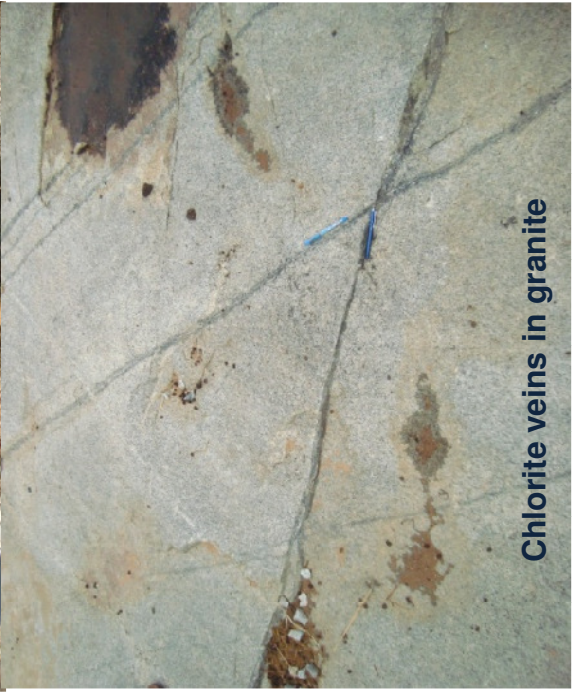


Figure 1.6. Rose diagrams of the structural features in the study area

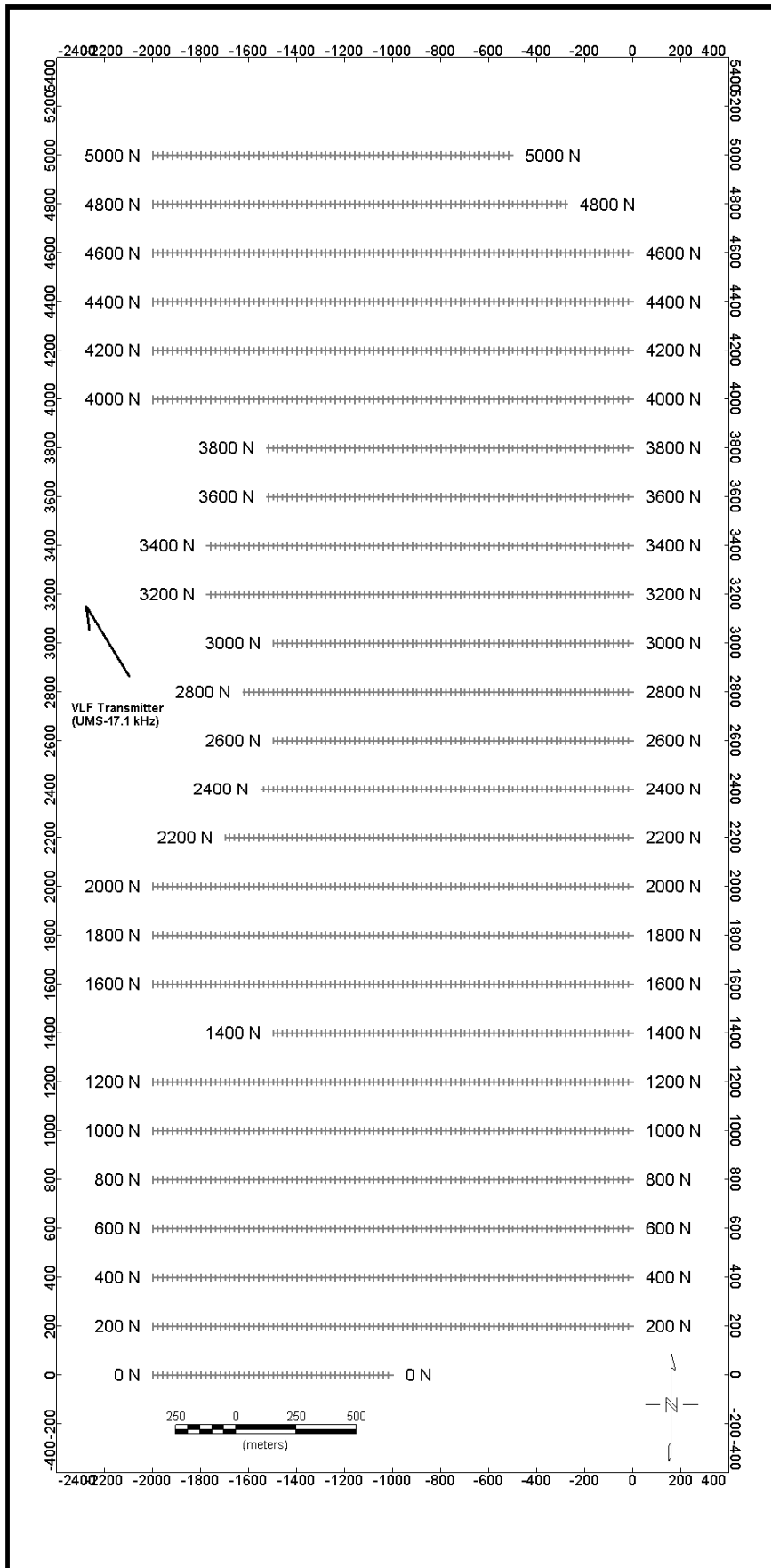


Figure 2.6 . Survey layout showing profile line and station points

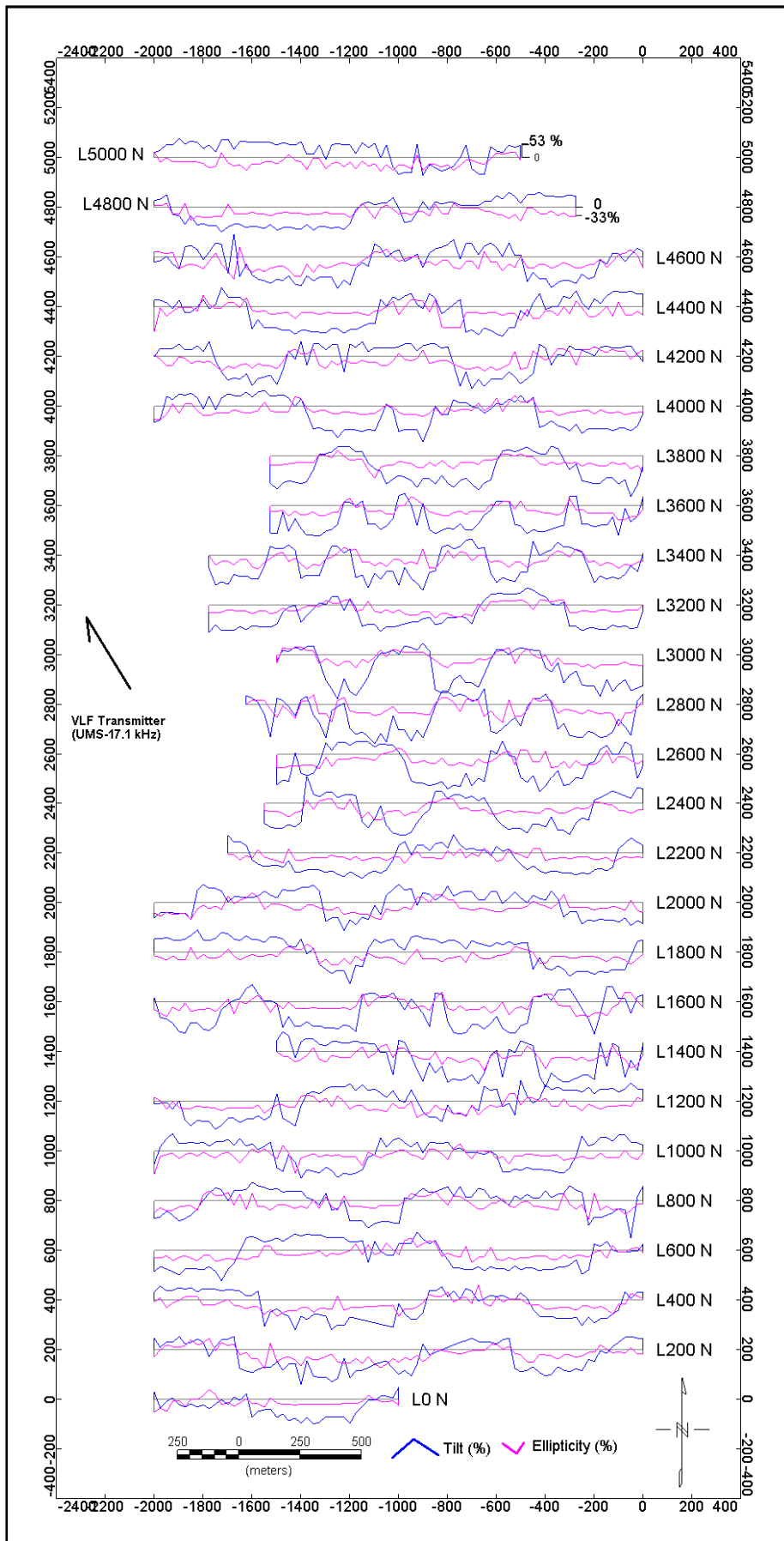
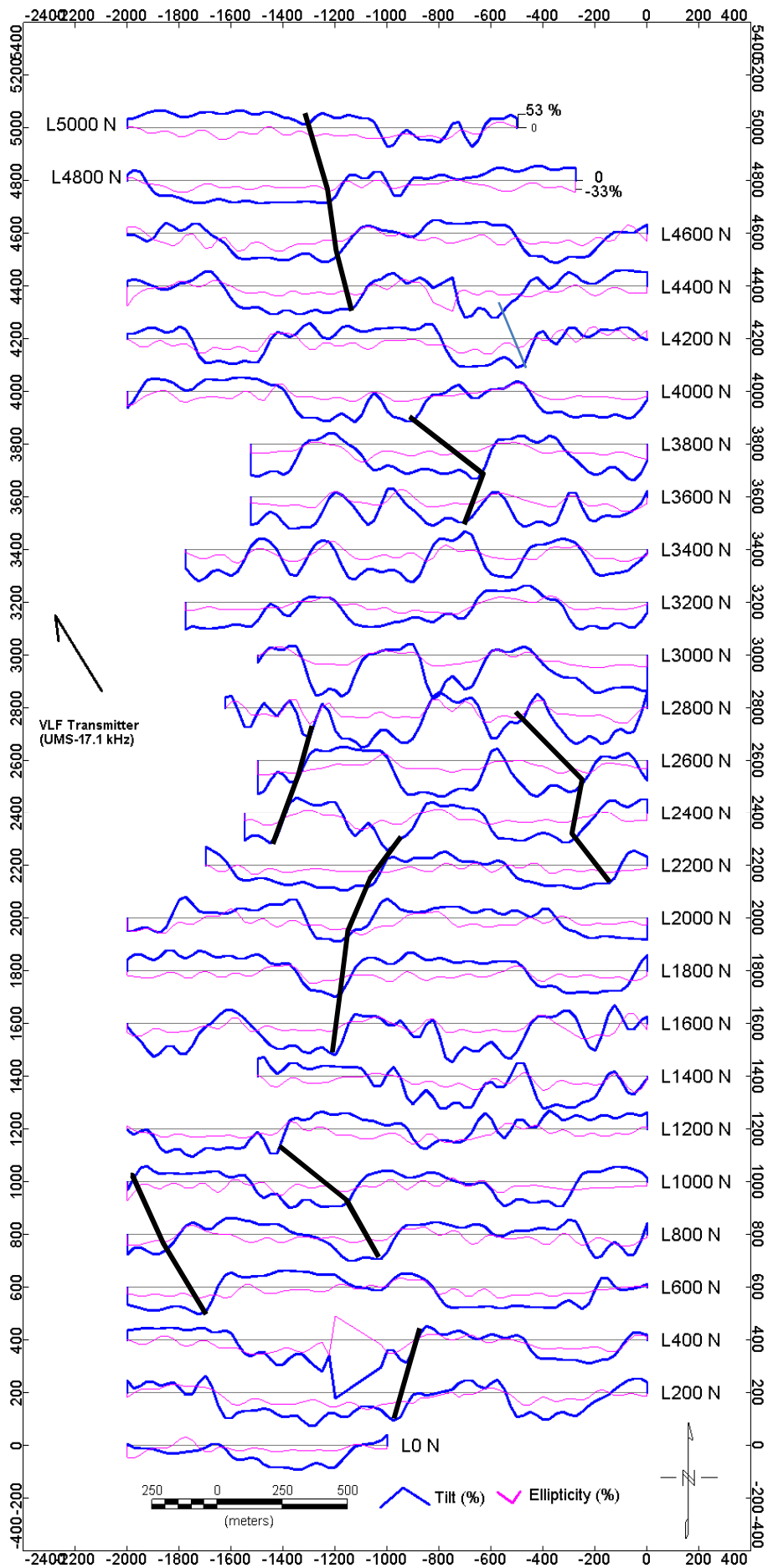


Figure 3.1 Stacked profiles of raw tilt (%) and ellipticity (%) data



**Figure 3.2 . Stacked profiles of low pass filtered tilt and ellipticity data with lines showing the conductor axis**

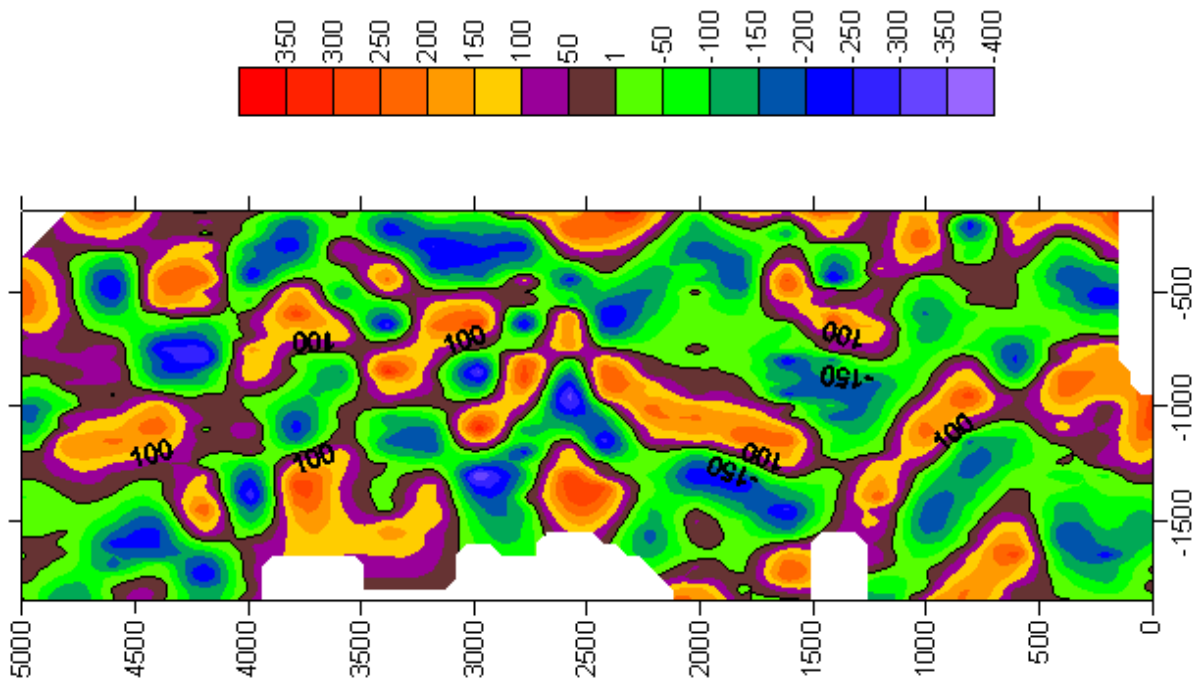


Figure 3.3. Fraser filtered output of inphase data

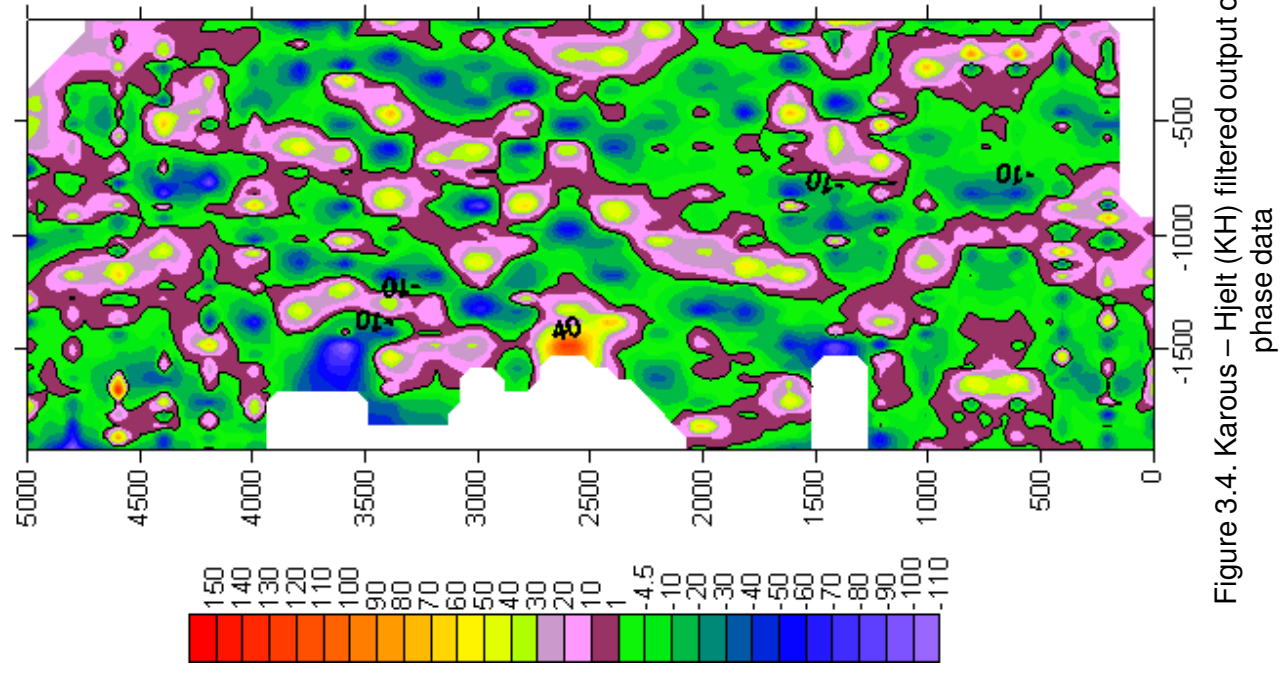


Figure 3.4. Karous - Hjelt (KH) filtered output of in phase data

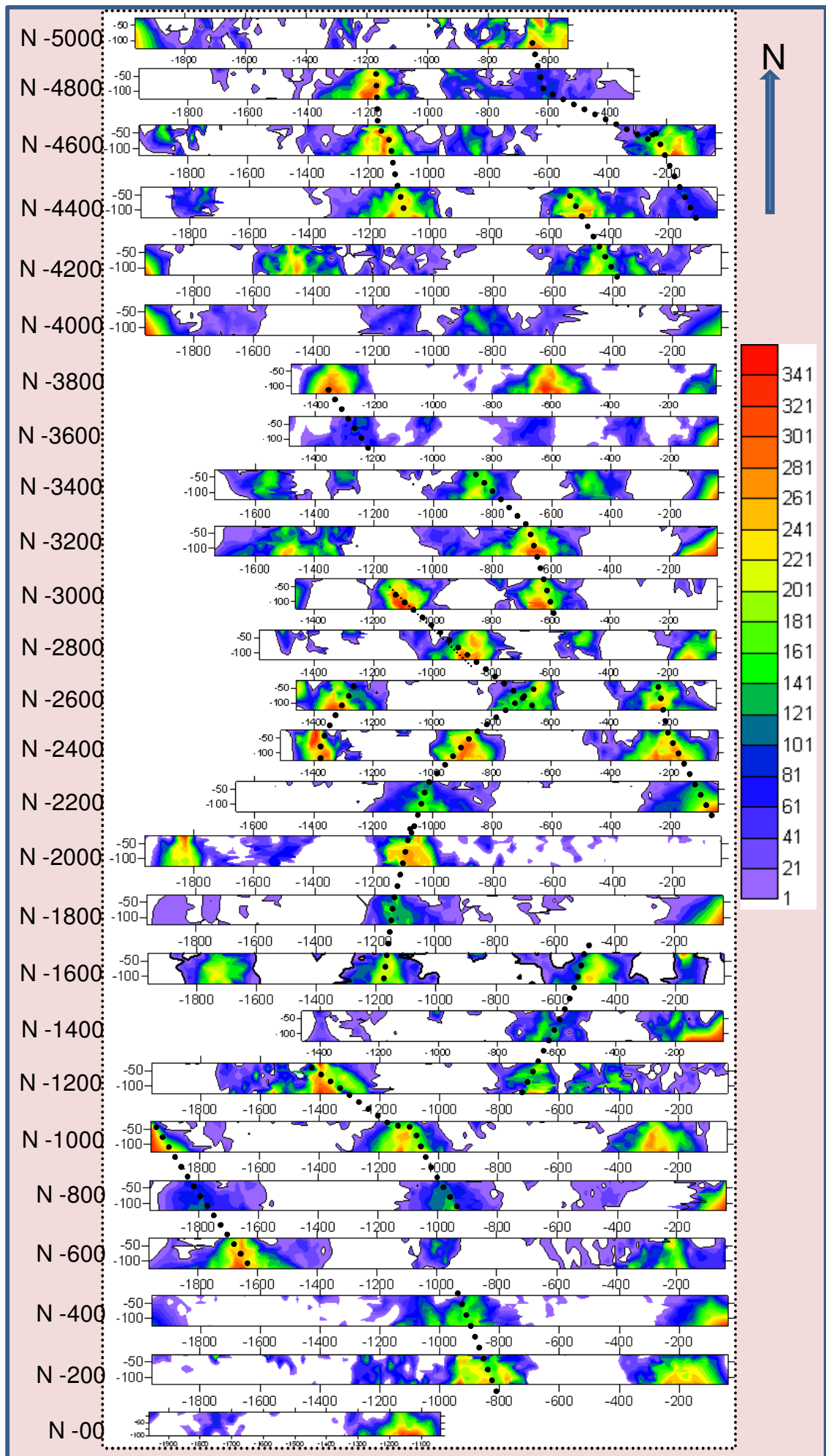


Figure 3.5 . Fraser filter pseudo sections of the profiles showing conductor axis

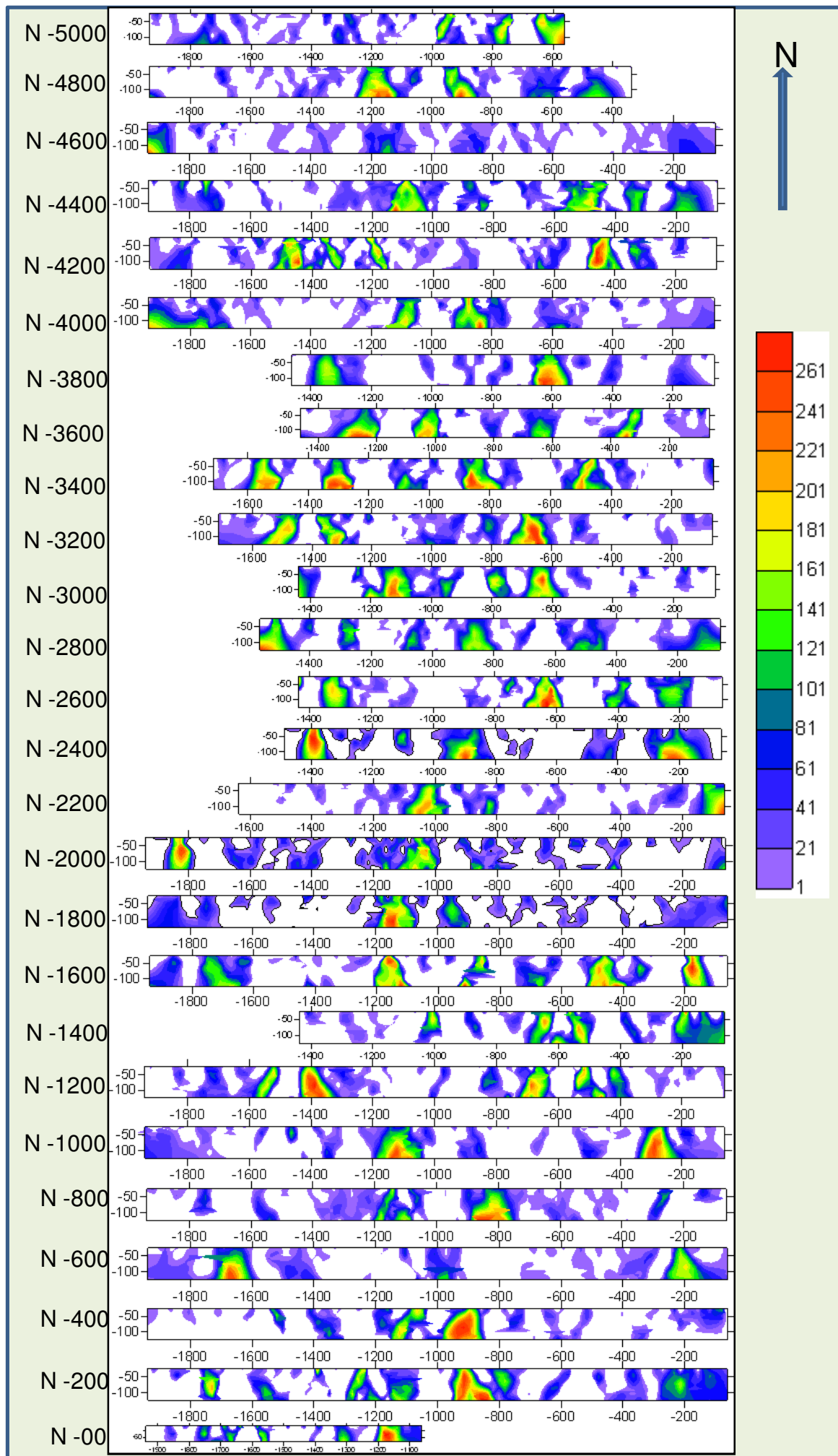


Figure 3.6 . Karous – Hjelt (KH) filter pseudo sections of the profiles

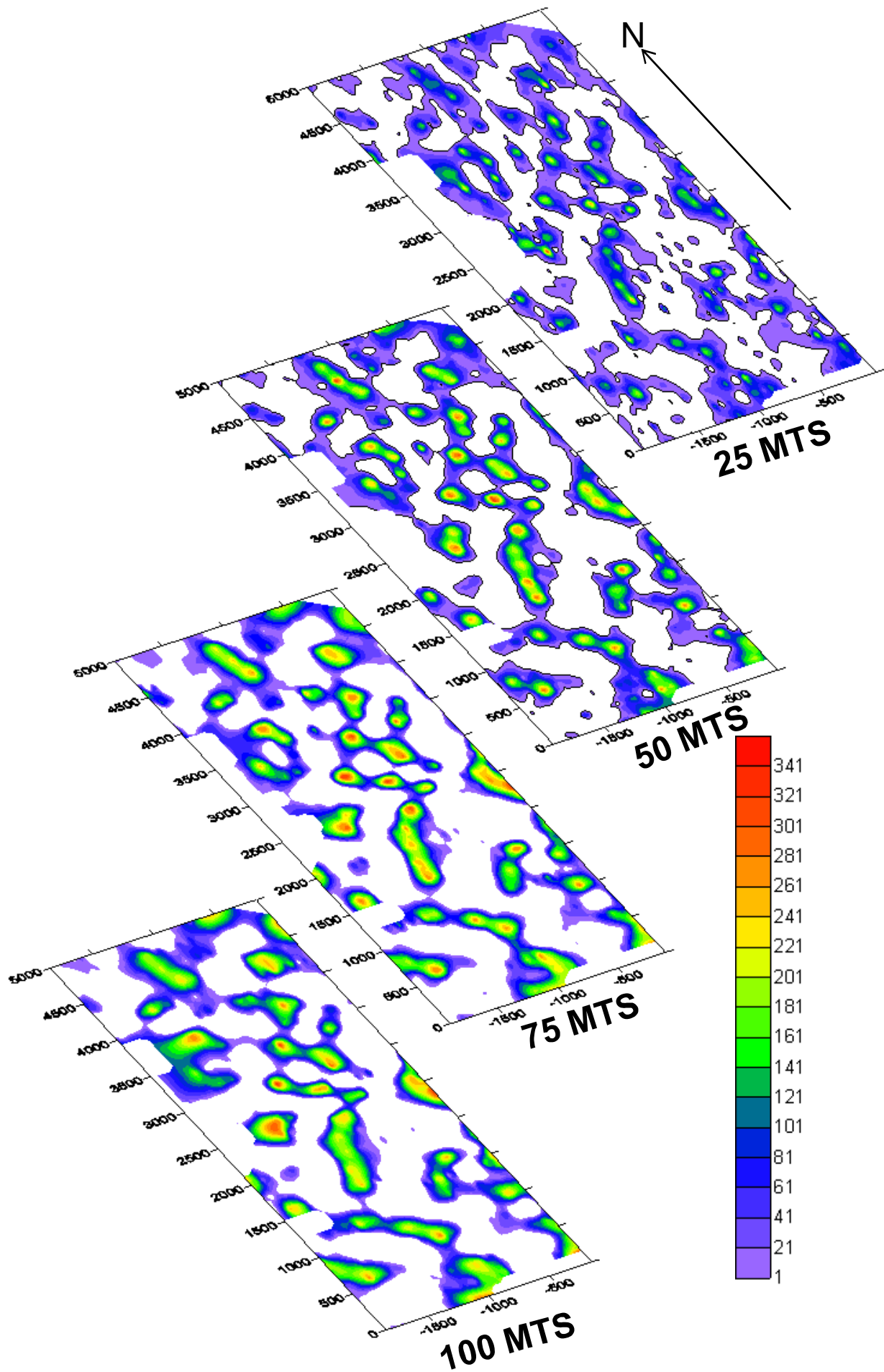


Figure 3.7 . Depth slices prepared using Fraser filter data

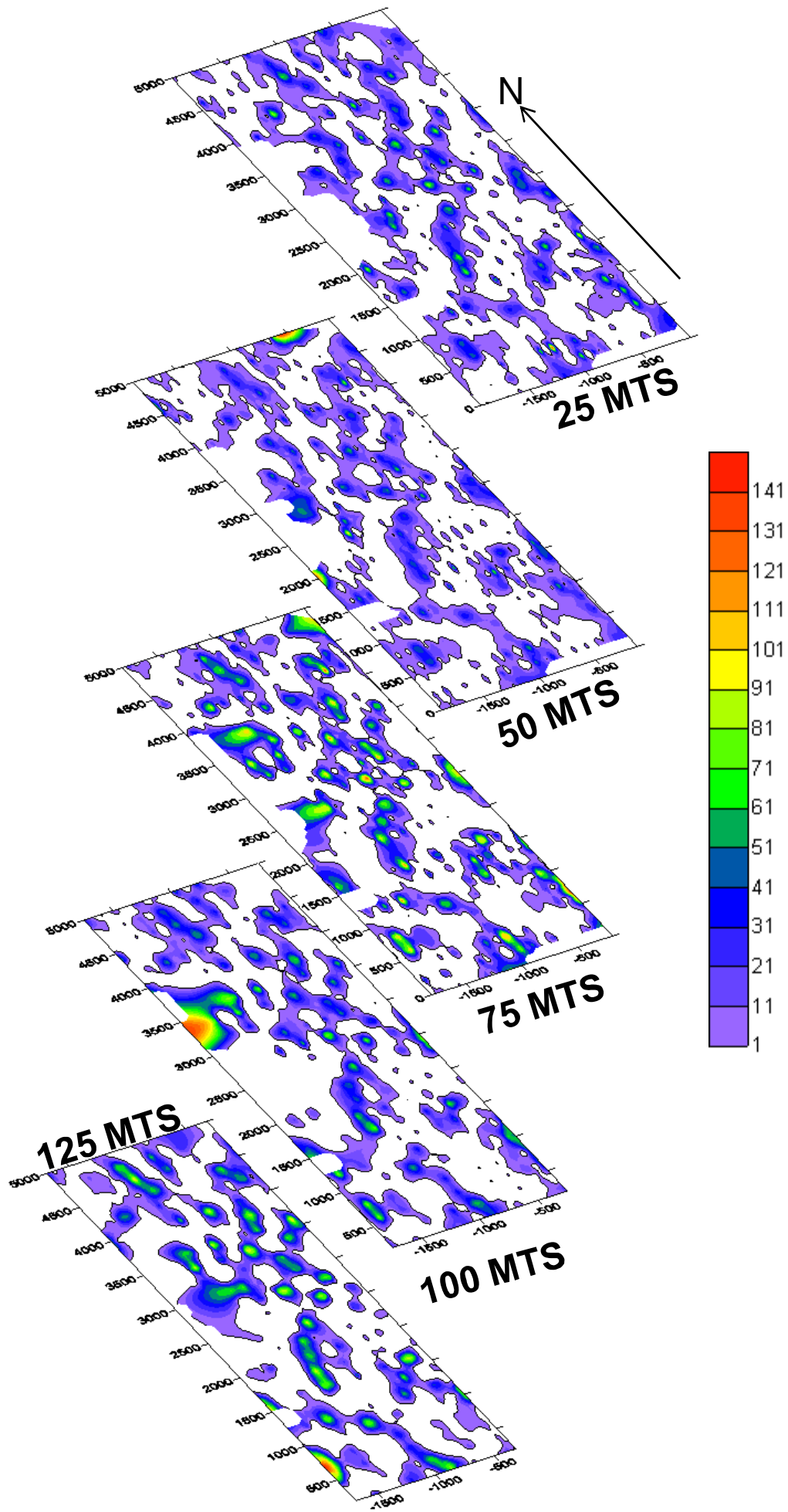


Figure 3.8. Depth slices prepared using Karous – Hjelt Filter data

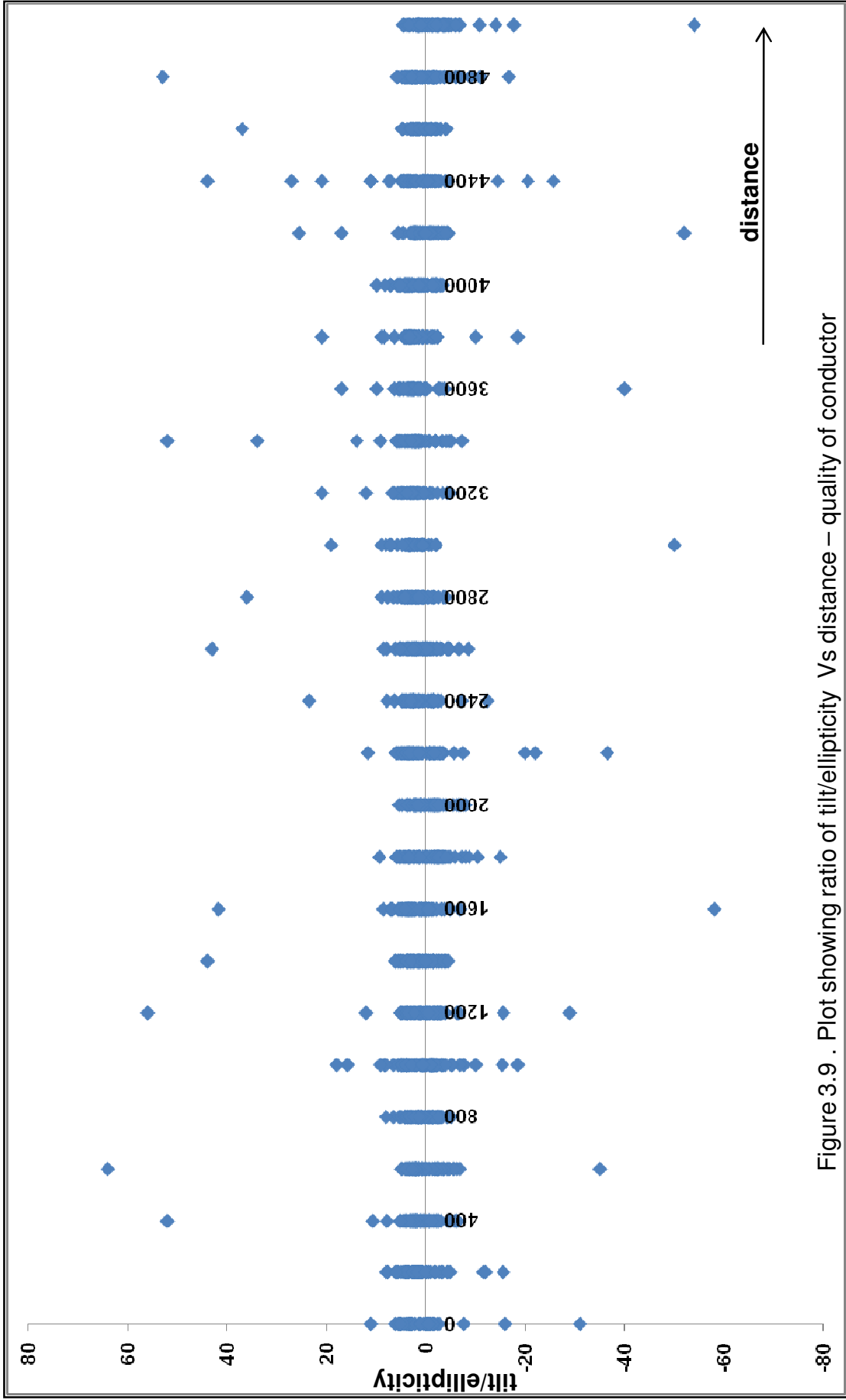


Figure 3.9 . Plot showing ratio of tilt/ellipticity Vs distance – quality of conductor

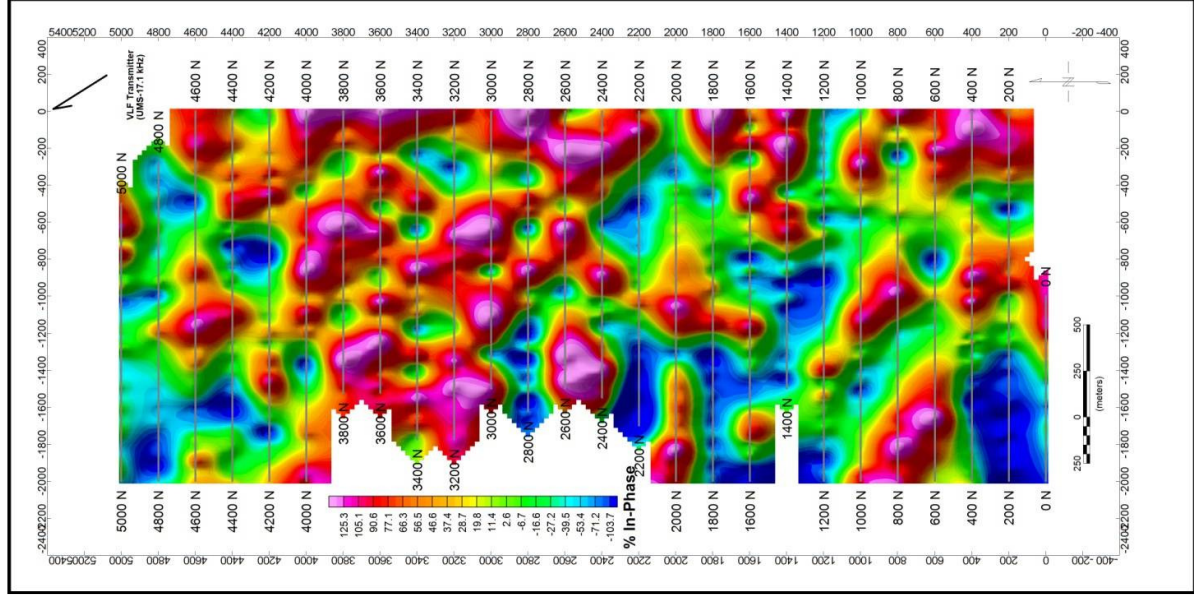


Figure 3.10. Hilbert Transform output image of In-phase data

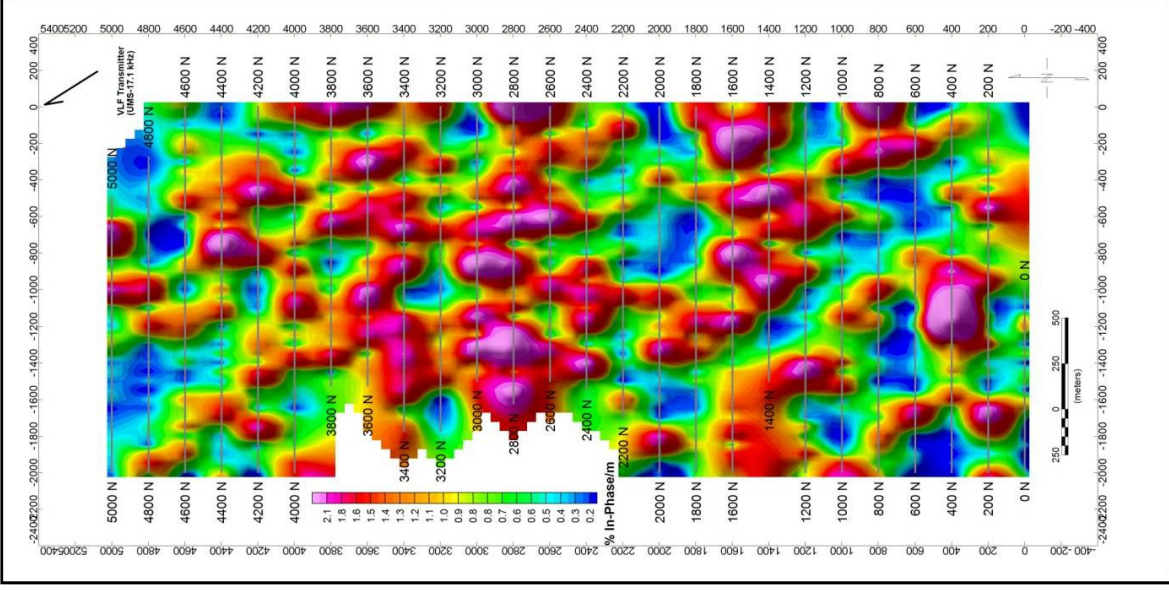


Figure 3.11. Amplitude of Analytical signal image of In-phase data

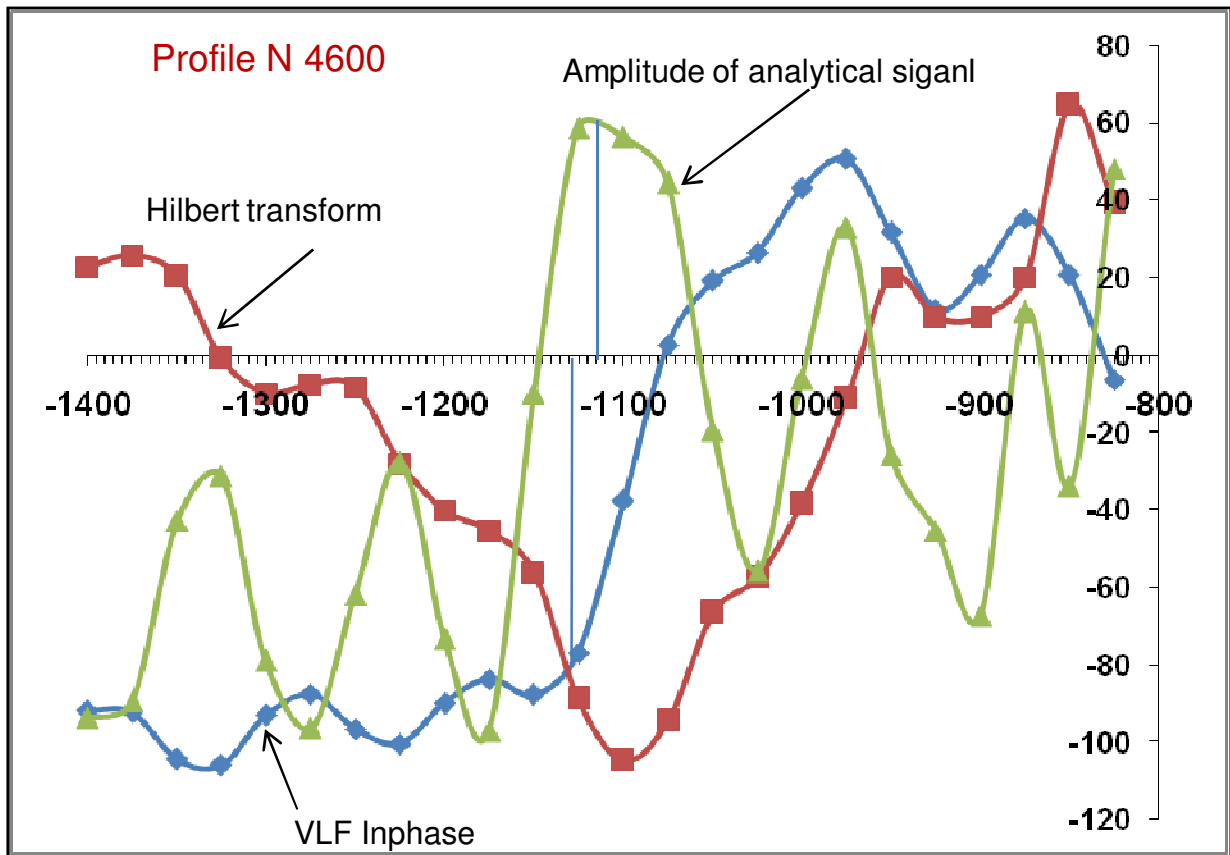
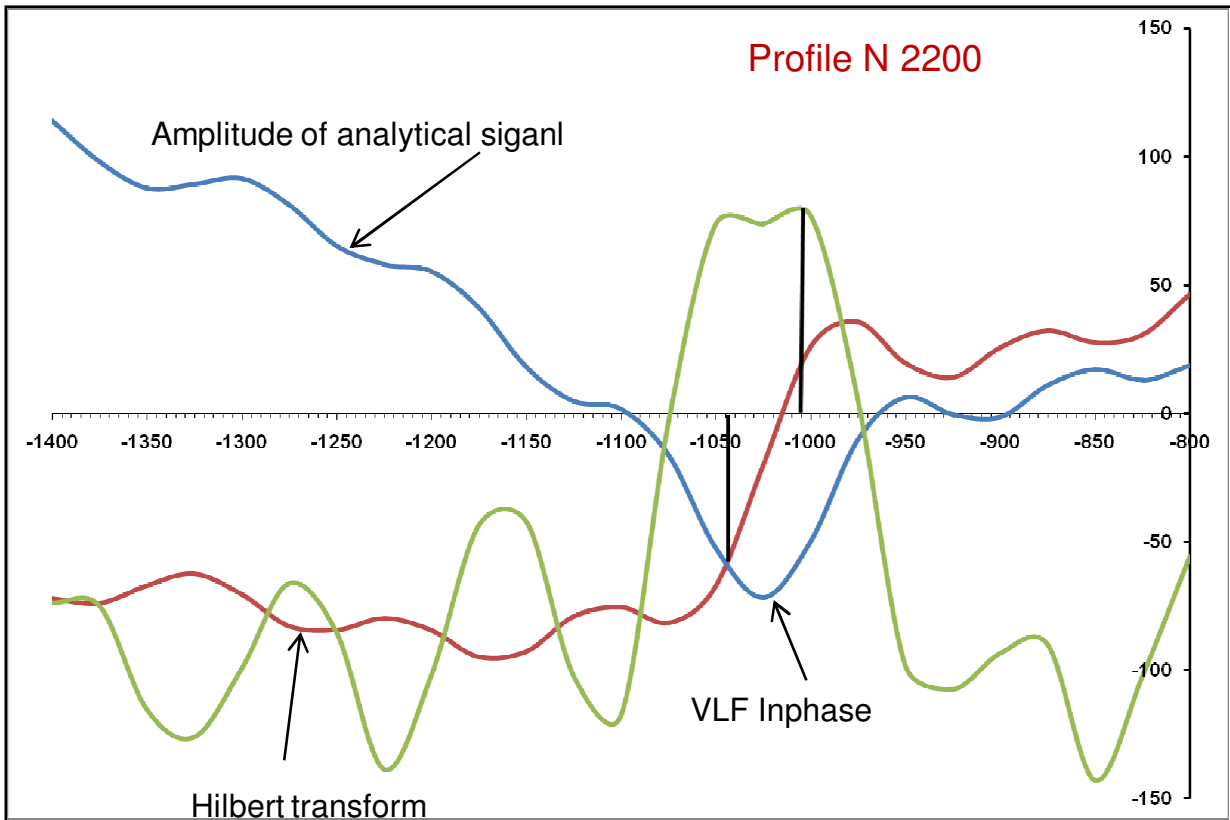


Figure 3.12 profiles ( N2200 and N 4600) showing depth to the top of the conductor using empirical method ( Sundararajan, et al, 2011)

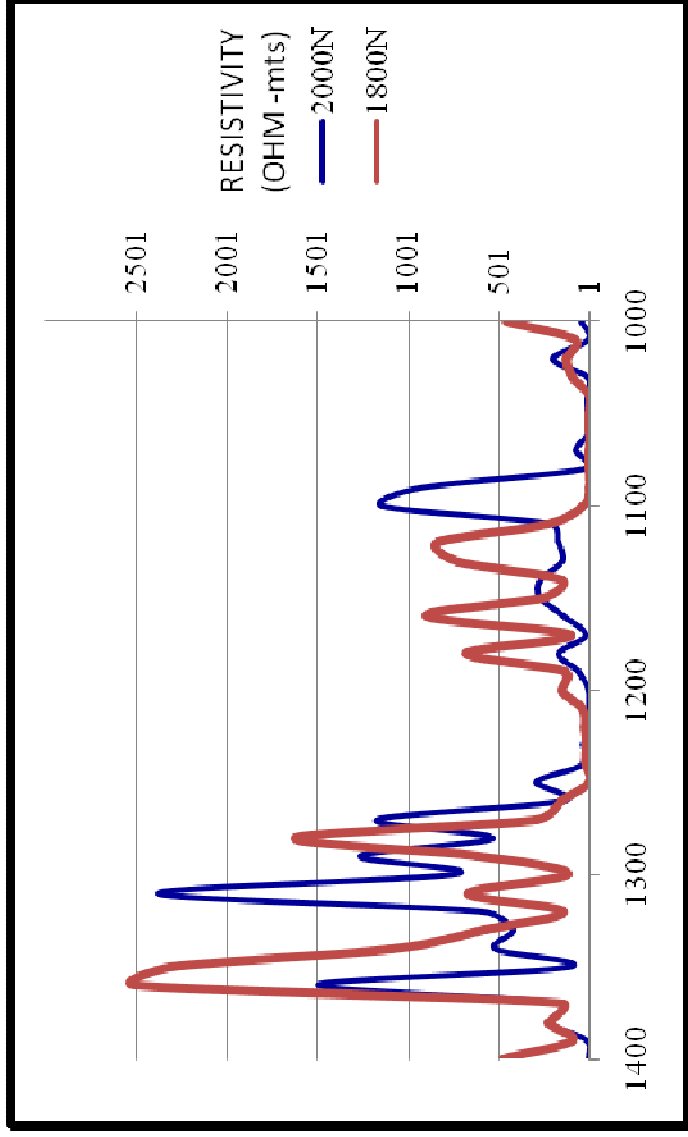
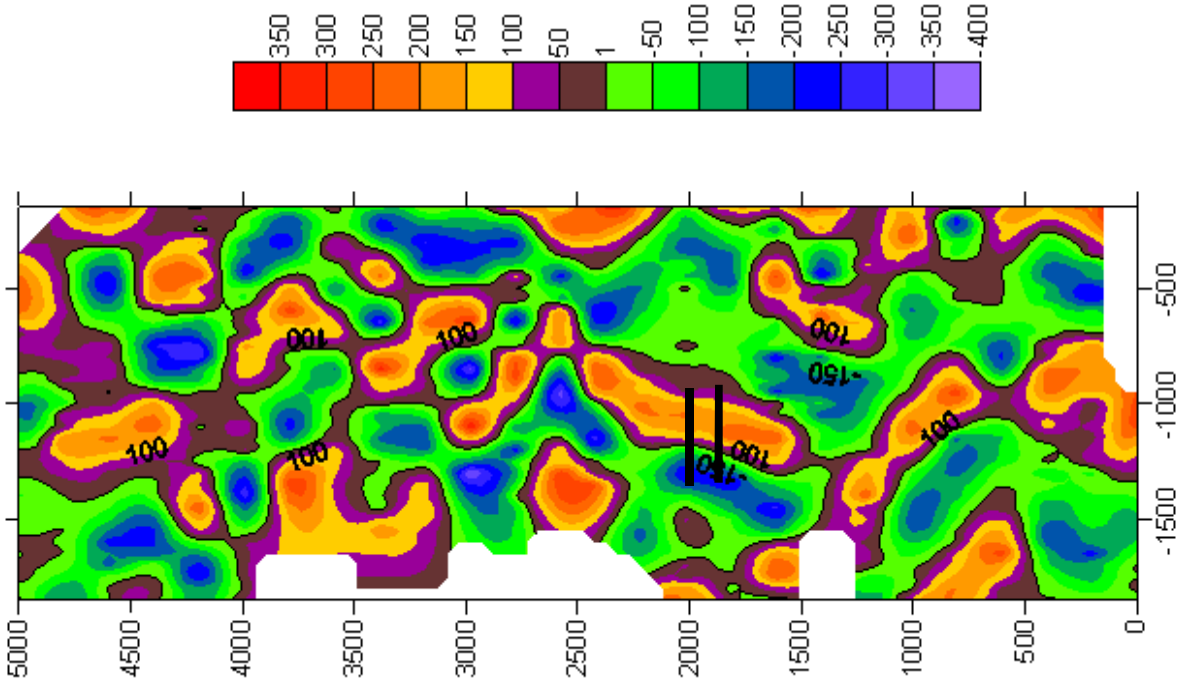


Figure 4.1b. measured apparent resistivity profiles

Figure 4.1a. Fraser filtered output of study area showing VLF resistivity profile lines

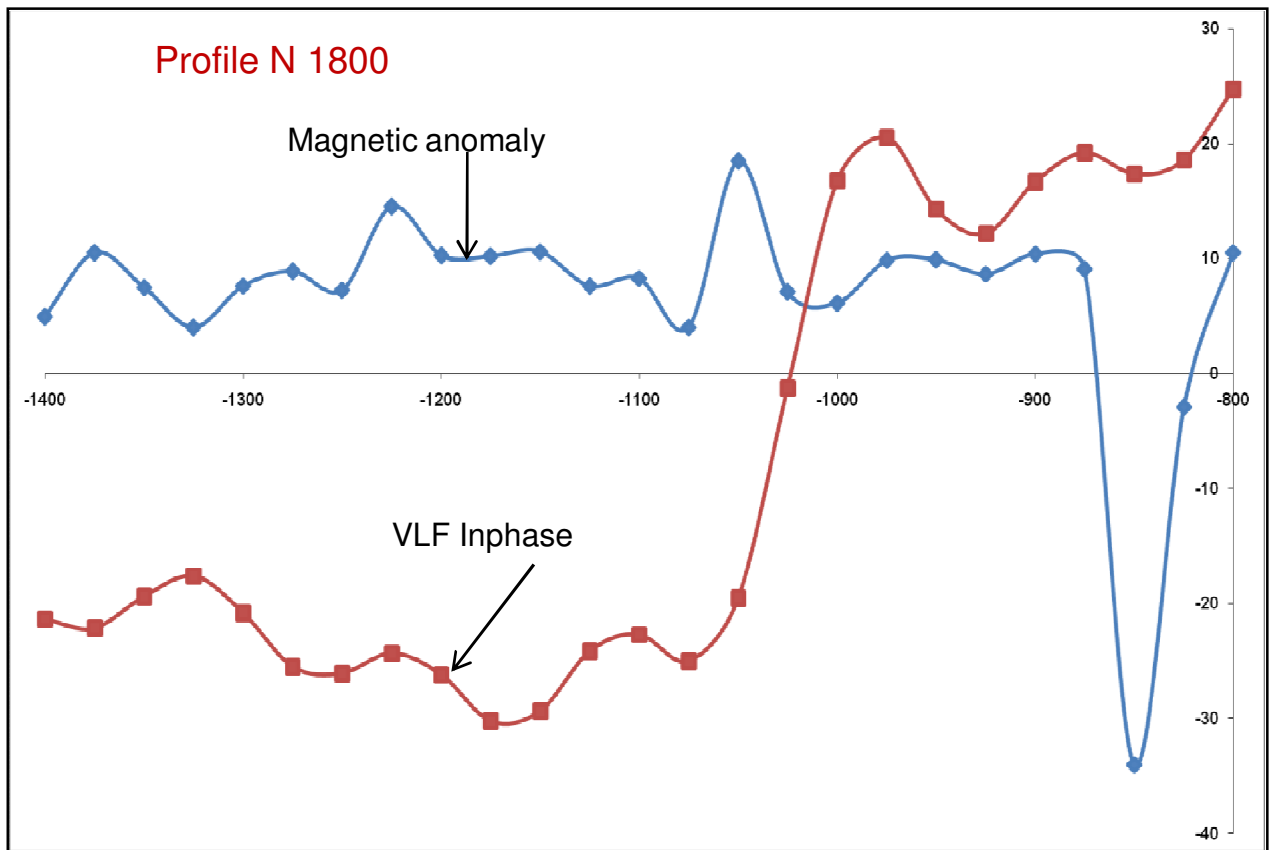
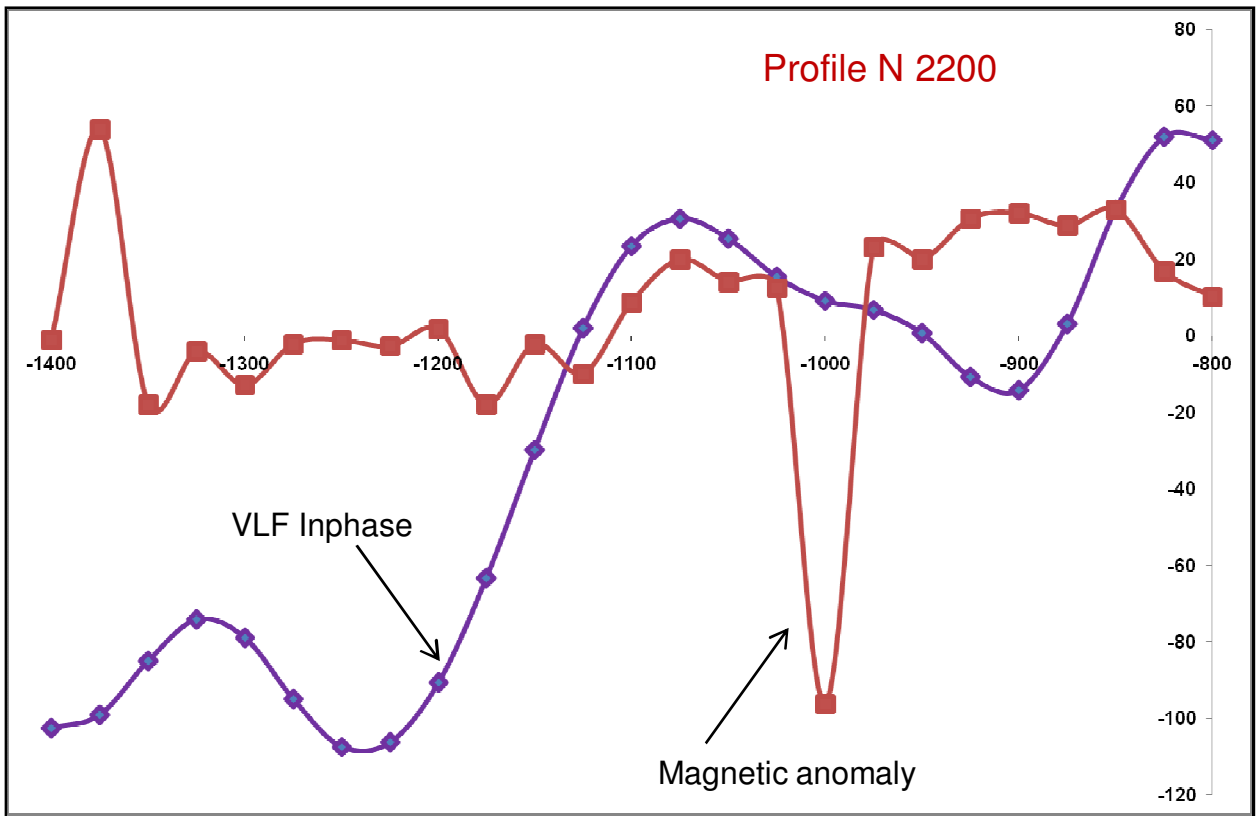


Figure 5.1 Profiles ( N2200 and N 1800) showing VLF in-phase and Magnetic anomaly

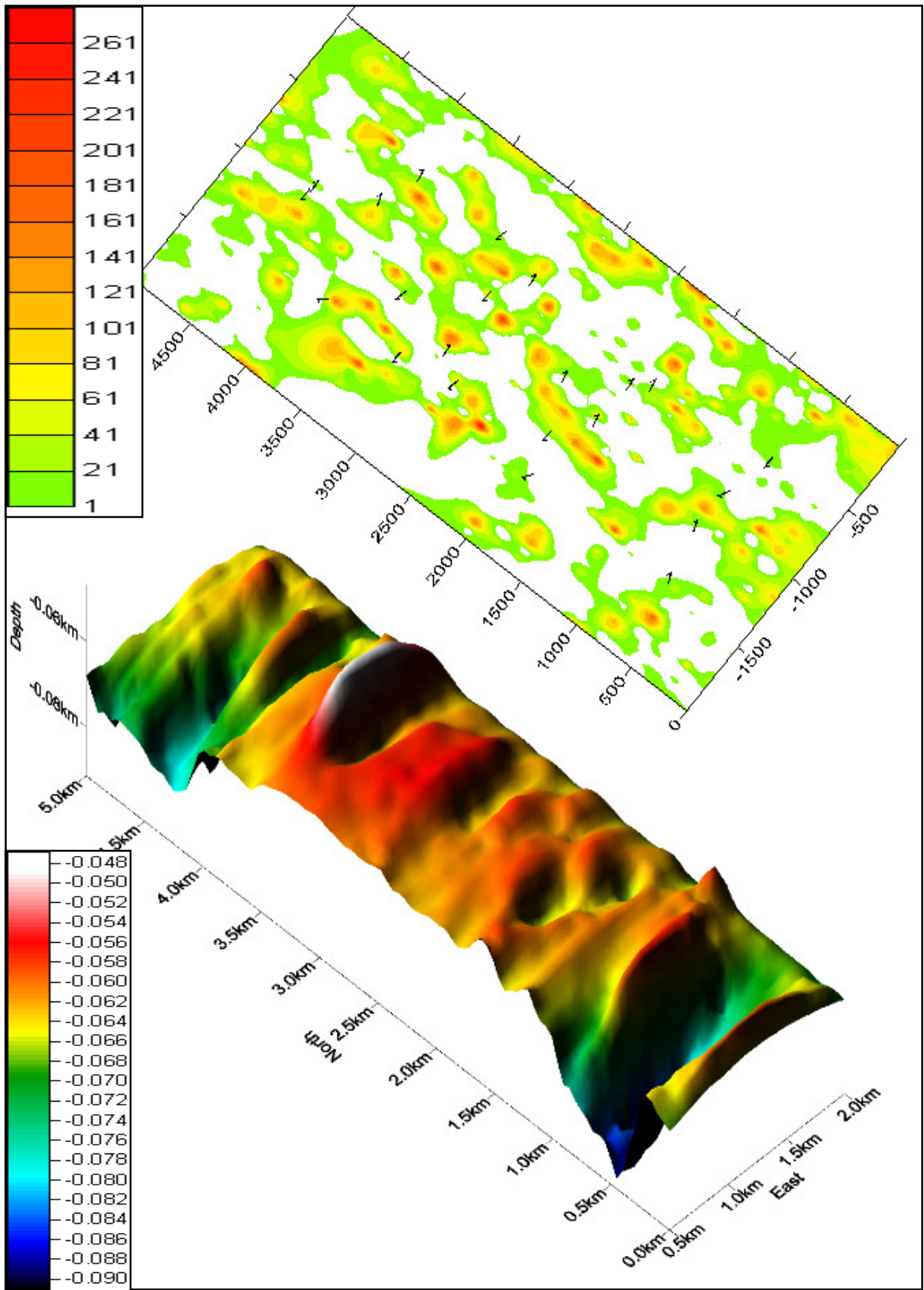


Figure 5.2 Superimposed map of magnetic 3D inverted image on the VLF Fraser filter contour map

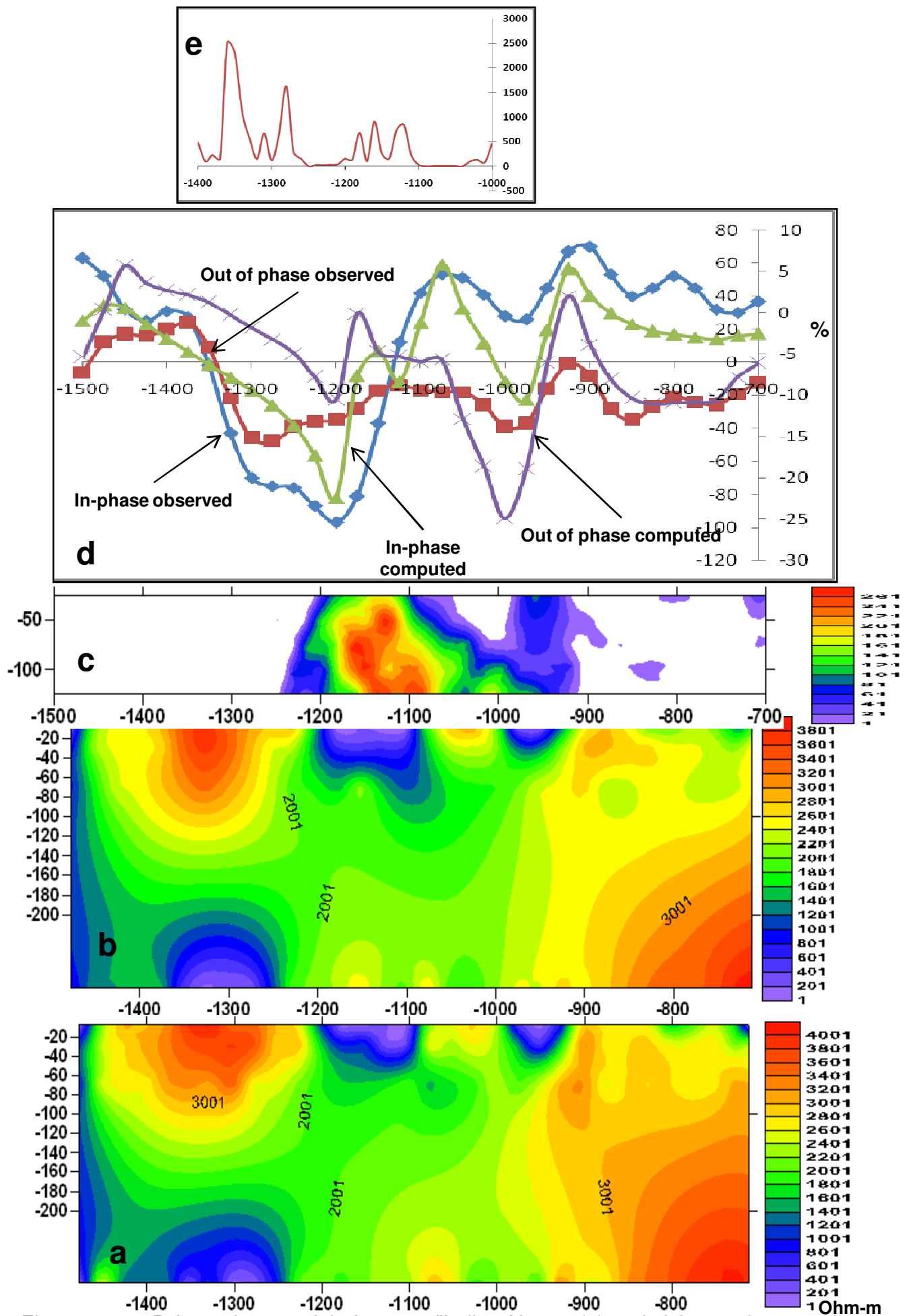


Figure 6.5: 2D Inversion model along profile line N1800 (a) resistivity section raw data (b) resistivity section low pass filter (c) pseudo depth section (d) curves of observed and computed data (e) measured apparent resistivity profile

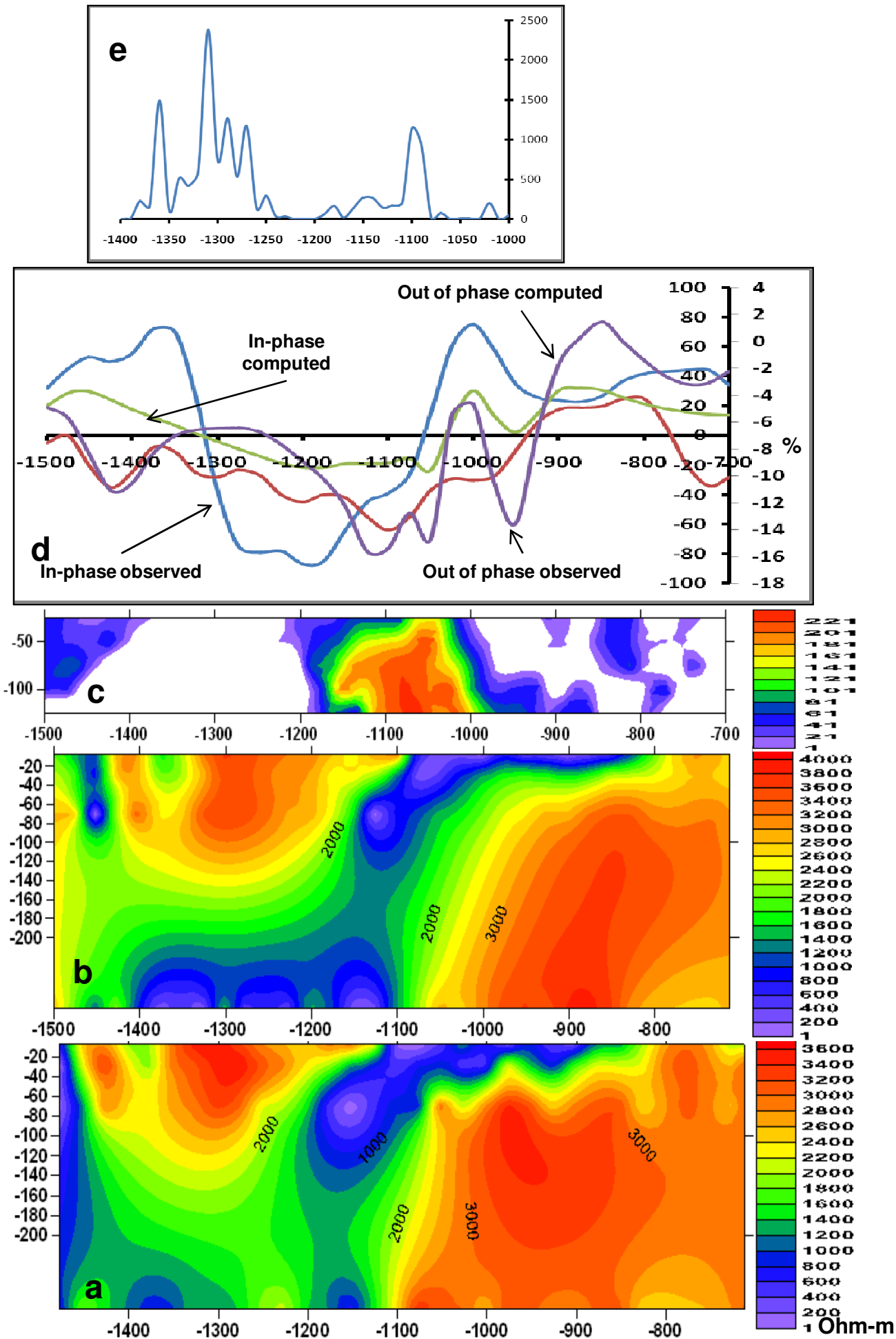


Figure 6.6: 2D Inversion model along profile line N2000 (a) resistivity section raw data (b) resistivity section low pass filter (c) pseudo depth section (d) curves of observed and computed data (e) measured apparent resistivity profile

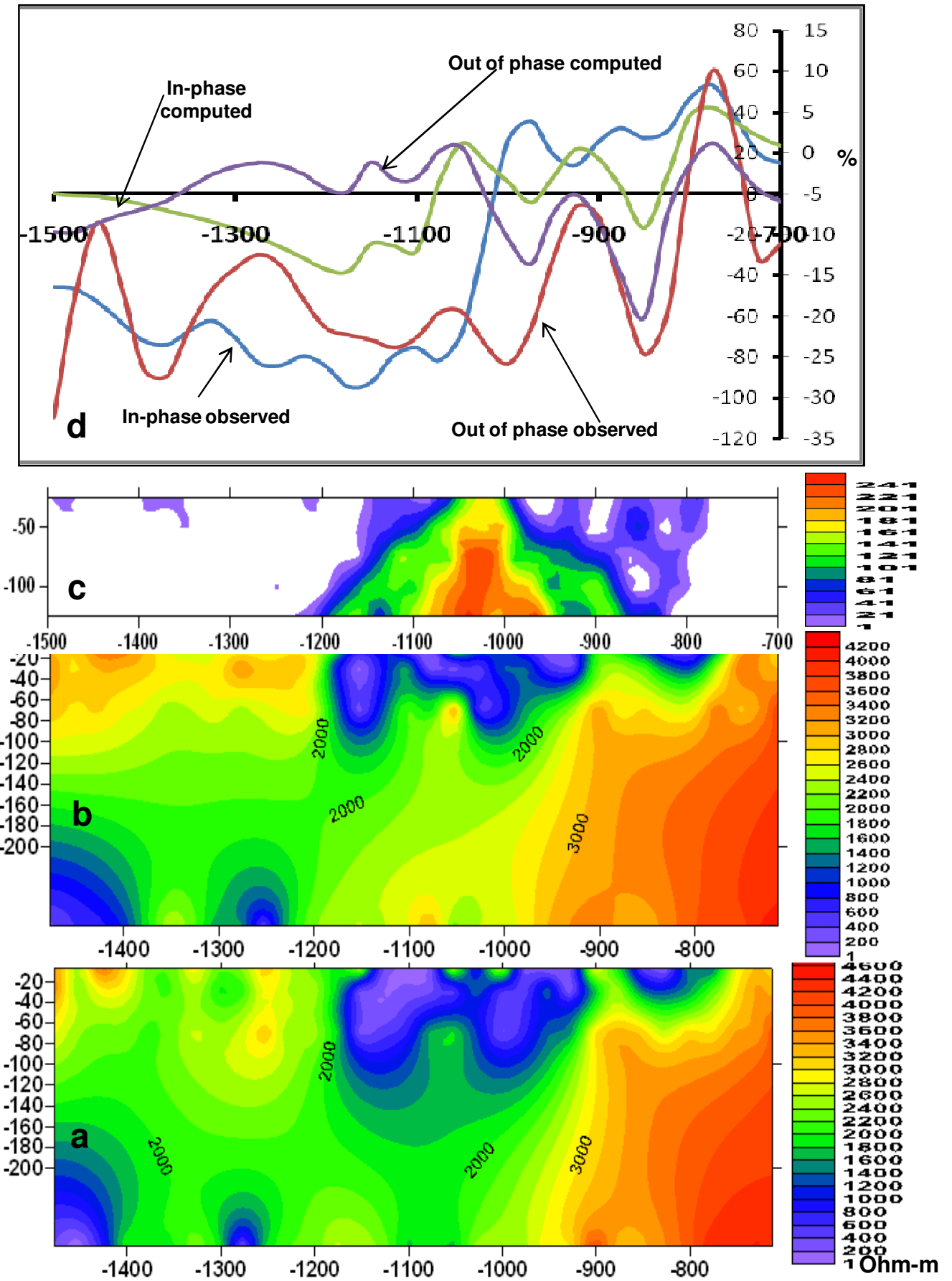


Figure 6.7: 2D Inversion model along profile line N2200 (a) resistivity section raw data (b) resistivity section low pass filter (c) pseudo depth section (d) curves of observed and computed data

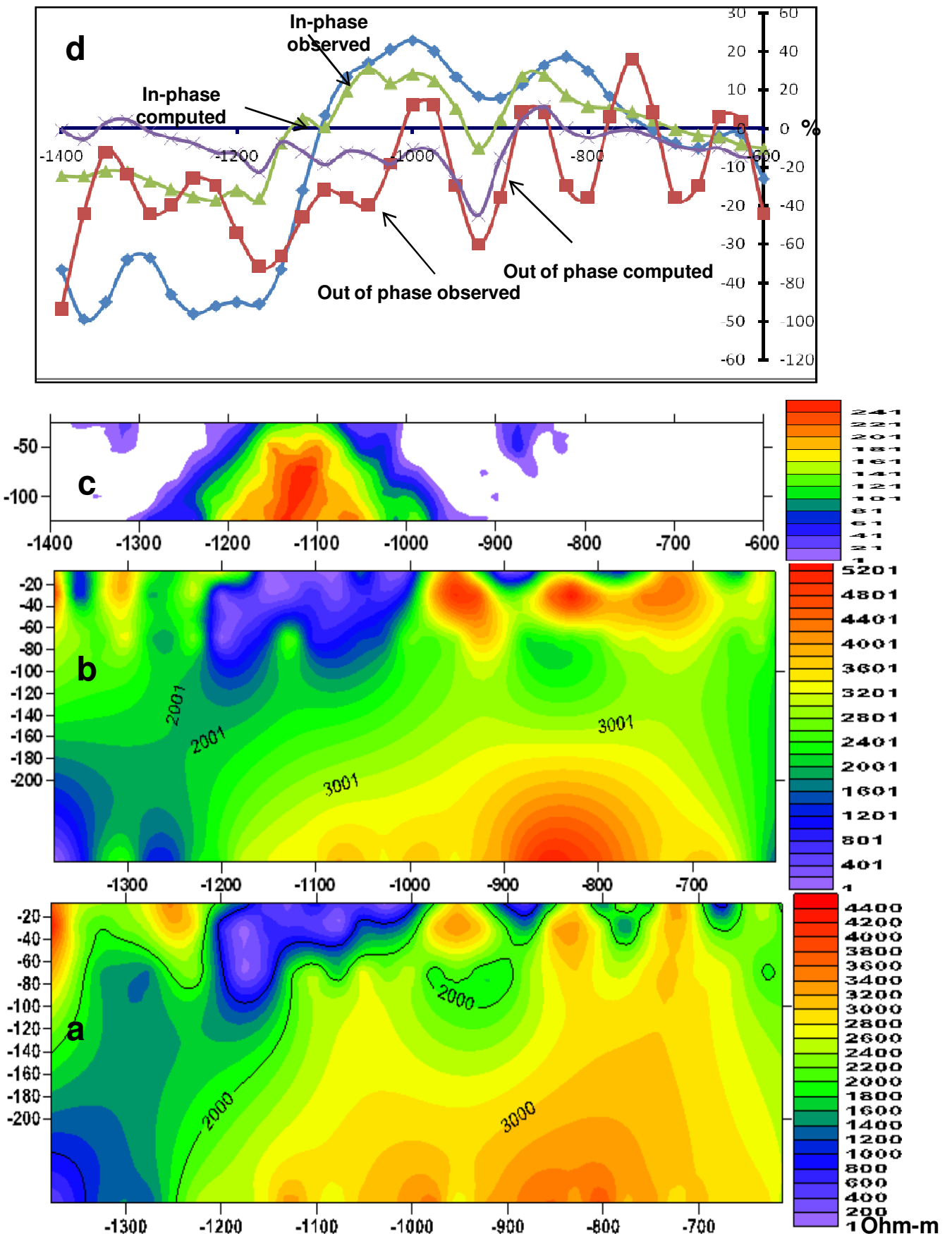


Figure 6.8 2D Inversion model along profile line N1000 (a) resistivity section raw data (b) resistivity section low pass filter (c) pseudo depth section (d) curves of observed and computed data



Figure 6.9: 2D Inversion model along profile line N4400 (a) resistivity section raw data (b) resistivity section low pass filter (c) pseudo depth section (d) curves of observed and computed data

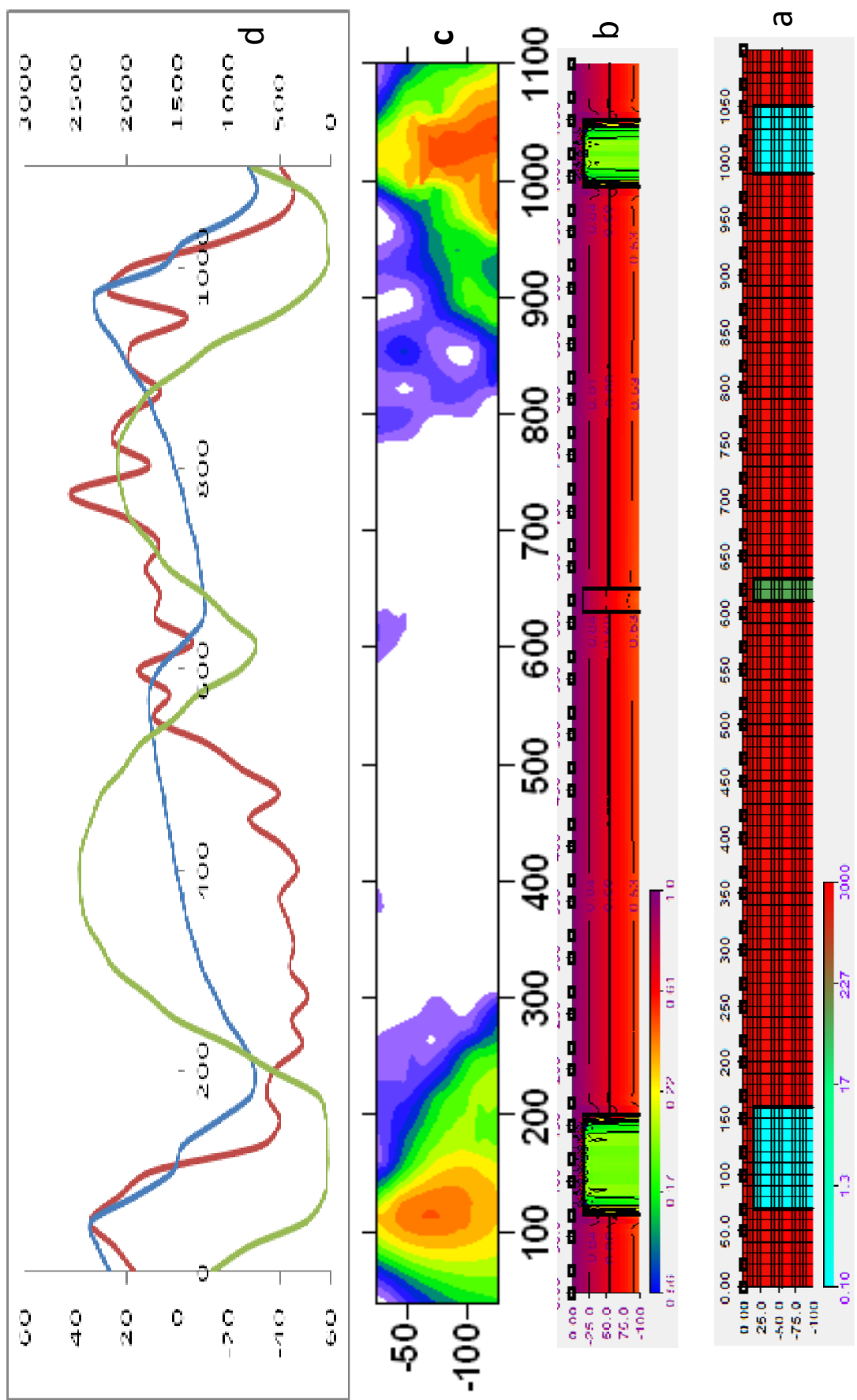


Figure 6.2 : 2D-MODEL FOR N-2200 line a) Model parameters b) obtained model c) current density Pseudo depth section d) Observed and computed tilt angle curves with computed resistivity profile